THE ROLE OF THE HERPES SIMPLEX VIRUS TYPE 1 UL25 PROTEIN IN DNA PACKAGING AND VIRION ASSEMBLY

by

Shelley Kristen Cockrell

Bachelor of Science, Duke University, 2003

Submitted to the Graduate Faculty of

the School of Medicine in partial fulfillment

of the requirements for the degree of

Doctor of Philosophy

University of Pittsburgh

2010

UNIVERSITY OF PITTSBURGH

SCHOOL OF MEDICINE

This dissertation was presented

by

Shelley Kristen Cockrell

It was defended on

August 23, 2010

and approved by

James Conway, Associate Professor, Department of Structural Biology

Roger Hendrix, Professor, Department of Biological Sciences

Neal DeLuca, Professor, Department of Microbiology and Molecular Genetics

Thomas Smithgall, Professor and Chair, Department of Microbiology and Molecular Genetics

Dissertation Advisor: Fred Homa, Associate Professor, Department of Microbiology and Molecular Genetics

THE ROLE OF THE HERPES SIMPLEX VIRUS TYPE 1 UL25 PROTEIN IN DNA PACKAGING AND VIRION ASSEMBLY

Shelley Kristen Cockrell, PhD

University of Pittsburgh, 2010

Herpes simplex virus type 1 replicates its DNA and builds progeny nucleocapsids in the nucleus of the infected cell. Replicated viral DNA is a concatemer that is cleaved to unit-length genomes and packaged into capsid precursors, and successful DNA packaging is required for the mature capsid to exit the nucleus and become incorporated into virions. The DNA cleavage and packaging machinery is highly conserved across herpesvirus subfamilies; they represent novel targets for anti-herpesviral treatments. Seven genes have been identified that are essential for the packaging reaction. Of these, the UL25 gene product is unique because it is required for the completion rather than the initiation of DNA packaging. In the absence of functional UL25, the nuclei of infected cells accumulate empty capsids and free, close to genome-length viral DNA. This phenotype differs from null mutations of the other packaging genes, which block cleavage of the concatemer and expulsion of the capsid scaffold protein. While the functions of several members of the packaging machinery have been deduced by analogy with the dsDNA bacteriophages, the role of UL25 protein (pUL25) in this process is unclear. pUL25 is stably associated with the capsid vertices, where it forms a heterodimer with the packaging protein UL17. The goal of this project is to elucidate the pUL25 capsid-binding mechanism and its significance for DNA packaging and virion assembly. Mutational analysis of UL25 mapped the capsid-binding domain to the pUL25 N-terminus. pUL25 interactions with the capsid surface proteins were visualized with cryo-electron microscopy and 3D image reconstructions of capsids

containing pUL25 fusion proteins. Finally, we demonstrated that UL25 mutants aberrantly cleave viral DNA before the second packaging signal. These data support a model in which pUL25 provides structural support to capsid vertices without interacting directly with DNA during the packaging reaction.

TABLE OF CONTENTS

LIST OF TABLES

LIST OF FIGURES

PREFACE

The data presented in this dissertation are the culmination of many individual contributions. I would like to thank Bill Goins, Jason Heming, Jamie Huffman, and Minerva Sanchez, who provided technical assistance in the laboratory and critical reading of manuscripts. James Conway and Katerina Toropova of the University of Pittsburgh Department of Structural Biology performed all cryo-electron microscopy and 3D image reconstructions. Mara Sullivan and Donna Stolz of the University of Pittsburgh Center for Biologic Imaging prepared the samples for thin section electron microscopy; Katerina Toropova performed the microscopy and collected images of the sectioned samples. Bill Newcomb and Jay Brown of the University of Virginia generated and supplied to us the UL25 antibody, 25E10. Other reagents and equipment were kindly provided by Joel Baines (Cornell University), Neal DeLuca (University of Pittsburgh), Paul "Kip" Kinchington (University of Pittsburgh), Bruce McClane (University of Pittsburgh), and Sandra Weller (University of Connecticut).

Much of the data and text in Chapters 2 and 3, and some data in Chapter 4, has previously been published. These publications are noted in Appendix B.

Commonly used abbreviations in this dissertation include: aa, amino acid(s); kb or kbp, kilobase pairs; bp, base pairs; wt, wild-type; min, minutes; h or hr, hours; ORF, open reading frame; MOI, multiplicity of infection; RT, room temperature; hpi, hours post-infection. Viruses

generated in this study are given a descriptive name referencing the UL25 genotype, preceded by a lowercase “v”. Proteins are designated by their gene name preceded by a lowercase “p”.

1.0 INTRODUCTION

1.1 HERPESVIRUSES AND DISEASE

The herpesviruses are a large group of animal viruses that infect many different vertebrate and one identified invertebrate species. The prototypical herpesvirus can be recognized by its virion morphology, and particularly, by the shape and size of the nucleocapsid. Negative staining and electron microscopy revealed that the herpesvirus virion is approximately 200 nm in diameter and contains an angular nucleocapsid, a protein tegument layer, and a glycoprotein-studded lipid envelope; the capsid is made of 162 capsomers that form an icosahedron of around 100 nm (238). Inside the nucleocapsid, herpesviruses have large (124-241 kbp), linear, double-stranded DNA (dsDNA) genomes. Recent approaches to herpesvirus classification have relied on comparative genomic and structural analysis (120). In the current nomenclature, three families of herpesviruses infecting different classes of animal hosts—the *Herpesviridae*, the *Alloherpesviridae*, and the *Malacoherpesviridae*—constitute the order *Herpesvirales* (Table 1). In addition to sharing a common evolutionary lineage, members of *Herpesvirales* are also predicted to share ancestry with the tailed dsDNA bacteriophages due to the commonalities in structure of the major capsid protein and the capsid portal (10, 120).

TABLE 1. The order *Herpesvirales.*

Family	Host classes
Herpesviridae	Mammals, reptiles, birds
Alloherpesviridae	Amphibians, fish
Malacoherpesviridae	mollusk

Herpesviruses are further divided into three subfamilies—the *alphaherpesvirinae*, the *betaherpesvirinae*, and the *gammaherpesvirinae*. These classifications were initially based on biological similarities and later adapted to accommodate genome sequence homology (181, 182). Phylogenetic analyses of the sequences encoding the viral DNA polymerase have shown that the last common ancestor of the *Herpesviridae* subfamilies existed about 400 million years ago, indicating that viruses from the same subfamily that infect different host species are more closely related than viruses of different families infecting the same host (119, 120). While acute disease manifestations between subfamilies vary, the herpesviruses have in common the ability to establish latent infections that can be periodically reactivated to the lytic cycle to cause recurrent disease. Eight human herpesviruses have been identified that fall into the three subfamilies (Table 2). The alphaherpesviruses have a rapid lytic replication cycle and typically establish latency in sensory neurons. Beta- and gammaherpesviruses are slower to replicate and target lymphoid tissue for latency. By serological testing for herpesvirus antibodies, it has been demonstrated that all of the human herpesviruses are fairly ubiquitous in the adult population (Table 2).

Like most microbial infections, the severity and resolution of herpesvirus lytic infections are largely dependent on host immunity [reviewed in (58, 96, 210)]. The majority of healthy individuals resolve the acute infection without serious complications. Populations at risk for life-threatening disease are those with undeveloped or waning immunity—neonates, the elderly, and immunocompromised patients with AIDS or undergoing transplantation and chemotherapy. In

these individuals, recurrent and/or disseminated infections can lead to virus invasion of the central nervous system (CNS), resulting in lethal encephalitis or meningitis. HSV-1 and HSV-2 invasion of the CNS is rare; CNS disease results most often from infection with CMV, but also with VZV, EBV, and HHV6. Less lethal but important for the elderly population are recurrent ocular HSV-1 infections, leading to corneal obstruction and blindness, and chronic pain (neuralgia) after the acute infection of HSV-1, HSV-2, or VZV is cleared.

TABLE 2. Human Herpesviruses

Virus[A]	Common name	Sub-Family[B]	Prevalence (%)[C]	Acute/Recurrent Disease	Site of latency
HHV 1	Herpes simplex virus 1 (HSV-1)	α	65	Orofacial lesions, ocular stromal keratitis	Sensory ganglia
HHV 2	Herpes simplex virus 2 (HSV-2)	α	22-26	Genital lesions	Sensory ganglia
HHV 3	Varicella zoster virus (VZV)	α	>95	Chicken pox, shingles	Sensory ganglia
HHV 4	Epstein-Barr virus (EBV)	γ	>90	Mononucleosis, lymphoproliferative disease	Lymphocytes
HHV 5	Cytomegalovirus (CMV)	β	54-91[D]	Mononucleosis	CD4 T cells
HHV 6		β	>95	Roseola infantum	CD4 T cells
HHV 7		β	75-85	Roseola infantum	B cells
HHV 8	Kaposi's sarcoma herpes virus	γ	8	Kaposi's sarcoma, lymphoproliferative disease	Lymphocytes

[A] HHV, Human herpesvirus.
[B] α, β, and γ are abbreviations of *alphaherpesvirinae*, etc.
[C] Prevalence indicates the percentage of blood donors that tested positive for antisera specific to each virus. Statistics are from adults in the United States (age $\geq$ 30 years) in references (40, 101, 172, 200, 243).
[D] increases with age from 54 % at age 30 to 91 at age 80.

1.2 HSV-1 PATHOGENESIS

The progression of HSV-1 disease follows three stages—primary infection, latency, and reactivation—which have been described in detail (8, 182). HSV-1 infection begins with the transmission of virus particles to naïve mucosa or abraded skin that are in direct contact with infected mucosa. The primary infection can be asymptomatic or result in the appearance of skin lesions at the site of virus acquisition. The occurrence of symptoms is usually associated with higher viral burden and/or an immunocompromised state in the host. Disseminated primary infection is rare, but it can occur in neonates that acquire HSV-1 during delivery. In these cases, the spread of virus into the CNS can lead to encephalitis, serious neurological damage, and death. During initial replication in the mucosal epithelium, the virus is able to infect sensory neurons innervating the tissue. By retrograde movement along the axon, HSV-1 spreads into the neuron cell body, which is located in a mass of neuron cell bodies (trigeminal ganglion) at the base of the skull. When virus reaches the ganglion, an initial round of virus replication is followed by the cessation of productive infection. The virus enters a dormant or latent state within the infected neuron cell body. During latency, the viral genome is maintained as a circular, histone-associated episome, and viral gene expression is restricted to a small set of latency-associated transcripts (LATs) that are not translated into protein (45, 87, 91, 203). There is increasing evidence that host immune surveillance of the ganglion induces and maintains latency (62, 63, 95).

HSV-1 latent infection is maintained for the lifetime of the host and can periodically be reactivated to the lytic replicative cycle. Reactivation is associated with physical trauma, environmental stress, emotional stress, or other events that downregulate host immunity (41, 153, 185). Some individuals may never reactivate virus replication. In healthy individuals,

reactivations are transient events, but it is a prolonged state in immunocompromised patients. After reactivation of lytic gene expression, new virus particles are synthesized, and they travel anterograde down the neuron axons. The newly synthesized virus is released from the nerve endings into the mucosal epithelium, which results in virus shedding, and potentially the recurrence of lesions, at or near the primary site of infection. Recurrent HSV-1 infection produces lesions around the mouth and lips (herpes labialis) and is also increasingly associated with genital lesions. These symptoms are usually mild and clear within two weeks. Immunocompromised patients are at greater risk for severe lesions and disseminated infection causing more serious complications in the CNS or other organs. Other types of recurrent herpes infection include herpetic whitlow—lesions on the hands or fingers—and keratitis of the cornea. Repeated HSV-1 infection and immune infiltration of the cornea can eventually cause blindness.

At present, all of the antiviral pharmaceuticals that are available for the treatment of HSV-1 target the viral DNA replication machinery (13, 58, 210). Acyclovir (ACV) is an acyclic nucleoside analogue that terminates DNA replication when it is incorporated into newly replicated DNA. ACV is specifically phosphorylated by the viral thymidine kinase (TK), so it is only activated and incorporated into viral DNA in infected cells. However, ACV is a poor drug because it requires frequent dosage; the ACV derivatives famcyclovir and valacyclovir have greater efficacy. Frequently, in immunocompromised patients taking ACV regimens, the virus acquires ACV-resistance mutations that map to TK or the viral DNA polymerase (58). Foscarnet and cidofovir are two alternative drugs, but both are very cytotoxic. Foscarnet and cidofovir target the viral DNA polymerase at the pyrophosphate binding site and the nucleoside-binding site, respectively. Recent investigation of HSV-1 antivirals has identified potential new targets within the DNA replication machinery: the helicase-primase complex of the virus proteins UL5,

UL8, UL52; the ribonucleotide reductase kinase domain; and interaction domains of the DNA polymerase subunits UL30 and UL42 (13).

1.3 THE HSV-1 PARTICLE

The HSV-1 virion consists of a double-stranded DNA genome, nucleocapsid, tegument layer, and a glycoprotein-studded lipid envelope (Figure 1). The tegument is a distinctive feature of herpesviruses, and it is a collection of proteins—both viral and cellular—that fills the space between the envelope and the nucleocapsid (or "capsid"). A recent study used mass spectroscopy (MS) to define the polypeptide content of purified extracellular virions; each of the identified proteins was validated by cross-referencing previously published data or by Western blot analysis (112). The host-derived lipid envelope contains 13 viral glycoproteins, and the tegument contains 23 viral proteins, including the viral transactivator proteins ICP0, ICP4, and VP16. Additionally, the MS analysis identified 49 human cell-derived proteins in the tegument, which included the transcription initiation factor eIF4H and components of the cell cytoskeleton. The tegument is generally asymmetric but can be regularly ordered around the capsid vertices (73, 253).

The capsid is 125nm in diameter and conforms to icosahedral symmetry, such that it has 20 faces and 12 vertices (see Section 1.5 for a detailed description of capsid structure and formation). The 162 capsomers are arranged to produce a triangulation number (T) of 16. Most of the capsomers are formed by the major capsid protein, UL19 (VP5), which is assembled into 5- and 6-membered rings (pentons and hexons). Pentons and hexons form the vertices and faces of the shell, respectively. At one vertex of the capsid, the penton is replaced with the DNA

portal complex, which is a dodecamer ring of UL6 protein (143, 221). The minor capsid proteins UL38 (VP19c) and UL18 (VP23) form a heterotrimeric complex ("triplex") that enhances the connections between hexons and pentons. Each triplex contains, on average, 2 copies of VP23 and one copy of VP19c (145). Another minor capsid protein, UL35 (VP26), is located at the tips of hexons.

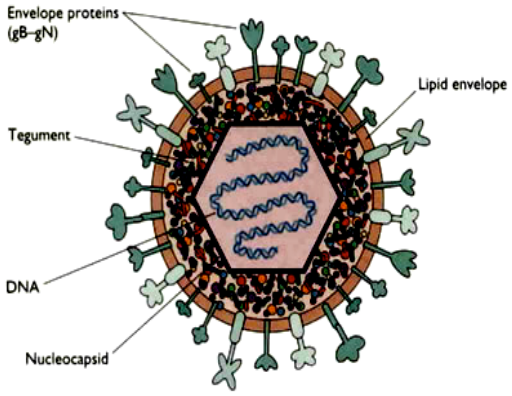

Figure 1. The HSV-1 virion. From Principles of Virology, 2nd ed. (59)

Enclosed within the capsid is the 152 kbp, double-stranded DNA genome, which is highly compressed and devoid of protein (16, 253). The genome consists of two segments of unique sequence—the unique long (U_L) and unique short (U_S) regions—that are flanked by repeat sequences (231) (Figure 2). Recombination between the terminal and internal repeat sequences generates four isomers in which the U_L and U_S segments are in different orientations with respect to each other; the isomers are found in equal proportion in infected cells and virions (75, 128). The long repeat, or *b* sequence, is approximately 10kbp, and it contains the coding sequences for the viral transactivators protein ICP0 and the latency-associated transcript (LAT). The short repeat, or *c* sequence, flanks the U_S segment and contains the ORF for the viral

transactivator protein ICP4 and an origin of replication (oriS). The *a* sequence is present in multiple copies at the U_L end of the genome, in one or more copies at the joint region between the long and short terminal repeats (*b* and *c* sequences), and in one copy at the U_S terminus (232). The *a* sequence contains short direct repeats (DR1, DR2, DR4) and unique sequences (Ub and Uc), which are organized in the following manner at the joint region: DR1-Ub-DR2-DR4-Uc-DR1 (Figure 2). At the ends of the genome, the *a* sequence is inverted with respect to the *a* sequence at the joint. The overall genome sequence can be represented as *a*-*b*-U_L-*b'*-*a'*-*c'*-U_S-*c*-*a*, in which the internal repeat sequences are in the inverse orientation to those at the genome termini.

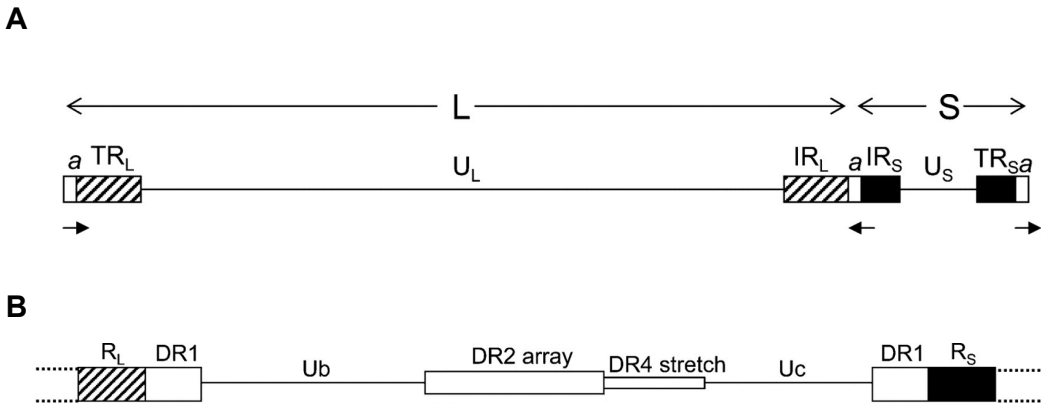

Figure 2. The HSV-1 genome and *a* sequence. A. Diagram of the HSV-1 genome, with the long (L) and short (S) genome segments marked. The orientation of the *a* sequence with respect to the unique regions is depicted as the black arrow. TR, terminal repeat. IR, internal repeat. B. Diagram of the *a* sequence in "inverted" orientation (DR1-Ub-DR2-DR4-Uc-DR1) at the junction between the long and short repeats (joint region of the genome). The *a* sequence contains three different direct repeats—DR1, DR2, and DR4—and two unique regions, Ub and Uc. This figure has been modified from reference (227).

1.4 OVERVIEW OF HSV-1 LYTIC INFECTION

The HSV-1 lytic replication cycle can be broken down into several major events that occur in different cellular compartments: virus attachment and entry at the plasma membrane; genome uncoating at the nuclear membrane; viral gene expression, DNA replication, and progeny capsid assembly in the nucleus; capsid egress from the nucleus to the cytoplasm; and finally, tegumentation, envelopment, and budding from the cell [reviewed in (182)]. The first stage of infection is the fusion of the virus with the host cell. Virus attachment and entry are mediated by viral glycoproteins in the virion envelope (23, 197). The initial attachment occurs via glycoprotein B and C (gB and gC) interaction with heparan sulfate (HS) on the cell membrane. gB and gC binding to HS are not absolutely required for viral entry, but they facilitate entry by concentrating virus particles at the cell surface. The viral glycoprotein D (gD) binds to one of three cell-surface entry receptors: nectin-1, HVEM, and modified HS. Receptor-bound gD then brings gB, gH, and gL into a fusion complex (9). Attachment at the cell surface also induces structural rearrangements in the tegument compartment (122). After the viral envelope fuses with the host cell plasma membrane, the envelope-associated viral glycoproteins are left at the cell surface (158) and the capsid plus tegument is released into the cytoplasm.

De-enveloped capsids are actively transported along microtubules from the cell periphery to the nucleus, where they release viral DNA (11, 113, 114, 149, 196). Incoming capsids colocalize with the microtubule motor dynein (52). It is unclear which of the capsid-associated proteins interacts with microtubules or motor proteins during viral entry. The small protein VP26 is not required for HSV-1 movement on microtubules, even though it was shown to interact with dynein (51, 57). The large tegument protein pUL36 is a likely candidate because it remains on incoming capsids and is required for their localization to the nuclear membrane (72,

113, 180). Copeland *et al* used antibodies to block several different capsid-associated proteins on incoming capsids; these experiments showed that pUL36—but not the tegument pUL37 or the capsid proteins pUL19 (VP5) and pUL18 (VP23)—was needed for docking the capsid at the nuclear pore (34). Depletion of the nucleoporins Nup214 and Nup358 inhibits binding of the capsid and delivery of viral genomes to the nucleus, and direct interaction between the capsid and Nup214 and Nup358 has also been demonstrated by immunoprecipitation and immunofluorescent localization assays (34, 156). Furthermore, the capsid-associated protein pUL25 interacts with Nup214, and pUL25 is required for release of the viral genome into the nucleus (4, 156, 169). Thus, it is likely that a complex of the nucleoporins Nup 358 and Nup214 form the capsid nuclear receptor, which binds to pUL36, pUL25, and/or other undefined capsid-associated proteins. Proteolysis of pUL36 and the DNA portal protein pUL6 may also be necessary for release of the viral genome into the nucleus (92, 133). When DNA is ejected, the U_S end of the genome exits the capsid first (136), so that the first viral gene exposed is ICP4.

Release of the HSV-1 genome into the nucleus initiates viral gene expression, which is a complex and tightly regulated process [reviewed in (173)]. Many HSV-1 genes are arranged with overlapping ORFs or with common initiation or termination sites (118). A temporal gene expression cascade segregates virus genes into 3 groups: immediate early (IE or α), early (E or β) and late (L or γ) (79, 80). Promoters that are specific to each group drive expression of the different gene classes. Generally, genes expressed at early times post infection have complex promoters with more regulatory elements than the promoters of genes expressed late in infection. The IE genes ICP0, ICP4, ICP22, ICP27, and ICP47 are the first genes transcribed, and their expression is dependent on the viral transactivator protein UL48 (VP16). UL48 is carried into the newly infected cell in the tegument compartment, and it binds to IE promoters. Thus, IE

genes are expressed in the newly infected cell without any viral protein synthesis. IE genes, in turn, serve as transactivators of the early and late genes. Most early genes are involved in DNA replication, while late genes are structural or virion proteins. Late genes fall into two sub-groups—γ1 (leaky late) and γ2—that have a relaxed or strict requirement, respectively, for DNA replication to occur before their expression.

The HSV-1 DNA replication machinery consists of the DNA polymerase (UL30 and UL42), single-stranded DNA binding protein ICP8 (UL29), helicase/primase (UL5, UL8, and UL52), and the origin-binding protein (UL9) (14). There are three origins of replication in the HSV-1 genome. One is in the unique long segment (oriL), and two copies of the other (oriS) are in the *c* sequences located at the internal repeat and short terminal repeat (204, 236). DNA replication produces a highly branched, intertwined concatemer that contains many copies of the HSV-1 genome connected through the terminal repeat sequences (46, 189, 190). The mechanism for DNA replication remains unclear. There is evidence that, similar to the dsDNA bacteriophages, HSV-1 utilizes a rolling-circle mechanism to produce a concatemer of head-to-tail linked genomes (14, 195, 207). However, the rolling-circle mechanism depends on circularization of the viral genome, and recent evidence suggests that the viral genome does not adopt the circular form during lytic infection (87). The concatemeric, branched replicative intermediate could also be synthesized by recombination of viral genomes during DNA replication (239). The viral alkaline nuclease, UL12, resolves the branched intermediate into its linear form (116, 163), which can be packaged subsequently into pre-assembled precursor capsids. Capsid assembly and the DNA packaging reaction are described in detail in Sections 1.5 and 1.6.

After completion of packaging, the DNA-filled progeny capsids exit the nucleus, and they acquire the tegument proteins and the virion envelope *en route* to the host cell plasma membrane. Capsids in the nucleus are transported along actin filaments (60), but they cannot access the nuclear membrane until the viral proteins UL31 and UL34 induce breakdown of the nuclear lamina, probably through protein kinase C recruitment and phosphorylation of lamin B (65, 155, 176, 193). Formation and localization of the UL31/UL34 complex is dependent on the viral kinase US3 (65, 125). Primary envelopment of capsids involves their budding through the nuclear membrane into a vesicle-like structure; the primary-enveloped capsid fuses to the outer leaflet of the nuclear membrane and is released into the cytoplasm (124, 125, 174). The primary envelope contains US3, UL31, UL34 and may also contain viral glycoproteins and tegument proteins (126). Conflicting reports have shown that the large tegument protein, pUL36, attaches to capsids in the nucleus (1, 22, 32, 106) or that pUL36 is cytoplasmic and not needed for capsid nuclear egress (44, 64, 129). Likewise, there is evidence for and against the addition of the tegument protein UL48 (VP16) to the capsid prior to its release to the cytoplasm (130, 154). Additional tegument proteins are added to the capsid in the cytoplasm. For secondary envelopment, capsids are recruited to the trans-Golgi network (TGN), where newly synthesized viral glycoproteins accumulate (225). During TGN envelopment, a double-layered lipid membrane is wrapped around the capsid. The outer portion of this double membrane acts as a vesicle that transports the virion to the cell surface; it fuses to the host cell plasma membrane when the virion exits the cell. The inner portion of the double membrane contains viral glycoproteins, and it becomes the envelope of the extracellular virion.

1.5 FORMATION AND MATURATION OF THE CAPSID

The function of the nucleocapsid is to protect and transport the viral genome. The HSV-1 capsid is an icosahedron with a triangulation number (T) of 16. Like other quasi-equivalent structures, the capsid is made of many subunits that are identical in peptide sequence but slightly different in structure and conformation; the flexibility of the subunits allows a single gene product to assemble into a large macromolecular complex (90). In the case of HSV-1, the major component of the capsid is the structural protein UL19 (VP5), a large protein of 1374 amino acids and molecular weight 149 kDa. VP5 is arranged into rings of five or six copies, which are visible by negative staining and electron microscopy of capsids (70, 145, 198, 202, 238). These capsomers are called hexons (6-mer rings) and pentons (5-mer rings), and they form the faces and the vertices of the capsid, respectively. Hexons and pentons are dissimilar not only in the copy number of VP5 but also in the conformation of VP5. VP5 in hexons and pentons have different exposed antibody epitopes, and the small capsid protein VP26 preferentially binds to hexons (17, 223, 241). A recent study of VP5 structure highlighted the differences in hexons and pentons (18). Bowman *et al* trypsin-digested VP5 and purified a 65 kDa fragment—the "upper" domain that faces the exterior of the capsid—that was used for x-ray crystallography. Folded VP5 is mostly α-helical and has charged faces, and it is the electrostatic interactions between these charged residues that likely hold the pentons and hexons together. Furthermore, these charged faces are arranged differently in pentons and hexons, so that hexons have a smaller inner channel that is positively charged, while pentons have a smaller channel of a less acidic nature (18). Hexons have also been segregated into three classes based on their distance from the penton vertex and the edge of the capsid face, but these hexon forms do not appear to have distinct structures (202).

Between the capsomers, a heterotrimeric complex—or "triplex"—fills in the capsid surface. Two copies of pUL18 (VP23) and one copy of pUL38 (VP19c) make up the triplex (145). VP19c and VP23 both interact with VP5, but since VP19c sits atop VP23, VP19c is probably more accessible to the upper domain of VP5, while VP23 interacts with the VP5 floor domain (184, 254). VP19c contains a nuclear localization signal (NLS) in amino acids 24-56 that localizes VP5 and VP23 to the nucleus (3, 179). Mutational analyses of the triplex proteins have identified regions that are important for the interactions between VP19c, VP23, and VP5 (150, 179, 199). The C-terminus (amino acids 450-465) and the region of VP19c around amino acid 100 appear to be required for its interactions with both VP23 and VP5, and additional contacts with VP23 may occur at VP19c amino acids 230-347. In VP23, mutations within several different regions (amino acids 22-67, 100-190, 206-239, 296-310) abrogated its interaction with VP19c.

At a single vertex of each capsid, the penton is substituted with a portal complex made of the DNA packaging protein UL6 (24, 26, 143). The portal has three putative functions: it is the docking site for the terminase complex (consisting of the DNA packaging proteins pUL15, pUL28, and pUL33), it is the passageway through which DNA enters and exits the capsid, and it is likely the foundation upon which the procapsid is built (138, 143, 237). The portal is made of twelve copies of pUL6 that are arranged into a barrel; the larger end of the barrel faces away from the interior of the capsid (24, 143, 221). The portal can be assembled in the absence of other viral proteins, but its cylindrical structure is deformed by mutations to a leucine zipper (LZ) motif in pUL6 (aa 409-473) (132, 143). Deletion of the LZ motif does not prevent pUL6 or pUL15 inclusion to capsids, indicating that the LZ region is important for pUL6 self-interaction but not for its interaction with scaffold or the DNA packaging machinery (132).

Capsid assembly is catalyzed by interaction of the portal with scaffold proteins (138, 144). The scaffold is composed of the viral proteins preVP22a (pUL26.5) and pUL26, which are both transcribed from the UL26 ORF (38, 110, 111). At the beginning of capsid assembly, a small region of the scaffold protein (amino acids 143-151) binds to and orients the portal so that its bulkier portion faces the exterior of the nascent capsid (24, 83, 194, 245). Following this initial event, capsomers and more scaffold proteins are added to the portal-scaffold complex. The scaffold forms multiple intramolecular contacts, and its C-terminus connects to the VP5 N-terminus (81, 82, 139, 167, 233). In this way, more scaffold and capsomers are added to the original "wedge" and continue extending it until the spherical precursor capsid—the procapsid—is completed (139-142, 144). The interior of the procapsid is thus filled with and supported by the scaffold. The triplexes are assembled separately and are added to the assembling procapsid shell (199).

As the precursor to the angularized capsid, the procapsid is porous, unstable, and requires several structural transformations to reach its mature form (220). Conversion of the procapsid to its angularized form is tightly coupled to the cleavage, disorganization, and removal of the scaffold (29, 36, 183). Within pUL26, there is an autocatalytic protease (VP24) that cleaves both scaffold proteins to form the processed scaffold, which consists of VP21 and VP22a (50, 108-110, 160, 170, 235). Scaffold is cleaved at its C-terminal end, near its connection to the capsid protein VP5 (50). Scaffold cleavage therefore physically separates the procapsid shell from the scaffold (256). These biochemical events are linked to global changes in capsid structure, which have been observed by cryo-electron microscopy and reconstruction of a temperature-sensitive protease mutant at different timepoints after procapsid assembly (76). These procapsids mature in "slow-motion" at the non-permissive temperature and allow collection of images at distinct

stages of maturation. The first major event in procapsid maturation is formation of the VP5 "floor" of connections between capsomers, accomplished by the rotation of VP5 in hexons. In both the pentons and hexons, conformational changes of VP5 close the central channels. Finally, the triplexes are re-ordered to reinforce the VP5 floor. After these transitions, VP5 in hexons and pentons are morphologically distinct in that they have different regions exposed to the capsid surface (223). These distinctions probably account for the preferential binding of the small capsid decoration protein VP26 to hexons (17, 222, 255).

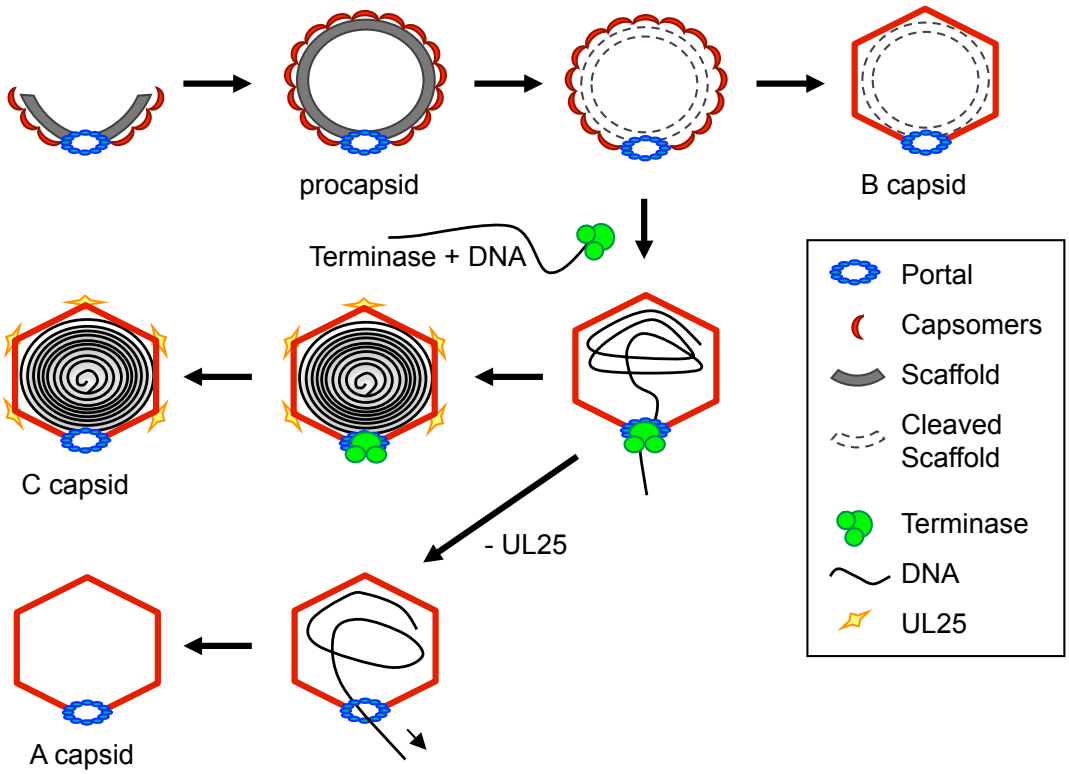

Figure 3. Precursor capsids mature into three different capsid forms. Unlike the spherical procapsid, all mature capsid types are angular, but they contain different materials in their interior. B-capsids are filled with the cleaved scaffold protein VP22a, and A-capsids are empty. Only C-capsids contain DNA and are incorporated into virions.

Maturation of the procapsid is an inefficient process; many of the capsids formed during productive infection are not assembled into virions. Three types of icosahedral capsids have been purified from the nuclei of wt HSV-1-infected cells, and they were designated based on their sedimentation through sucrose density gradients (70) (Figure 3). The most dense form, the C-capsid, contains tightly packed DNA (16, 70). C-capsids exit the nucleus and become incorporated into virions. A- and B- capsids are restricted to the nucleus; they are considered defunct by-products of the capsid maturation and DNA packaging reactions (16, 70, 139). Empty A-capsids have no inner core, and B-capsids contain the cleaved scaffold proteins VP21, VP22a, and VP24. Because DNA packaging is dependent on scaffold proteolysis and expulsion from the capsid (69, 117, 166, 170), A-capsids are thought to be the result of abortive packaging events, while B-capsids may form when DNA packaging is blocked but scaffold proteolysis proceeds normally.

1.6 THE HSV-1 DNA PACKAGING REACTION

1.6.1 Model from the dsDNA bacteriophages

Because HSV-1 shares an evolutionary lineage with the tailed dsDNA bacteriophages (10, 120), the pathway for packaging of the HSV-1 capsid is presumed to resemble that observed in phage [reviewed in (25, 66, 89)] (Figure 4). Generally, the machinery involved are a terminase enzyme—so named because it generates genome termini out of a DNA concatemer—and a portal that provides the gateway for DNA into the procapsid. The process of DNA encapsidation in bacteriophages begins when the terminase recognizes a packaging sequence at the ends of

genomes in the DNA concatemer. At or near this sequence, terminase makes a double-strand cut to free one end of the DNA. The terminase-DNA complex then docks onto the procapsid at the portal vertex. Terminase acts as a motor to propel the free DNA end into the capsid through the central channel of the portal. As DNA enters, the procapsid is transformed into its mature morphology. DNA is driven into the capsid by the terminase until it senses that a full genome has been packaged; this can be accomplished by a head-full mechanism (i.e. a certain length or amount of DNA packaged) or by a second packaging site at the end of the genome. Terminase cleaves the end of the genome to release it into the capsid. After the second DNA end has entered the capsid, head completion proteins close the portal and stabilize the capsid.

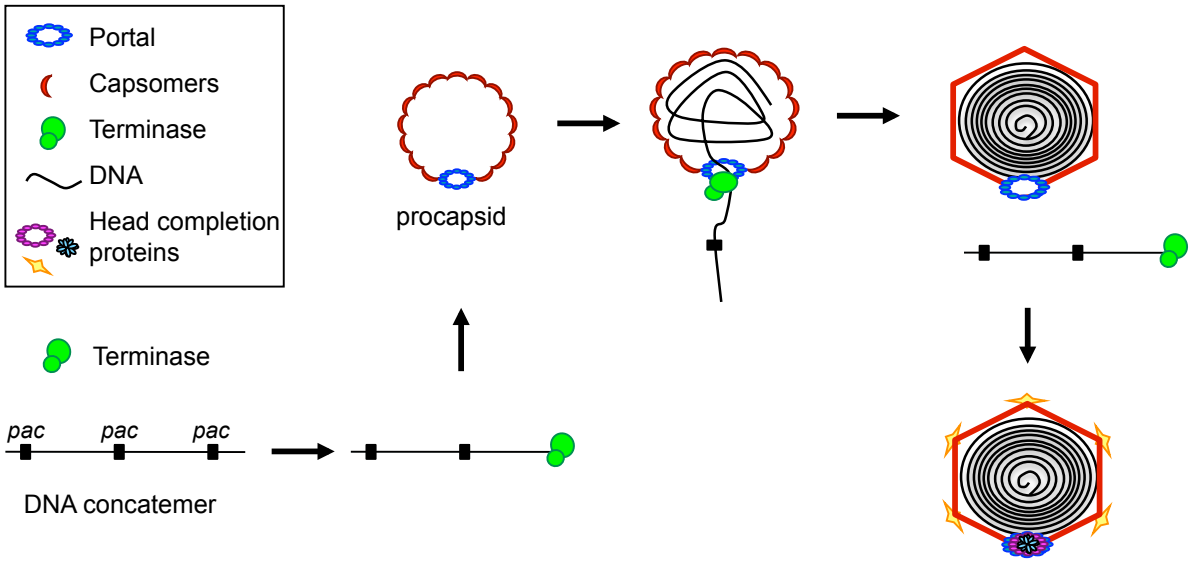

Figure 4. DNA packaging in the double-strand DNA bacteriophages. Modified from (25). Initiation of packaging occurs when the terminase complex recognizes packaging sequences (*pac*) in the concatemer of replicated genomes. The initial terminase cleavage frees an end of DNA. Terminase docks on the portal and propels DNA into the procapsid, which triggers procapsid expansion and angularization. Termination of packaging results in terminase cleavage of the end of the genome and dissociation from the filled capsid. Head completion proteins seal off the portal and reinforce the capsid.

In bacteriophage, the terminase complex is composed of multiple subunits that together provide the site-specificity for DNA cleavage and the force required to drive DNA into the capsid, by hydrolysis of ATP. In the *E. coli* bacteriophage λ, the terminase is a trimer of two copies of the small subunit gpNu1 and one copy of the large subunit gpA (115). gpNu1 binds to the DNA packaging signal and recruits gpA into the complex. The gpA subunit contains both endonuclease and ATPase domains that are responsible for the energy-dependent cleavage and translocation of DNA into the procapsid. A similar division of labor—site-specificity directed by the small subunit, DNA cleavage and ATP hydrolysis carried out by the large subunit—has been observed in the terminases of phages T4, P22, and SPP1 (25). Association of the terminase with packaging sequences may require host factors that bend DNA into an appropriate conformation for terminase binding, as is the case for the λ terminase small subunit gpNuI and the *E. coli* host factors IHF and HU (152, 209). In all cases, the initial cleavage requires the recognition of specific packaging signals, for example, the *cos* sequence of λ phage and the *pac* sites of phages T4, P22, and SPP1 (25).

For completion of bacteriophage DNA packaging, three events are required: 1) addition of accessory proteins to the capsid exterior to stabilize it against the increasing internal pressure of packaged DNA; 2) cleavage of DNA at the next packaging signal to release a free genome into the capsid; and 3) addition of head completion proteins that block off the portal to prevent DNA release. When the packaging reaction is nearly complete, structural proteins that reinforce the capsid are added to maintain capsid integrity, and thus, to allow terminase to package the full-length genome. The T4 phage protein Soc is one such protein; it is present in a homotrimeric complex between T4 capsomers (85, 86, 201). The λ phage gpD protein also decorates the capsid surface, and it is only added to the expanded capsid after the initiation of

DNA packaging (84). In the absence of gpD, capsids are unable to retain viral DNA, and many empty expanded capsids are produced (244). However, truncated DNA substrates lacking the final 15-20% of the viral genome can be successfully packaged in the absence of gpD (249). Although gpD is a structural protein, these data indicate that gpD is required for the second cleavage reaction, inasmuch as the terminase requires the structural stability gpD provides to the capsid in order to reach the second cleavage site. The second genome cleavage can occur at a specific DNA sequence, or terminase can cleave after it senses that a specific amount of DNA has been packaged, i.e. the head-full mechanism. Most phages employ the head-full mechanism, with the exception being λ, which terminates packaging at a second *cos* sequence.

Head completion proteins attach to the capsid portal to prevent DNA expulsion from the mature capsid and to build a connector complex that is the foundation for the phage tail fiber. The connectors typically consist of two or more proteins that attach in multiple copies to the portal. Some examples include gpW and gpFII from λ phage (161) and gp4, gp10, and gp26 from phage P22 (208). In the phage SPP1, which infects *Bacillus subtilis*, the structure of the connector has been resolved (107, 151). The SPP1 head completion proteins gp15 and gp16 form dodecamer rings that sit on top of the portal. These rings are connected to each other and to the portal via interaction between charged faces of the multimer rings (107). When bound to the connector, the portal protein gp6 has a different conformation than when unbound, suggesting that completion of DNA packaging triggers changes in gp6 structure that promote connector attachment. gp16 is the "stopper" that blocks the opening at end of the connector. gp15 and gp16 null mutants produce unit-length genomes that are not encapsidated; these mutants also produce empty, expanded capsids (151).

1.6.2 HSV-1 packaging signals

The HSV-1 genome ends are defined by the presence of the *a* sequence, which contains the signals for cleavage and packaging of DNA (43, 206). Adjacent genomes in the replicated concatemer share overlapping *a* sequences that are joined by the common DR1 element; cleavage between genomes occurs in this DR1 (131, 227) (Figure 5). In the *a* sequence, the minimal packaging signals are located within the 200bp fragment containing Uc-DR1-Uc (42, 78). Genome termini are made by two different cleavage events (229). Accordingly, there are two packaging signal sequences, pac1 and pac2, which are located in the Ub and Uc portions of the *a* sequence, respectively (131). While pac2 is required for the initial cleavage of DNA from the concatemer, pac1 is important for the secondary cleavage at the termination of packaging (78, 219). The cleavage site is not sequence-specific but is instead located at a set distance from the packaging signals (229). Thus, deletions within pac1 or pac2 are more detrimental to packaging than substitution mutations (78, 219). Both pac1 and pac2 have structural elements—GC-rich elements and T tracts—that are important for DNA packaging (Figure 5). Taken together, the spacing requirement between the packaging signal and the cleavage site, along with the inhibitory effects of substitutions in the GC and T tracts, has prompted the hypothesis that these DNA elements are modeled into secondary structures that are recognized by the packaging machinery (5, 242).

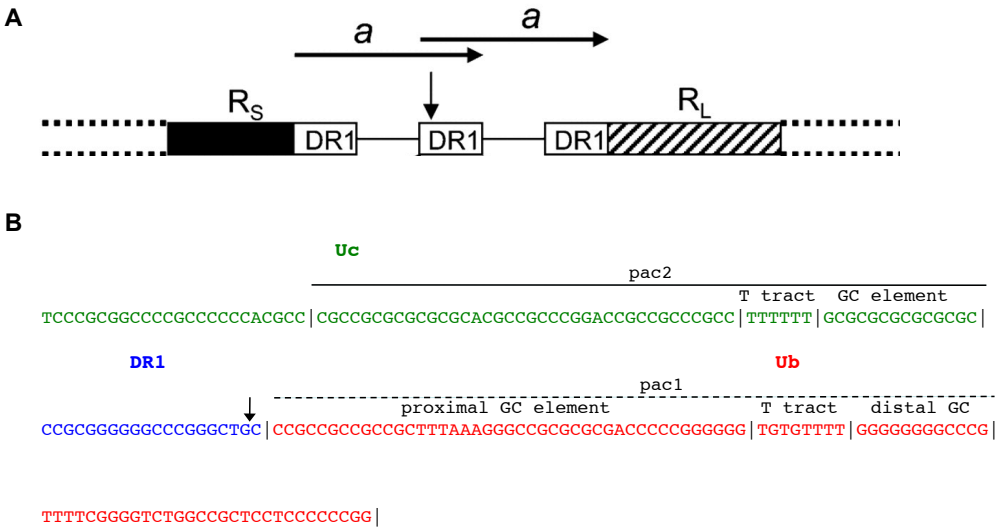

Figure 5. The *a* sequence mediates HSV-1 DNA cleavage and packaging. A. Genomes in the DNA concatemer are punctuated by overlapping copies of the *a* sequence between the short terminal repeat (R_S) and the long terminal repeat (R_L). Cleavage (black arrow) occurs in the direct repeat (DR1) shared by adjacent *a* sequences, leaving a single copy of the *a* sequence at the U_S terminus and multiple copies on the U_L terminus. Modified from (227). B. Diagram of the Uc-DR-Ub junction between adjacent *a* sequences. The sequences are colored green (Uc), blue (DR1), and red (Ub). The pac2 is marked with a solid line, and pac1 is marked with a dashed line. Structural features within each pac site are noted. The cleavage site in DR1 is shown (black arrow). Modified from (219).

1.6.3 HSV-1 DNA packaging machinery

The HSV-1 packaging genes have been identified as UL6, UL15, UL17, UL25, UL28, UL32, and UL33 (6, 103, 104, 121, 186, 214). These genes are essential for virus replication and are members of a set of core genes that are conserved across herpesvirus subfamilies (120). Null mutations of the UL6, UL15, UL17, UL32, and UL33 genes completely eliminate DNA cleavage and packaging, such that the DNA concatemer is unresolved and only B-capsids are formed (103, 157, 175, 186, 214, 250). The observed phenotype suggests that these gene products catalyze the initial stages of packaging including terminase assembly, the initial cleavage of the concatemer, and relocation of terminase to the DNA portal. In contrast, the packaging gene UL25 seems to have a unique role in packaging. The UL25 null mutant accumulates free,

approximately genome-length DNA and almost equal amounts of A- and B-capsids (121, 205). It has been inferred from the A-capsid phenotype that UL25 is required for completion of packaging or retention of DNA in the capsid rather than initiation of packaging. The packaging machinery is localized to intranuclear centers of viral replication, which are characterized by the presence of the HSV-1 single-stranded DNA binding protein UL29 (ICP8). These replication compartments, or assemblons, are distinct areas within the nucleus where capsids and packaging proteins accumulate (179). Both UL17 and UL32 have been implicated in the localization of capsids to assemblons (103, 211). The packaging proteins UL6 and UL25 are imported into cell nuclei independently of terminase, although UL25 nuclear localization requires expression of the triplex protein UL38 (VP19c) (148, 247).

The putative HSV-1 terminase complex consists of three subunit proteins: UL15, UL28, and UL33. The assignment of HSV-1 proteins to the terminase complex has been due to a) their functional and sequence similarity to terminase subunits in bacteriophage (25, 127, 171), and b) the mapping of resistance mutations to DNA cleavage and packaging inhibitors to the CMV homologues of UL15 and UL28 (100, 146, 228). The ATP-binding motifs Walker box A (PRRHGKT, aa 259-265) and Walker box B (LLFVDE, aa 352-357) have been identified in UL15, and they are common to the terminases of other herpesviruses and many bacteriophages (127). The importance of the ATPase domain of UL15 was demonstrated by the G263A mutation in Walker box A, which abrogated DNA cleavage and packaging as well as viral replication (171, 251). In addition to the ATPase domains, UL15 shares >70% sequence homology with bacteriophage terminases in at least 10 different regions of the protein (171). Thus, UL15 is presumed to be the motor that hydrolyzes ATP and drives DNA into the capsid. In UL28 protein, a highly conserved zinc finger motif is located between amino acids 197 and 225

(100). Because UL28 and its homologues in CMV have been shown to bind to packaging signals (5, 15), UL28 is the proposed terminase endonuclease subunit, which carries out the cleavage of viral DNA. Because the U_L end of the genome is preferentially packaged first (46, 136), UL28 also must distinguish between the pac2 and pac1 packaging signals, which initiate and terminate packaging, respectively. UL33 is not known to have any enzymatic activity, but it may regulate the activity of the other terminase subunits. Transposon insertions within two highly conserved regions of UL33—aa 46-77 and 101-130—inhibit the ability of UL33 to complement the UL33 null virus, indicating that these regions are important for UL33 function (12). In order to insert DNA into the procapsid, terminase must dock on the capsid portal after the initial cleavage of DNA at the U_L terminus. UL15 is the most likely candidate for terminase-portal attachment because UL15 co-immunoprecipitates with the portal protein UL6 (247). Terminase proteins are not found in intact virions (112). Thus, after DNA is translocated, terminase dissociates from the capsid surface, and this dissociation may require proteolysis of UL15 (187, 240, 252).

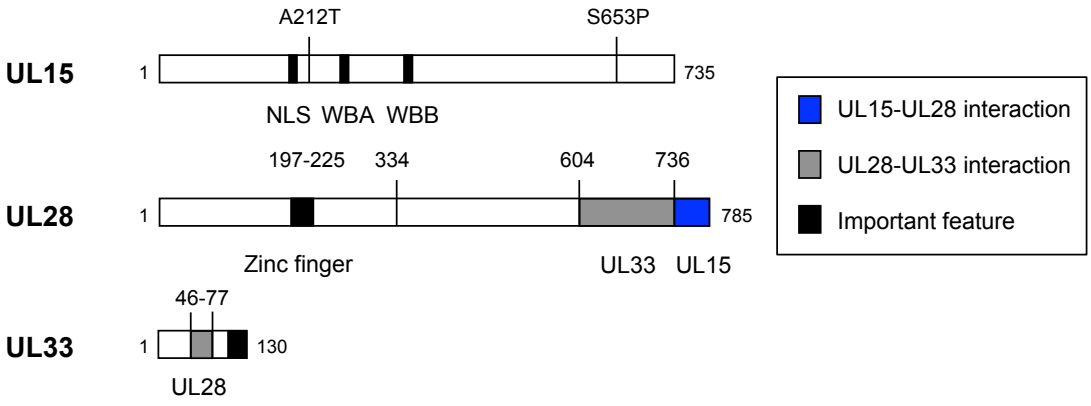

Figure 6. Features of the terminase subunit proteins UL15, UL28, and UL33. UL15 contains a nuclear localization signal (NLS) that mediates terminase complex import to the nucleus. UL15 also contains two potential ATPase domains in the form of Walker box A and B (WBA, WBB) motifs. UL28 has a zinc finger motif that may allow it to bind to DNA. Interaction domains between UL15, UL28, and UL33 have also been mapped.

Co-immunoprecipitation studies with UL15, UL28, and UL33 mutants have illuminated regions of these proteins that are important for terminase assembly (Figure 6). In the assembled complex, the largest subunit UL28 hinges UL15 and UL33, which do not contact each other (246). Single amino acid substitutions at aa 653 of UL15 or aa 61 of UL33 disrupt their binding to UL28 (162, 248). It has also been demonstrated that small insertions (5 aa) in aa 46-77 of UL33 inhibits co-immunoprecipitation of UL28, so this region likely represents an interaction domain with UL28 (12). Within the UL28 protein, UL33 and UL15 binding domains have been mapped to aa 604-736 and 736-785, respectively (2, 88). There is evidence of additional contact between UL28 and UL15 at aa 334 and 212, respectively, as the UL15 A212T mutation complements the UL28 linker insertion mutation 334i (88). These interactions likely drive assembly of terminase in the cytoplasm of infected cells, and subsequently, the nuclear localization signal located in aa 183-189 of UL15 directs nuclear import of the complex (88, 99, 247). After import to the nucleus, UL15 is required to localize the complex to replication compartments (77). However, when individually expressed, UL15 retains a diffuse nuclear staining pattern (251), suggesting that inclusion of the terminase into replication compartments requires other viral proteins.

1.7 COMPLETION OF PACKAGING AND BEYOND: ADDITION OF THE CAPSID-STABILIZING PROTEIN PUL25

Completion of DNA packaging is dependent on expression of the essential gene UL25. The UL25 ORF occupies bp 48813-50553 of the 152kbp HSV-1 genome (118). By genome sequence analyses, UL25 gene homologues have been identified in each of the eight human

herpesviruses: HSV-2 (55), VZV (37), EBV (53), CMV (54), human herpesvirus 6 (56), human herpesvirus 7 (123), and KSHV (177) (see Table 3). The estimated similarity between the UL25 gene products of HSV-1 and the other human alphaherpesviruses HSV-2 and varicella-zoster virus are 93% and 64%, respectively, while the sequence similarity of HSV-1 UL25 to UL25 proteins in the human beta- and gammaherpesviruses drops to 40% (19). UL25 is conserved in members of the alphaherpesvirus family that infect other animals, such as pseudorabies virus (PrV) (49), herpes B virus (159), equine herpesvirus 1 (EHV-1) (213), and bovine herpesvirus 1 (BHV-1) (47, 74). Altogether, 40 UL25 homologues have been identified and catalogued (NCBI Entrez Gene database). The conservation of UL25 across virus families in humans and other animals is illustrative of its core function in herpesvirus replication.

TABLE 3. UL25 Homologues

Virus	UL25 homologue
Herpes simplex virus 1	UL25
Herpes simplex virus 2	UL25
Varicella-zoster virus	Orf 34
Epstein-Barr virus	BVRF1
Human cytomegalovirus	UL77
Human herpesvirus 6	U14
Human herpesvirus 7	U14
Kaposi's sarcoma herpes virus	Orf 19

The UL25 gene is predicted to encode a protein of 580 amino acids with a molecular weight of 62 kDa (118). In the initial characterization of the UL25 gene product, the genome fragment containing UL25 was sub-cloned into an expression vector, which was transfected into cultured cells. Lysates from transfected cells and cells infected with HSV-1 and HSV-2 were analyzed by Western blot with an antibody raised against a GST-fusion containing the predicted

C-terminus of UL25 protein (pUL25). A specific band running at 60 kDa reacted with the pUL25 antibody in all three cases. This peptide could be detected in purified extracellular virions and could be immunoprecipitated from HSV-1 or HSV-2 infected cells (7). Thus, pUL25 does not appear to have post-translational modifications that significantly alter the molecular weight predicted from the coding sequence. The temporal range of pUL25 expression occurs between 2-20 hours post-infection and peaks at 9-12 hours (7, 121). pUL25 expression is partially blocked by the addition of phosphonoacetic acid, an inhibitor of viral DNA replication (7). Because expression of pUL25 is somewhat dependent on DNA synthesis, it is classified as a γ1 or leaky late HSV-1 protein.

UL25 null mutant viruses exhibit a variety of phenotypes that distinguish them from wt virus and from other packaging gene mutants. Similar to the other packaging genes, UL25 is essential to viral replication, and the null mutant produces many B-capsids. Unlike the other packaging mutants, the UL25 null mutant also accumulates a large number of empty A-capsids in infected cell nuclei (30, 121). In this aspect, the UL25 null phenotype is identical to the bacteriophage SPP1 mutants gp15- and gp16-; gp15 and gp16 act as head completion proteins that seal off the portal after DNA is packaged (151). Due to the similarity in phenotype, pUL25 is presumed to be the equivalent of a head completion protein that is required for the completion but not the initiation of packaging. The UL25 homologue in BHV-1 is similarly required for completion of packaging, while in PrV, UL25 does not appear to be needed for formation of C-capsids (48, 102). Secondly, the UL25 null mutant produces near-to-full-length viral genomes that are (a) sensitive to DNase digestion and (b) missing, or are significantly reduced in, the U_S genome terminus (30, 121, 205). These data suggest that in the absence of UL25, the packaging machinery can process viral DNA from the concatemer, but the DNA is not stably packaged into

capsids. Furthermore, these observations suggest that UL25 null mutations impair the second terminase cleavage at the U_S terminus, but not the first cleavage event at the U_L terminus. This phenotype is similar to that observed for the λ phage gpD mutant (249). Lastly, several UL25 mutations can also impair capsid trafficking and genome uncoating (4, 98, 147, 169). These deleterious effects occur after successful DNA packaging and effect cell-to-cell spread of virus.

As demonstrated by multiple studies in which capsids containing pUL25 were immunogold-labeled, pUL25 is incorporated into the exterior surface of capsids at their vertices (33, 121, 137, 148, 192, 216, 224). At the capsid vertex, pUL25 is a member of a proposed heterodimer with pUL17 (224). This heterodimer—termed the C-capsid specific component, or CCSC—was observed by cryo-electron microscopy; it is present on wt but not UL25-null capsids. The assignment of pUL17 to the heterodimer was based on the observation that pUL17 is necessary for the attachment of pUL25 to capsids (216). Densitometric analyses of Western blots showed that in the absence of pUL17, the amount of pUL25 associated with the capsid dropped to 10% of wt (216). Conversely, pUL17 occupancy was only reduced by 50% in the UL25-null mutant. These data indicate that pUL17 attaches to the capsid prior to pUL25, but the addition of pUL25 stabilizes the CCSC. pUL25 attachment to the capsid surface is most likely influenced also by its interactions with the capsid proteins pUL19 (VP5) and pUL38 (VP19c), which have been demonstrated by co-immunoprecipitation of these proteins with pUL25 from infected cells and by far-Western assays in which pUL25 was attached to a membrane containing immobilized pUL19 and pUL38 (148, 188). pUL25 may also bind the portal protein, pUL6 (156). Pasdeloup *et al*. demonstrated that transiently co-expressed pUL6 and pUL25 could be co-immunoprecipitated, but they could not determine if pUL6 was in monomers or in its ring structure as the assembled portal. This result prompted the suggestion that pUL25 has a second

site of attachment near the portal. At the portal, pUL25 may adopt a different conformation or different interaction partners, as the dodecameric portal is structurally distinct from the pentons containing five-mer rings of VP5. To date, there is no indication in capsid reconstructions that pUL25 associates with the portal. However, the reconstructions are limited by the imposition of icosahedral symmetry, which conceals the unique portal vertex, and it is also possible that pUL25 at the portal could dissociate from capsids during their preparation for cryo-electron microscopy.

Capsid-associated pUL25 has several functions. Most importantly, pUL25 provides structural reinforcement for the capsid (183). Because pUL25 occupancy on the capsid surface increases during maturation of the capsid from procapsid to the C-capsid (137, 192), pUL25 addition to the capsid is probably used to counteract the increasing internal pressure of packaged DNA, but it could also be an indirect signal to the terminase that DNA packaging should be completed. If pUL25 is present at the DNA portal, it could also be used to seal off the portal, in the manner of a bacteriophage head completion protein. After packaging, pUL25 is required for the egress of capsids from the nucleus (98, 102, 147). It has been estimated that more pUL25 is in the virion (239 copies) than in intranuclear C-capsids (178 copies), suggesting that a threshold amount of pUL25 on the capsid is a requirement for nuclear egress (217, 224). pUL25 initiates tegumentation of the cytoplasmic capsid via its interaction with the large tegument protein, pUL36 (VP1/2) (32, 156). The pUL25-pUL36 interaction organizes tegument around capsid vertices (253). pUL36 has two independent pUL25-binding domains located at pUL36 aa 2037-2353 and 3104-3164 (156). Finally, capsid-associated pUL25 has roles in virus entry. In PrV, pUL25 associates with microtubules in the absence of other viral proteins (93), but in the context of HSV-1 infection, this association is probably mediated by pUL36, which is known to interact

with microtubules during capsid transport (191). A temperature-sensitive mutation that maps to pUL25 aa 233 causes incoming capsids to aggregate at the nuclear periphery and prevents release of viral DNA into the nucleus (169). In reciprocal co-immunoprecipitation experiments, transiently-expressed pUL25 was shown to pull down the nucleoporins CAN/Nup214 and hCG1; this interaction was supported by pUL25 interaction with nucleoporins in a yeast-2-hybrid assay (156). pUL25 interaction with the nuclear pore would complement that of pUL36, which binds to the nucleoporin Nup358 (34). Thus, pUL25 helps to dock the incoming capsid at the nuclear pore prior to uncoating of the viral genome.

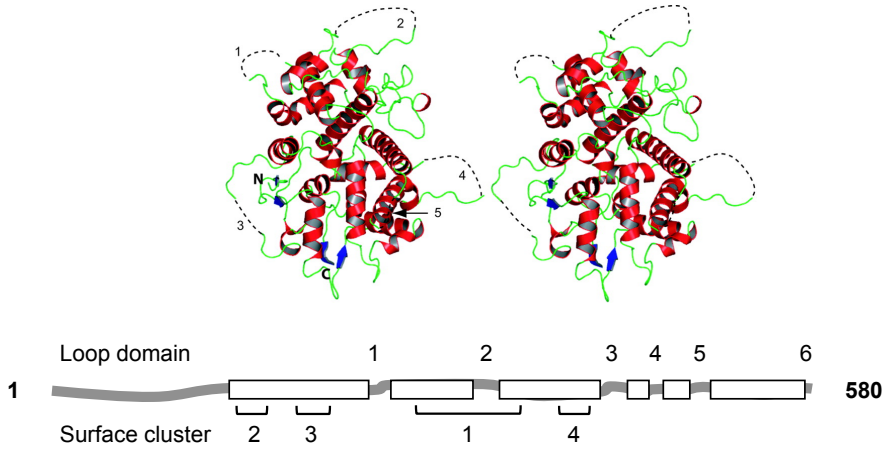

Figure 7. pUL25 structure. (Top) UL25 protein secondary structure was determined by x-ray crystallography (19). Flexible loops are shown as dashed lines. (Bottom) Diagram of linear UL25 protein. White boxes are regions of the protein that form the folded core. The gray line represents unstructured regions. Loop domains and surface clusters identified by Bowman *et al* (19) are indicated. The regions marked as surface clusters are not contiguous sets of residues, but instead represent the general area of each cluster. The specific residues in each cluster are noted in Table 4.

The structure of a truncated version of pUL25 has been determined by x-ray crystallography (19). During protein expression and crystallization, pUL25 was proteolytically cleaved between aa 116 and 130, with subsequent analysis finding that the first ordered residue was aa 134. Thus, the structural prediction effectively includes pUL25 aa 134-580. Bowman *et*

al. described the structure of folded pUL25 as a core of packed α-helices with an overall unique α plus β folding pattern that has not been previously observed (Figure 7) (19). Six unstructured loops and a long flexible N-terminus extend from the pUL25 core, and based on the charge distribution of the surface residues, pUL25 has two polar faces, one positively charged and one negatively charged. Comparison of 38 pUL25 homologues revealed four evolutionarily conserved clusters of residues on the protein surface. The location of these structural features in the pUL25 sequence are listed in Table 4 and illustrated in Figure 7.

TABLE 4. Mutational analysis of pUL25 structural features.[A]

			Phenotype		
Structure	**Amino Acid Sequence**	**Mutation**	**Virus replication**	**DNA Packaging**	**Capsid egress**
Loop domain 1	249-AADDSD-254	Δ249-254	+	n.d.	n.d.
2	335-RDASTHVNPDG-345	Δ335-345	+	n.d.	n.d.
3	417-PSEAIARGA-425	Δ417-425	-	+	-
4	479-PVGST-483	Δ479-483	+	n.d.	n.d.
5	511-RTN-513	Δ511-513	-	-	n.d.
6	578-SAV-580	Δ578-580	-	+	+
Surface cluster 1	G225, R288, R305, P327, G331, H348, R362, G363, N365	n.d.	n.d.	n.d.	n.d.
2	R148, D150, N152, D156, L214, N508	n.d.	n.d.	n.d.	n.d.
3	G169, S170, G172, R180, G202, R203, K206, P413	G169A, S170A, G172A, G202V, R203A, K206A	-	-	n.d.
4	R390, N396, Y398, D400, L402, R552	N396A, Y398A, D400A, L402A	-	+	-

[A]Adapted from (147). n.d. not determined. +, no effect. -, inhibitory effect.

The surface cluster and loop domains are the most accessible regions of pUL25 and are predicted to be the sites of pUL25 interaction with other proteins. Recently, mutational analysis of pUL25 tested the importance of the unstructured loop domains and conserved surface clusters

for virus replication, DNA packaging, and capsid trafficking (147). With UL25 supplied in *trans* from a plasmid vector, the mutations deleted each of the loop domains and substituted point mutations at each of the surface cluster residues of pUL25. Mutant UL25 plasmids were transfected into cells that were subsequently infected with the UL25-null virus. Several different mutant phenotypes were generated, as summarized in Table 4. Interestingly, three of the loop domains (1, 2, and 4) could be removed without deleterious effects on virus replication. Loop domain 5 and surface cluster 3 mutants were defective in DNA packaging, while mutants of loop domains 3 and 6 and surface cluster 4 successfully packaged viral DNA. Ultrastructural analysis of the latter three mutants showed that two produced C-capsids that were sequestered to the nucleus (loop domain 3 and surface cluster 4), and one (loop domain 6) produced extracellular virions that were not infectious. These results led the authors to conclude that residues 417-425 and 396-402 were important for capsid nuclear egress, while aa 578-580 were involved in entry of the capsid to the newly infected cell.

In studies of herpesviral protein interactomes by yeast-2-hybrid screens, pUL25 homologues in VZV and KSHV were found to interact with the orthologues to HSV-1 pUL15 and pUL31—proteins that are implicated in the terminase complex and in capsid nuclear egress, respectively (61, 94, 97, 124, 226, 251). Although pUL25 interaction with pUL15 and pUL31 have not been tested directly, it could be hypothesized that the DNA packaging and capsid egress null phenotypes generated by O'Hara *et al*. affected pUL25 interaction with one or both of these proteins. A summary of the predicted interactions of pUL25 with other viral and cellular proteins is presented in Table 5.

In sum, UL25 is involved in a diverse array of events in the virus replication cycle, beginning with DNA packaging and including capsid nuclear egress, tegumentation, and

uncoating of the genome from the capsid in the newly infected cell. These features are all intrinsically linked to the unique structure of pUL25—which allows it to participate in dynamic interactions with different binding partners—and pUL25 attachment to the capsid surface, which provides access to those binding partners.

TABLE 5. Summary of predicted pUL25 interactions with viral and cellular proteins.

Predicted binding partner	Function	Confirmation of interaction	References
pUL6	Capsid portal	IP[A]	(156)
pUL15	Terminase complex	No	(226)
pUL17	DNA packaging	IP	(188, 216, 224)
pUL19	Major capsid protein (VP5)	IP; far-Western assay	(148, 188)
pUL31	Capsid nuclear egress	No	(226)
pUL35	Small capsid protein (VP26)	No	(105)
pUL36	Large tegument (VP1/2)	IF[B]	(32, 156, 226)
pUL38	Triplex protein (VP19c)	IP; far-Western assay	(148, 188)
CANCt/hCG1	Nucleoporin	IP	(156)

[A] IP, Immunoprecipitation
[B] IF, co-localization by immunofluorescence

1.8 SPECIFIC AIMS AND RATIONALE

The goal of this project is to elucidate the biological functions of UL25 protein through (a) analysis of its interactions with the HSV-1 capsid and (b) determination of the importance of

pUL25 capsid-attachment for DNA packaging. To address these goals, the specific aims focused on the protein-protein interactions that drive pUL25 incorporation to the capsid, the effects of UL25 mutations on HSV-1 genome retention in the capsid, and the effects of UL25 mutations on genome cleavage. These studies explain the role of UL25 in the HSV-1 DNA packaging reaction and generally improve our knowledge of herpesvirus virion assembly.

1.8.1 Specific aim I: To map the pUL25 capsid-binding domain.

UL25 protein is added to the capsid exterior during the DNA packaging reaction. It has been postulated that accumulation of UL25 stabilizes the capsid and promotes completion of DNA packaging. In this aim, the UL25 capsid-binding domain(s) were identified by mutational analysis of UL25. To address the importance of UL25 capsid attachment, UL25 null mutants were examined for changes in DNA packaging phenotype. These studies defined functional domains of pUL25 that are important for capsid binding and DNA packaging.

1.8.2 Specific aim II: To identify UL25 protein interactions by structural analyses

UL25 protein is predicted to contact multiple proteins on the capsid surface. To identify these connections, capsid-associated pUL25 was visualized by cryo-electron microscopy and 3D image reconstruction of capsids. pUL25-fusion proteins were used to add extra density to the capsid surface and to facilitate prediction of pUL25 location(s).

1.8.3 Specific aim III: To investigate the potential role of UL25 in stabilizing secondary DNA cleavage or in direct DNA-binding.

Equimolar amounts of both long and short genome termini (TR_L and TR_S) are produced by DNA cleavage and packaging during wild-type HSV-1 infection. TR_S has been reported to be truncated or missing in the UL25 null virus. We characterized the effect of UL25 mutations on the cleavage of viral genome termini. Additionally, purified UL25 protein has been bound to HSV-1 DNA immobilized on a membrane (148), but is not known if this observation reflects a similar phenomenon in HSV-1-infected cells. In this study, pUL25 was purified from infected cells and used for an *in vitro* DNA-binding assay.

2.0 UL25 PROTEIN ATTACHES TO CAPSIDS THROUGH A SMALL N-TERMINAL DOMAIN

2.1 ABSTRACT

The herpes simplex virus type 1 (HSV-1) UL25 protein (pUL25) attaches to the external vertices of capsids and is required for the stable packaging of viral DNA. To define regions of the protein important for viral replication and capsid attachment, the 580 amino acid (aa) UL25 open reading frame was disrupted by transposon mutagenesis. The UL25 mutants were assayed for complementation of a UL25 deletion virus, and *in vitro*-synthesized protein was tested for binding to UL25-deficient capsids. Of the 11 mutants analyzed, 4 did not complement growth of the UL25 deletion mutant, and analysis of these and additional mutants in the capsid-binding assay demonstrated that UL25 aa 1 to 50 were sufficient for capsid binding. Several UL25 mutations were transferred into recombinant viruses to analyze the effect of the mutations on pUL25 capsid binding and on DNA cleavage and packaging. Studies of these mutants demonstrated that aa 1 to 50 of UL25 are essential for its stable interaction with capsids. A short region of the putative capsid-binding domain (aa 26-39) is highly conserved throughout the alphaherpesviruses. To investigate the importance of these residues for pUL25 capsid-

attachment and DNA packaging, recombinant viruses were generated that expressed pUL25 with point mutations and small deletions in the highly conserved region. With the exception of the deletion of aa 40-50, deletions within the N-terminus of pUL25 prevented viral replication and DNA packaging. The paired point mutations F26A I27A and F35A W36A partially supported viral replication and DNA packaging but did not allow cell-to-cell spread of virus. Immunoblotting of purified capsids determined that pUL25 amino acids 1-36 were required for capsid attachment, and amino acids 37-50 were dispensable for capsid attachment but not for virus replication. To account for the possibility that N-terminal truncations prevented nuclear import of pUL25, indirect immunofluorescence assay was used to observe pUL25 protein in Vero cells infected with the N-terminal truncation mutant, vΔ1-50. The Δ1-50 protein was present in infected nuclei, indicating that deletion of the capsid-binding domain did not mislocalize pUL25. Taken together, these data suggest that pUL25 attaches to capsids with a small N-terminal domain and that capsid attachment is required but not sufficient for completion of the DNA packaging reaction.

2.2 INTRODUCTION

The herpes simplex virus type 1 (HSV-1) virion consists of a 152 kbp double-stranded DNA genome, an icosahedral capsid (T=16), an amorphous protein layer called the tegument, and a lipid envelope containing viral glycoproteins. The HSV-1 genome contains several kbp of repeat sequences that flank and separate the unique long (U_L) and unique short (U_S) regions, which contain most of the ORFs for viral genes. Viral DNA is replicated as a concatemer of head-to-tail genomes in the nucleus of the infected cell (189, 190). DNA replication is concurrent with the

expression of the HSV-1 capsid structural proteins VP5 (UL19), VP19c (UL38), VP23 (UL18), and VP26 (UL35) [reviewed in (173)]. Using a protein scaffold—made of the viral proteins VP22a and pUL26.5—these structural proteins self-assemble into a spherical capsid precursor, or procapsid (139, 215, 220). Packaging of viral genomes into procapsids requires several tightly coupled events: 1) proteolysis and expulsion of the scaffold proteins, 2) recognition and cleavage of viral genome termini by the terminase complex, 3) docking of the terminase-DNA complex on the capsid portal, and 4) insertion of DNA into the procapsid. Terminase preferentially cleaves and packages the U_L end of the genome first; conversely, the U_S end is ejected first from the progeny capsid (46, 133). The product of DNA packaging is an angular capsid that contains tightly packed viral DNA (16, 70). This mature capsid, also known as a C-capsid, exits the nucleus and is incorporated into virions.

In the absence of successful packaging, two capsid by-products accumulate in nuclei. B-capsids contain the cleaved scaffold proteins VP21, VP22a, and VP24; A-capsids are empty (70). The three types of capsids are distinguishable in electron micrographs, and they can be separated from each other preparatively by sucrose density gradient ultracentrifugation. B- and A-capsids are thought to form when DNA packaging is terminated prior to or after insertion of DNA, respectively. DNA packaging can be blocked by null mutations of the UL6, UL15, UL17, UL25, UL28, UL32, and UL33 genes (6, 103, 104, 121, 157, 186, 214). For most of the packaging genes, deletion or null mutation completely eliminates DNA cleavage and packaging, such that the DNA concatemer is unresolved and only B-capsids are formed. UL25 mutants, however, have a dissimilar phenotype to that of the other packaging gene mutants. Deletion of UL25 results in the formation of A-capsids and nearly unit-length genomes that are aberrantly cleaved at the U_S end of the genome (30, 121, 205).

The UL25 gene product is a 580 amino-acid, 62 kDa protein that contains an unstructured N-terminal tail and core of packed alpha helices (19). UL25 protein (pUL25) attaches to the external vertices of HSV-1 capsids (30, 137, 224). Based on the crystal structure of a truncated pUL25 lacking the N-terminal 134 amino acids, pUL25 was predicted to occupy the penton-distal region of the UL25-UL17 heterodimer (CCSC), which is present in five copies at each capsid vertex (224). pUL25 interaction with the capsid structural proteins has been tested directly by immunoprecipitation and far-Western assays (148, 188). Formation and stability of the CCSC is dependent on its interaction with the major capsid protein pUL19 (VP5) and the triplex protein pUL18 (VP23) (188), and pUL25 may also bind to the triplex protein pUL38 (VP19c) (148). Much like the accessory proteins of the double-stranded DNA bacteriophages, accumulation of UL25 protein may reinforce the capsid to prevent loss of DNA (121, 137). pUL25 has been shown to interact with pUL6, which forms a dodecameric ring that serves as the portal of entry for DNA into the procapsid and the docking site for the terminase complex (143, 156, 221, 237). In structural studies, pUL25 has not yet been observed around the portal. However, because pUL25 prevents aberrant cleavage of viral genome termini (205), pUL25 could be involved in stabilizing the terminase complex on the portal while DNA is being actively packaged, or in sealing off the portal for DNA retention after completion of packaging.

Its flexible nature and accessibility on the capsid surface has implicated pUL25 in interactions required for trafficking capsids through infected cells. Quantification of pUL25 copy numbers on intranuclear C-capsids and those in virions revealed that more pUL25 is present on capsids that leave the nucleus, suggesting that capsid-associated pUL25 is required for nuclear egress (98, 217, 224); UL25 involvement in nuclear egress has been confirmed in HSV-1 and pseudorabiesvirus (98, 102, 147, 169). It has been suggested that conformational changes of the

capsid proteins induced by DNA packaging expose pUL25 binding sites at the capsid surface, such that accumulation of pUL25 serves as a signal for nuclear egress (224). pUL25 recruits the large tegument protein pUL36 to virus assembly compartments, and it is the pUL25 interaction with pUL36 that initiates tegumentation around the capsid pentons (27, 32, 156, 253). The pUL25/pUL36 complex may also contact microtubules and the nucleoporins; these interactions would transport capsids from the cell periphery to the nucleus and dock them on the nuclear pore before the viral genome is released (93, 156, 169). Finally, UL25 is required at a very early stage in infection, in the uncoating of the viral genome (169).

In this study, we completed a mutational analysis of UL25 to define regions of UL25 protein important for viral replication and capsid attachment. The pUL25 capsid-binding domain is located in the N-terminal 50 amino acids and is essential for successful viral replication and DNA packaging *in vivo*. The capsid-binding domain of pUL25 was further defined by making small deletions and point mutations within the N-terminal 50 amino acids. In addition, UL25 mutants that bind capsids *in vivo* without promoting the formation of infectious particles were isolated. These mutations may span regions of UL25 protein that are required for capsid maturation from the nucleus or other downstream events in virion assembly.

2.3 MATERIALS AND METHODS

2.3.1 Cells, viruses, and antibodies

African green monkey kidney cells (Vero; American Type Culture Collection, Rockville, MD) and UL25-transformed 8-1 cells (121) were propagated in 5% FBS/DMEM with penicillin

(10U/ml) and streptomycin (10μg/ml) at 37° and 5% CO_2. HSV-1 wild-type KOS strain and UL25-null virus KUL25NS have been previously described (121). The rabbit polyclonal antibody NC1 (31) was used in Western blots to detect the HSV-1 major capsid protein, pUL19 (VP5). Baculovirus-expressed UL25 protein (121) was purified and used to prepare a UL25 monoclonal antibody, 25E10, that was provided by W. Newcomb, University of Virginia (33).

2.3.2 Transposon mutagenesis

The transposition reaction was done following the GPS-LS protocol (New England Biolabs). The GPS-LS system is an *in vitro* method for random insertion of a 1.7 kbp transposon (Tn7-based transprimer) that encodes a kanamycin resistance gene, Kan^R. The mutagenesis is accomplished by introduction of a transposon that contains the 8 bp *Pme*I site; the majority of the transposon is then removed by restriction digestion with *Pme*I. Religation results in a 15 bp insertion, which retains the unique *Pme*I site. Plasmid pAPV-UL25 contains the UL25 gene expressed from the HSV-1 ICP6 promoter and was used as the template for the transposition (121). Following transposition, the plasmid was transformed into bacteria and plated on selective agar containing kanamycin and ampicillin. DNA extracted from individual colonies was analyzed using a restriction enzyme (*Pme*I) to map the site of the transposition. Plasmids with insertions that mapped within the UL25 open reading frame were digested with *Pme*I to remove transposon sequences, religated, and transformed into bacteria. The mutants were sequenced (University of Pittsburgh DNA sequencing core laboratory) to confirm the positions and residues inserted as a result of the transposition.

2.3.3 Construction of UL25 mutants

UL25-expressing plasmids were made by PCR using pAPV-UL25 as a template followed by Topo cloning of the gel-purified PCR products into pcDNA3.1/V5/His-TOPO (Invitrogen) such that the UL25 gene was under the transcriptional control of the cytomegalovirus (CMV) promoter. PCR primers contained *Bam*HI and *Eco*RI restriction sites that were used for further subcloning. UL25 plasmids pFH274, pFH284, pFH368, and pFH379 contained the coding sequences for UL25 amino acids 37 to 580, 1 to 580, 1 to 50, and 51 to 580, respectively. The primers used to amplify these regions of UL25 are listed in Table 9 (Appendix A). The UL25 Topo clones were digested with *Bam*HI, and UL25 sequences were then ligated into the *Bam*HI site of plasmid pFH118. pFH118 expresses proteins (using the CMV promoter) with a C-terminal tandem affinity purification (TAP) tag and was constructed from plasmid pZOME-1-C (obtained from EUROSCARF, Institute of Microbiology, University of Frankfurt, Germany) (178). pZOME-1-C was digested with *Bam*HI and *Eco*RI, and a 540-bp fragment containing the TAP ORF was cloned into pcDNA3 at the *Bam*HI and *Eco*RI sites to generate pFH118. Plasmids pFH290, pFH373, and pFH392 expressed UL25-TAP fusion proteins 1-580-TAP, 1-50-TAP, and 51-580-TAP, respectively.

2.3.4 Complementation assay

Vero cells (1.0×10^5 cells/well in a 24-well plate) were transfected with 0.5 μg of plasmid DNA and 1 μl of Lipofectamine 2000 (Invitrogen) diluted in 100 μl of serum-free medium. The DNA-lipid complexes were allowed to form at room temperature for 20 min, added to the cells, and incubated overnight at 37°C. The next day, the cells were infected with UL25-null virus

(vΔUL25) at a MOI of 5 PFU/cell. After 90 min at 37°C, the medium was removed and unabsorbed virus was inactivated by washing the cells three times with citrate buffer (pH 3). The cultures were incubated for an additional 18 h, after which the cells were scraped from the plate and rinsed with PBS. A 10% aliquot of total cells was frozen and used to determine virus titers on 8-1 cells and Vero cells. The remainder of the cell pellet was resuspended in 20 μl PAGE loading buffer (Invitrogen) and used for Western blot analysis.

2.3.5 *In vitro* binding of pUL25 to capsids

Binding was performed with capsids lacking pUL25 that were prepared from Vero cells infected as described below with the UL25-null mutant virus, vΔUL25. Synthesis of [^{35}S]-methionine-labeled UL25 was carried out in a rabbit reticulocyte lysate using a coupled transcription and translation system (TNT T7Quick; Promega) according to the manufacturer's instructions using pGEM-4z, pcDNA3.1/V5-HIS-TOPO, or pFH118 vectors expressing wild-type or mutant UL25 genes. The [^{35}S]methionine-labeled UL25 (45 μl of the 50 μl *in vitro* translation reaction) was mixed with 50 μl of pooled A- and B-capsids plus 400 μl of phosphate-buffered saline (PBS), and the mixture was incubated for 90 min at room temperature with constant rotation. Capsids were isolated from the reaction mixture by centrifugation on a gradient of 20% to 50% sucrose in TNE (500 mM NaCl, 10 mM Tris, 1 mM EDTA [pH 7.5]) on an SW41 rotor at 24,000 rpm for 1 h at 4°C. After centrifugation, capsids were harvested from the gradient, precipitated by addition of an equal volume of 16% trichloroacetic acid, and analyzed by sodium dodecyl sulfate-polyacrylamide gel electrophoresis (SDS-PAGE). Gels were stained with Coomassie blue and dried onto Whatman 3M filter paper prior to autoradiography.

2.3.6 Construction of recombinant BACs

Production and characterization of a bacterial artificial chromosome (BAC) containing the entire HSV-1 (KOS-37 strain) genome was described previously (71). The KOS BAC clone (bFH439) containing a deletion that removed the entire UL25 ORF was produced with a counter-selection BAC modification kit (Genebridges). Briefly, the Red/ET expression plasmid pSC101-BAD-gbaA (Genebridges) was transformed into EPI300 bacteria containing the wild-type KOS-37 BAC. After induction of Red/ET expression, cells were transformed with a PCR product consisting of the rpsL-neo antibiotic selection cassette flanked by sequences homologous to 50 bp immediately upstream and downstream of the UL25 ORF. Recombinant clones were isolated on selective agar medium, and deletion of UL25 from BAC DNA was confirmed by PCR with primers external to the recombination locus. To create specific UL25 mutations, the KOS BAC clone was transferred to GS1783 bacteria (gift from G. Smith) and mutagenesis was performed using the two-step bacteriophage Red-mediated homologous recombination system described by Tischer *et al.* (218). PCR was used to produce a construct that contained the Kan^R gene (alphAI from plasmid p-EP-Kan-S) flanked by UL25 homologous sequence repeats containing the desired mutation or deletion. Integration of this construct into the BAC was followed by a second recombination that removed alphaAI and left the seamless mutation within the UL25 gene. The list of primers for production of PCR amplicons that were used for isolation of the UL25 deletion and insertion mutants can be found in Tables 10 and 11 (Appendix A). To confirm mutations in UL25 mutant viruses, viral DNA was amplified by PCR with the primers 5'-GCAGAAGGTCTCCGGTAATATCACC-3' and 5'-GGTGATCAGGTACAACAGGCGCTC-3'. The 2.9 kb PCR product was extracted from agarose gels and used for restriction digest and

for sequencing with primers 5'-GCGGCGGCCGCAAGACTCATTTGGATCCG-3' and 5'-TCTCCGCGACGGCCAGAC-3' (GeneWiz sequencing core).

2.3.7 Virus generation and propagation

To recover mutant viruses, BAC DNA (5 μg) was transfected into 8-1 cells with Lipofectamine. Recombinant viruses harvested from transfected cell lysates were plaque purified on 8-1 or Vero cells. The third round plaque isolate was used to generate a mini-stock of virus in a T25 flask of Vero or 8-1 cells. Cell lysates were freeze-thawed, and virus mini-stock concentrations were determined by plaque assay on 8-1 cells. To prepare a large stock of virus, 1.5×10^8 Vero or 8-1 cells were infected at a MOI of 0.01. At 3 days post-infection, cell lysates were harvested by freeze-thaw. Clarified cell lysates were centrifuged at in a Sorvall SS34 rotor at 10000 RPM for 2 hours to pellet virions from the media. The virion pellet was resuspended in 10% glycerol/DMEM overnight on ice. The resultant virus stock was titrated on Vero and 8-1 cells.

2.3.8 Preparation of viral DNA

Viral DNA was prepared essentially as described in (21), with the following modifications. A T-175 flask (3×10^7) of Vero cells was infected with virus at a MOI of 1 PFU per cell. At 48 h post-infection, the medium was removed and the cells were washed in 1x PBS, scraped off the plate, and pelleted. The cells were resuspended in TE and lysed in Triton X-100 (1.5%) on ice for 15 minutes. Nuclei were pelleted by centrifugation at 2000 rpm for 10 minutes and subsequently discarded. Virus was lysed by incubation at 50°C with SDS (0.5%) and Proteinase K (0.5μg/μl) for 1 h. DNA was extracted with phenol once and chloroform twice before being

precipitated with 1/10 volume sodium acetate and 2 volumes ethanol. Pelleted DNA was dried and resuspended in TE or sterile ddH_2O with RNAse A.

2.3.9 Southern blot and hybridization analysis

Viral DNA (10μg) was digested with *Bam*HI and *Pme*I to confirm the transposon mutations. DNA was separated by agarose gel electrophoreses and transferred in alkaline buffer to a positively-charged nylon membrane. The 1.8 kbp fragment of plasmid pFH283 containing UL25 was recovered by *Bam*HI digest and agarose gel extraction. The UL25 fragment was radiolabeled by nick translation reaction (GE Biosciences) with ^{32}P-dCTP (PerkinElmer). Unincorporated nucleotides were removed from the probe by CentriSep gel filtration columns (Princeton Separations). Southern blots were pre-incubated with hybridization buffer (5X SSC, 5X Denhardt solution, 1% SDS, 100μg/ml denatured salmon sperm DNA) at 68°C for 3h. The probe was boiled, quick-cooled on ice, added to hybridization buffer, and incubated with blots overnight at 68°C. The next day, blots were washed twice in 2X SSC/0.1% SDS and once in 0.1X SSC/0.1% SDS at 68°C before autoradiography.

2.3.10 Immunoblotting

Protein extracts were separated on a 5 to 12% SDS–polyacrylamide gel, and proteins were transferred to nitrocellulose. The nitrocellulose was washed twice in Tris-buffered saline (TBS) and blocked overnight in TBS-T (20 mM Tris, 0.5 M NaCl [pH 7.5] plus 0.5% Tween 20) supplemented with 10% nonfat dry milk. The UL25 monoclonal antibody, 25E10, and the VP5 rabbit polyclonal antibody, NC1, were diluted to 1:5000 in blocking buffer. The diluted

antibodies were reacted with the blocked nitrocellulose for 2 h at room temperature, washed, and reacted with horseradish peroxidase-conjugated anti-goat or anti-mouse immunoglobulin G (IgG) diluted at 1:5000 in TBS-T plus 10% nonfat dry milk. The bound Igs were revealed by enhanced chemiluminescence (Pierce ECL kit).

2.3.11 Capsid preparation

Vero cells (1.5×10^8) were infected overnight (18 h at 37°C) at a MOI of 5 PFU/cell. Infected cells were harvested, rinsed with PBS, and resuspended in 20 mM Tris (pH 7.5) plus protease inhibitors (Roche), adjusted to 1% Triton X-100, and incubated for 30 min on ice. The resulting nuclei were harvested by low-speed centrifugation at 2000 rpm, resuspended in 10 ml TNE (500 mM NaCl, 10 mM Tris, 1 mM EDTA [pH 7.5]), and then sonicated to lyse the nuclei. The nuclear lysate was adjusted to 20 mM $MgCl_2$ and incubated with DNase I (100 μg/ml) at room temperature for 30 min. The lysate was then cleared by low-speed centrifugation, and the resulting supernatant was layered on top of a 10-ml cushion of 35% sucrose (SW28 rotor; 23,000 rpm for 1 h). The pellets were suspended in 3 ml TNE and adjusted to 1 mM dithiothreitol, and capsids were separated by centrifugation on 20 to 50% sucrose (in TNE) gradients (SW41 rotor at 24,000 rpm for 1 h). The positions of A-, B-, or C-capsids were observed as light-scattering bands, with A-capsids being found highest (least dense) on the gradient and C-capsids found lowest (dense fractions) on the gradients. The different capsid fractions can also be identified based on the presence or absence of the scaffold protein, VP22a, since only B-capsids contain the scaffold protein. The fractions were collected using a Beckman fraction recovery system (Beckman catalog no. 34890). The apparatus has a mechanism to puncture the bottoms of the tubes, and fractions are collected from the bottom to top. Fractions (0.75 ml) were collected, and

protein was precipitated by adding an equal volume of 16% trichloroacetic acid. Pellets were resuspended in 35 μl of 2x PAGE loading buffer (Invitrogen) supplemented with 0.4 M Tris-base. Gradient fractions were run on 5 to 12% SDS-PAGE, and the gels were either stained with Imperial blue (Pierce) to visualize capsid proteins or analyzed by immunoblotting with the UL25 (25E10) antibody**.**

2.3.12 Indirect immunofluorescence assay

2 x 10^5 Vero cells grown on coverslips were infected at a MOI of 5 for 1 h on ice. Cells were washed twice with DMEM to remove unattached virus, then incubated in DMEM at 37°C to 16 h post-infection. Coverslips were rinsed twice in PBS, and cells were fixed in 2% PFA in PBS for 15 minutes. Coverslips were rinsed 3x in PBS and 5x in 0.5% BSA/PBS (PBB). Cells were blocked in 20% goat serum/PBB for 30 minutes, then incubated with the 25E10 antibody (1:200 in blocking buffer) for 1 h. After rinsing 5x with PBB, coverslips were incubated with Cy3-conjugated secondary antibody (1:1800) for 1 h. Cells were rinsed 5x in PBB, stained with DAPI, washed 3x in PBS, and mounted on glass slides with Immunomount medium. Fluorescence was visualized on a Leica DMI4000B microscope. Images were captured with the Leica application software and imported to Adobe Photoshop for cropping and resizing.

2.3.13 Thin section electron microscopy

Vero cells (2 x 10^6) were infected overnight (18 h at 37°C) at a MOI of 5 PFU/cell. Cells were rinsed in 1X PBS, fixed in 2.5% glutaraldehyde for 1 h at RT, and rinsed several times with 1X PBS to remove the fixative. The samples were stained (1% OsO_4/1% potassium ferricyanide),

sectioned, and prepared onto carbon grids for transmission electron microscopy by Mara Sullivan of the Center of Biologic Imaging, University of Pittsburgh. Images were captured with a T12 electron microscope with the assistance of Katerina Toropova (University of Pittsburgh Department of Structural Biology).

2.4 RESULTS

2.4.1 Transposon mutagenesis and functional assessment of UL25 mutants

In order to identify regions of UL25 protein that are important for viral replication and for attachment to capsids, the UL25 ORF was randomly disrupted by linker scanning mutagenesis. A plasmid vector (pAPV-UL25) containing the UL25 gene was subjected to Tn7 transposon-mediated insertion of a 15 bp fragment that contained a *Pme*I restriction site. Eleven clones with unique DNA insertions in the coding region of the UL25 gene were mapped by restriction digestion and DNA sequencing. The resulting amino acid insertions into the UL25 protein are shown in Figure 8. The mutations were scattered across the UL25 ORF with a clustering of three insertions between amino acids 143 and 155. Three of these mutants contained in-frame stop codons after amino acids 12, 212, and 560.

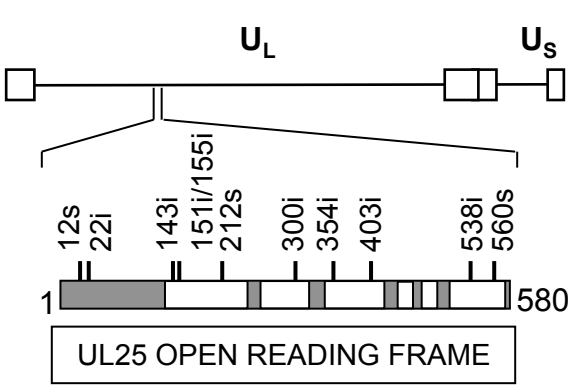

MUTANT	AMINO ACID CHANGE FROM	TO	PREDICTED MW (kDa)
12s	D-V	D-V*TLD-V	1.5
22i	D-S	D-LFKHD-S	64.1
143i	N-D	N-CLNSN-D	64.1
151i	T-N	T-CLNNT-N	64.1
155i	V-D	V-VFKHV-D	64.1
212s	T-A	T-V*TMT-A	23.2
300i	A-A	A-CLNTA-A	64.1
354i	R-A	R-CLNNR-A	64.1
403i	N-N	N-LFKIN-N	64.1
538i	L-A	L-CLNML-A	64.1
560s	S-S	S-V*TVS-S	60.4

Figure 8. Diagram of UL25 transposon mutations. (Top left) Physical map of the HSV-1 genome showing the location of the UL25 gene. U_L and U_S refer to the long and short unique region sequences. (Bottom left) Schematic representation of the 580 amino acid UL25 protein. White boxes are the folded protein core, and gray boxes are the flexible, unstructured regions, as determined by characterization of the UL25 crystal structure (19). Numbers above the line indicate the amino acid location where 15 base pairs were inserted into the UL25 open reading frame resulting in either the insertion (i) of five amino acids or an in-frame stop codon (s). (Right) The location of the insertions and the predicted amino acid changes are shown along with the predicted molecular weight for each mutant. *, stop codon. This figure was used with permission from reference (30).

The ability of the UL25 transposon mutants to support virus replication was tested using a genetic complementation assay. Vero cells were transfected with wild-type and mutant plasmids, and the next day the cells were infected with the UL25 deletion virus, vΔUL25. Following another day of incubation, the cell lysates were harvested, tested for UL25 protein expression by Western blot analysis, and assayed for virus progeny yield by plating the lysates on UL25-complementing cells (8-1 cells). With the exception of the 12s mutant, all of the plasmids produced proteins of the expected sizes (Figure 9A). Eight of the transposon mutants expressed a UL25 protein that was similar in size to the wild-type UL25 protein. For these mutants, a size difference would not be apparent since only five amino acids were added to the mutant UL25 proteins. The two nonsense mutants 212s and 560s produced proteins of 23 and 60 kDa, respectively. No immunoreactive proteins were observed for the 12s mutant, but this plasmid was predicted to make only a small peptide that would probably not be recognized by

the UL25 antiserum. Using the HSV-1 major capsid protein (UL19) as a loading control, all of the mutants except the 12s mutant were found to express similar amounts of pUL25 (Figure 9A). The ability of the UL25 mutants to complement growth of the UL25-null mutant was determined by titrating the cell lysates on 8-1 cells. Figure 9B shows that, with the exception of the three truncation mutants (12s, 212s, and 560s) and the 143i mutant, the remaining mutants were able to complement the UL25-null virus, although the 155i and 403i mutants complemented at less than 10% of the wild-type UL25 protein.

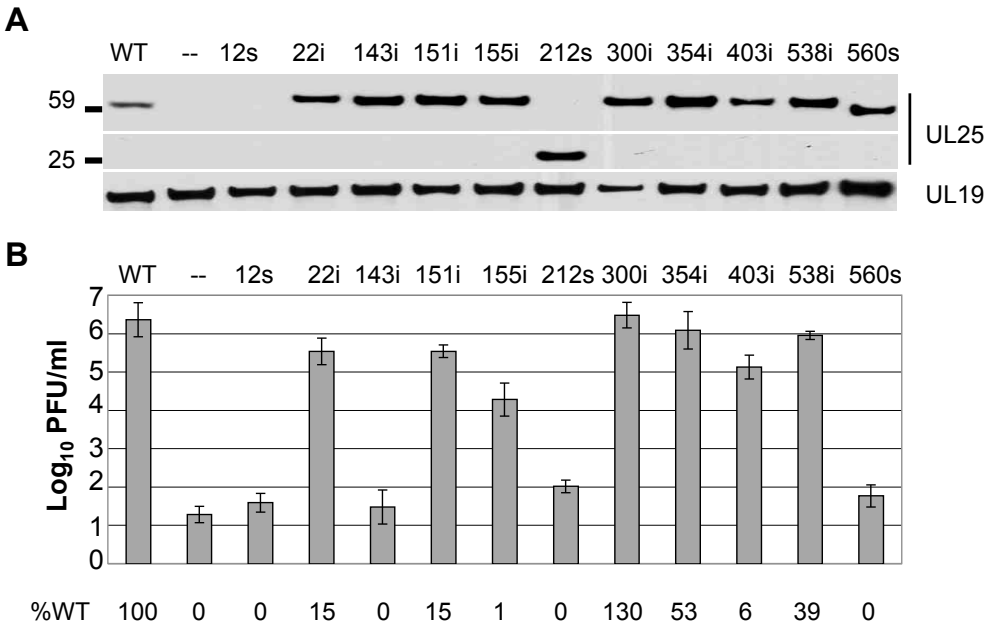

Figure 9. Complementation assays of the UL25 transposon mutants. The UL25 transposon mutants were examined for their ability to complement the growth of the UL25 null virus. A. Western blots for UL25 protein and major capsid protein, UL19. Molecular weight standards in kDa are shown at left. B. The progeny virus was titrated on the UL25 complementing cell line, 8-1, and the results shown are averages of at least six experiments. Error bars represent the standard deviation. The data listed at the bottom is the percentage of complementation relative to the wild-type UL25 protein. This figure was used with permission from reference (30).

2.4.2 The N-terminus of pUL25 is required for capsid attachment *in vitro*

Previously, we showed that [^{35}S]-methionine-labeled UL25 synthesized in a coupled *in vitro* transcription-translation system attached to the surface of UL25-deficient capsids during *in vitro* incubation (137). To determine if mutations that eliminated complementation also affected pUL25 capsid attachment, the 12s, 143i, 212s, and 560s mutants were tested for *in vitro* capsid binding. *In vitro* translation of plasmids containing the 143i, 212s, and 560s mutants produced proteins corresponding to their predicted molecular weights (Figure 10A). Unexpectedly, *in vitro* translation of the 12s mutant produced a nearly wild-type-size protein (Figure 10A). Capsid binding was determined by adding an aliquot of the [^{35}S]-methionine-labeled UL25 to pooled A- and B-capsids derived from the nuclei of cells infected with the UL25-null mutant, vΔUL25 (Table 6). After incubation to allow pUL25 attachment, the capsids were separated from other reaction components by centrifugation on a sucrose gradient, and gradient fractions were analyzed by SDS-PAGE followed by autoradiography. Capsid attachment was indicated by comigration of UL25 protein with capsids in the sucrose gradient (Figure 10B and C).

The 143i, 212s, and 560s proteins attached to capsids. Although the 212s protein was found to be primarily associated with the fractions containing A- and B-capsids, significant levels of the protein were found in fractions denser than capsids. This was probably the result of aggregation of the truncated UL25 protein, as evidenced by the observation that this protein is found in the same dense fractions when the *in vitro*-translated protein was run on the gradient in the absence of A- and B-capsids (Figure 10C). In contrast to the 143i, 212s, and 560s mutants, the 12s translation product did not attach to capsids, although we cannot rule out that there may be some low-level binding since the amount of radiolabeled 12s protein was reduced compared to the amounts of the other UL25 proteins.

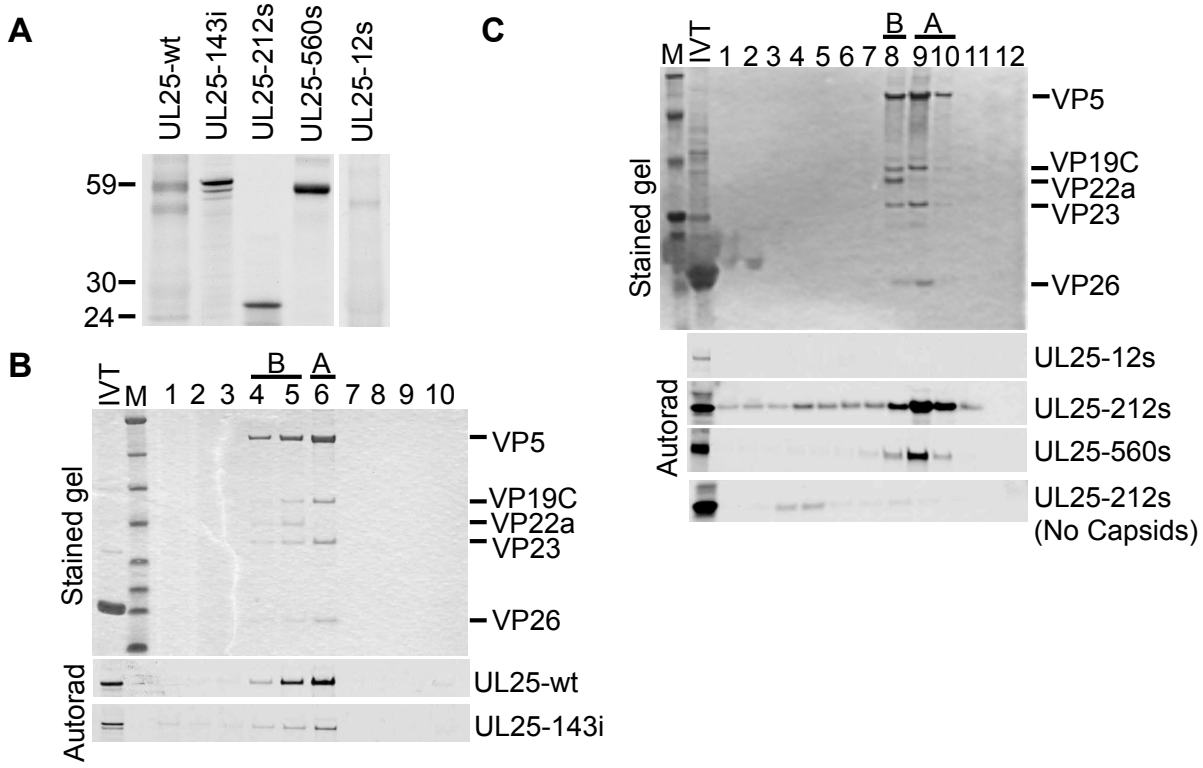

Figure 10. Capsid binding by UL25 transposon mutants. A. Autoradiograph of [35S]Met-labeled UL25 protein after SDS-PAGE. The sizes of the 143i, 212s, and 560s proteins were consistent with predicted molecular mass for each protein, while the 12s mutant unexpectedly produced a near wild type sized UL25 protein. B, C. *In vitro* capsid-binding assay. *In vitro*-translated protein was incubated with pooled A- and B-capsids isolated from Vero cells infected with the UL25 null virus, vΔUL25, and then purified by sucrose gradient centrifugation. The sucrose gradients were fractionated and analyzed by SDS-PAGE followed by Coomassie staining (top panel, representative gel) and autoradiography (bottom panels). The fractions containing A- and B-capsids are indicated. The capsid proteins visible in the stained gel are listed at right. Capsid-binding was demonstrated by co-migration of the UL25 protein with A- and B-capsids. Aggregation of the truncated 212s protein may explain the presence of this protein in the same dense fractions as in the gradient lacking A- and B-capsids (bottom of panel C). IVT, *in vitro* transcription-translation; M, molecular weight markers (from top, 194, 104, 60, 41, 27, 21, 16, 7 kDa). Lane 1 is the bottom and lane 10 is the top of the gradient. This figure was amended with permission from reference (30).

Examination of the UL25 coding sequence revealed that after the first AUG, the next in-frame AUG start codon was located 120 bp downstream. This start site corresponded to UL25 amino acid 37. To determine if the 12s mutant was initiating at this downstream start site, the codons for amino acids 1 to 36 were deleted from the UL25 expression plasmid (Figure 11A). The resulting *in vitro* synthesized protein, containing UL25 amino acids 37 to 580, was identical in size to the 12s mutant *in vitro* translation product (Figure 11B).

Similar to the result with the 12s protein, the UL25 N-terminal truncation (37 to 580) mutant did not bind capsids when tested in the *in vitro* capsid-binding assay (Figure 11C). In addition, this mutant did not complement the UL25-null virus (data not shown). These results demonstrated that the sequences within the N-terminus of the UL25 protein are required for capsid binding. To determine if the UL25 N-terminus was sufficient for capsid binding, three plasmids were generated that expressed portions of UL25 protein fused at its C-terminus to a tandem affinity purification (TAP) tag (Figure 11A). The TAP tag consists of the IgG-binding peptide protein A, the cleavage site for the tobacco etch virus protease, and the calmodulin binding domain; the tag adds 178 amino acids (20 kDa) to the C-terminus of the UL25 fusion protein (178). The three constructs 1-580-TAP, 51-580-TAP, and 1-50-TAP contained the full-length UL25 protein, UL25 amino acids 51 to 580, and UL25 amino acids 1 to 50 fused to the TAP tag, respectively (Figure 11A). *In vitro* translation produced proteins corresponding to their predicted size, and each protein was tested for binding to UL25-deficient A- and B-capsids (Figure 11A to C). Like the 12s and 37-580 mutants, the UL25 fusion protein 51-580-TAP did not attach to capsids. In contrast, the full-length 1-580-TAP and truncated 1-50-TAP fusion proteins were able to bind capsids. When incubated with A-, B-, and C-capsids purified from KOS-infected cells, the 1-50-TAP but not the 51-580-TAP was found to bind all three capsid

types by binding to unoccupied sites on the capsids and/or competitively displacing wild-type protein from capsids (Figure 11D). These results demonstrated that UL25 amino acids 1 to 50 mediate capsid attachment in the *in vitro* capsid-binding assay.

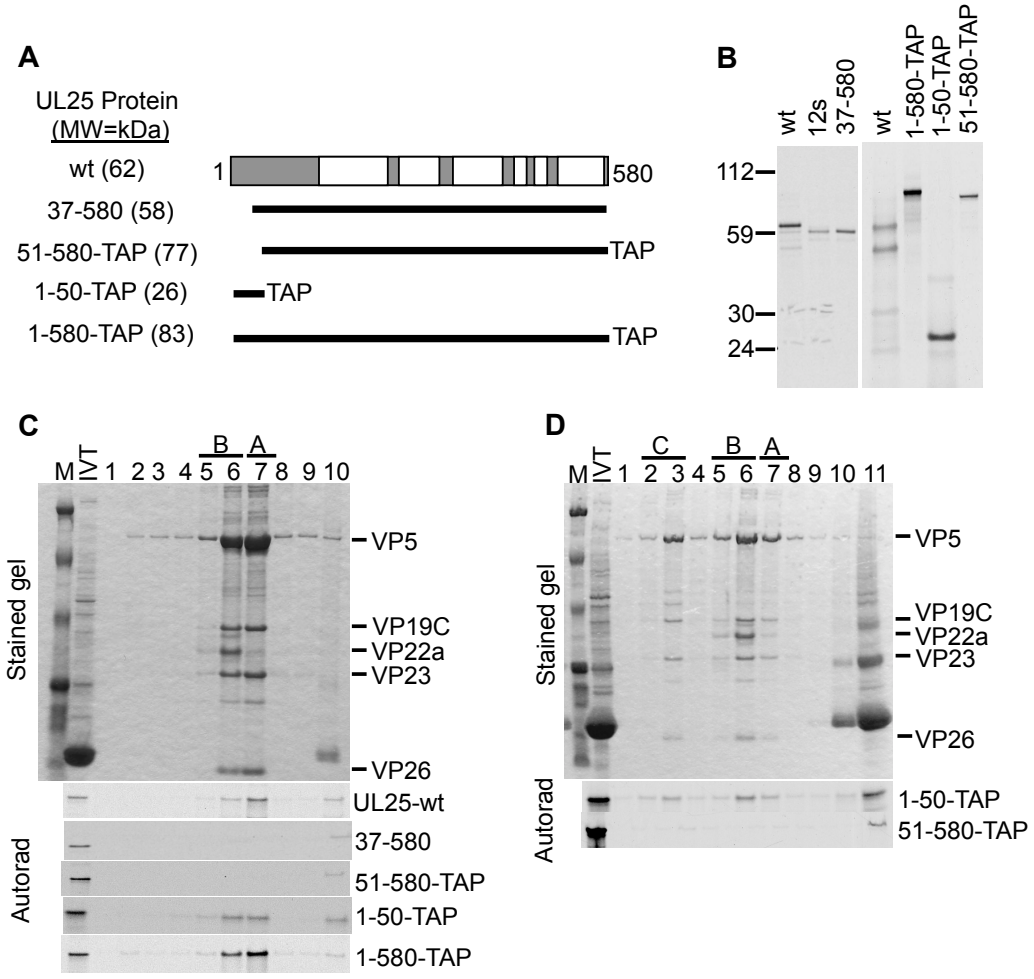

Figure 11. Capsid binding by UL25 N-terminal mutants. A. UL25 N-terminal truncation and TAP fusion constructs are shown. The numbers listed on the left indicate the UL25 amino acids included in each construct. The TAP constructs contained the tandem affinity purification (TAP) tag fused to the C-terminus of UL25. The predicted MW of each protein is listed in parentheses. B. Autoradiograph of in vitro translation products after SDS-PAGE. Molecular weight markers in kDa are shown at left. Each protein showed appropriate MW either due to addition of the TAP tag or deletion of the UL25 N-terminal amino acids. C. *In vitro* capsid-binding assay. *In vitro*-translated protein was incubated with pooled A- and B-capsids isolated from Vero cells infected with the UL25 null virus, vΔUL25, and then purified by sucrose gradient centrifugation. A representative Coomassie stained gel of the gradient fractions is shown (top panel). Autoradiographs of dried gels demonstrated the binding of the proteins 1-580-TAP and 1-50-TAP, but not the 51-580-TAP or the 37-580-TAP, to the two capsid types (bottom panel). D. *In vitro*-translated protein was incubated with pooled wild type KOS A-, B-, and C-capsids and then purified by sucrose gradient centrifugation. A representative stained gel of the gradient fractions is shown (top panel). Autoradiographs of dried gels demonstrating the binding of the 1-50-TAP but not the 51-580-TAP to all three capsid types (bottom panel). The fractions containing A-, B-, and C-capsids are indicated. The capsid proteins visible in the stained gel are listed at right. IVT, *in vitro* transcription-translation; M, molecular weight markers (from top, 194, 109, 59, 30, 22, 13, 6 kDa). Lane 1 is the bottom and lane 10 or 11 is the top of the gradient. This figure was amended with permission from reference (30).

2.4.3 Introduction of UL25 mutations to the viral genome

Several of the UL25 mutations were introduced into the viral genome through the genetic manipulation of an HSV-1 (KOS) genome maintained in a recombinant bacterial artificial chromosome (BAC). The genotypes of the viruses used in these studies are listed in Table 6. Virus vΔUL25 contains the rpsLneo antibiotic resistance genes, which replace the entire UL25 ORF. Recombinant viruses v143i, v155i, v212s, and v560s contain the indicated UL25 linker insertion mutations (Figure 5A). Recombinant virus vΔ1-50 contains a deletion that removed the coding sequences for UL25 amino acids 1 to 50, which were replaced with an ATG start codon. The BACs used to generate each virus were confirmed by digesting them with *Bam*HI and *Pme*I. The UL25 ORF is contained within the HSV-1 2.3 kbp *Bam*HI U fragment (118, 164) (Figure 12A). Since there are no *Pme*I sites in the HSV-1 genome, the presence of the *Pme*I linker in the UL25 gene of the HSV-1 BACs 143i, 155i, 212s, and 560s resulted in the loss of the 2.3 kbp *Bam*HI U fragment, which was shifted to a smaller fragment that comigrates with other HSV-1 *Bam*HI fragments (Figure 12B). The HSV-1 BAC Δ1-50 contained the deletion of 150 bp in UL25, which was detected as a shift in the *Bam*HI U fragments (Figure 12B). The BACs were transfected onto UL25-complementing 8-1 cells, and the recovered viruses were plaque purified on Vero or 8-1 cells. Each mutant was titrated on Vero and 8-1 cells to determine the effects of UL25 mutations on viral replication (Table 6). Vero cells were nonpermissive for the replication of vΔUL25, v143i, v212s, v560s, and vΔ1-50. The virus v155i displayed an intermediate phenotype with a six fold reduction of growth on Vero cells as compared to the UL25-complementing cell line. To verify the presence of the mutations in the progeny virus, viral DNA was digested with *Bam*HI and *Pme*I and subjected to Southern blot analysis with the ^{32}P-labeled UL25 probe (Figure 12C). As seen in the restriction enzyme digestion analyses of the individual

BAC preparations, a prominent 2.3 kbp fragment was detected in the KOS lane, which was reduced to two smaller fragments in v143i, v155i, v212s, and v560s and one smaller fragment in vΔ1-50. The 400 bp fragment for v560s was observed on longer exposure (not shown). The 2.3 kbp fragment containing the UL25 ORF was not detected in the UL25 deletion virus vΔUL25. These results demonstrated that that the UL25 mutants had the desired insertions or deletions.

TABLE 6. Virus stock titers: Transposon insertion and N-terminal truncation mutants

Virus strain	UL25 protein expressed (amino acid positions)	PFU/ml in: Vero cells	8-1 cells
KOS	Wild type (1–580)	2×10^8	2×10^8
KUL25NS	Null (1–107)	3×10^4	2×10^8
vΔUL25	Null	$<1 \times 10^2$	9×10^7
v143i	143i (1–580)	$<1 \times 10^2$	3×10^7
v212s	212s (1–212)	$<1 \times 10^2$	1×10^7
v560s	560s (1–560)	$<1 \times 10^2$	2.7×10^7
v155i	155i (1–580)	1×10^7	6×10^7
vΔ1-50	Δ1-50 (51-580)	$<1 \times 10^2$	3×10^8

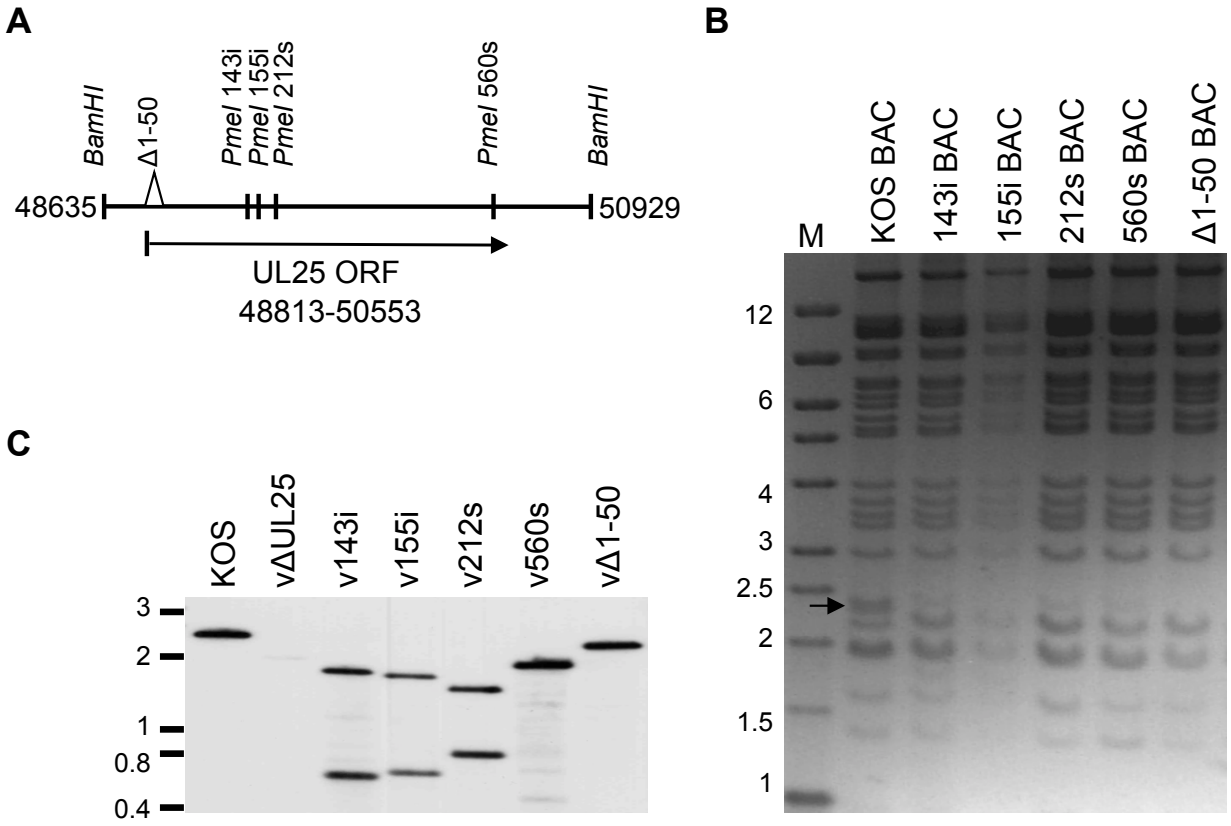

Figure 12. Characterization of BAC DNA and HSV-1 infected cell DNA. A. Schematic representation of the *Bam*HI region located between nucleotides 48635-50929 of the HSV-1 genome that contains the UL25 ORF. The sites where unique *Pme*I restriction sites are found in the UL25 gene and the resulting BACs and viruses (143i BAC, 155i BAC, 212s BAC, 560s BAC) are listed on top. Δ1-50 BAC contained a deletion that removes the coding sequences for UL25 amino acids 1-50 and inserts a new ATG start codon. B. BAC DNA was digested with *Bam*HI and *Pme*I and run on a 1.2% agarose gel. The wt 2.3 kbp *Bam*HI fragment is present in the KOS BAC lane (arrow). This fragment was cleaved to smaller fragments by *Pme*I in 143i BAC, 155i BAC, 212s BAC, and 560s BAC. The UL25 fragment of Δ1-50 BAC is shifted to 2.1 kbp , which comigrates with another viral band. C. Southern blot of viral DNA. Viral DNA was purified from cells infected with the indicated viruses. Viral DNA (10μg) was digested with *Bam*HI and *Pme*I and run on 1.2% agarose gel. DNA was blotted to a nylon membrane, and the blot was hybridized with the ^{32}P-labeled UL25 probe. The wt *Bam*HI fragment containing UL25 is visible at 2.3 kbp in the KOS lane and was cleaved to smaller fragments by *Pme*I in v143i, v155i, v212s, and v560s. The UL25 fragment of vΔ1-50 is shifted to 2.1 kbp. M, DNA markers in kbp. This figure was amended with permission from reference (30).

2.4.4 Association of pUL25 with capsids *in vivo*

Intranuclear capsids were purified from Vero cells infected with wild-type KOS or UL25 mutant viruses. The nuclear lysates were subjected to sucrose gradient centrifugation, and capsids were viewed as visible light-scattering bands (Figure 13). In cells infected with wild-type KOS or v155i, which replicate on Vero cells, all three capsid forms were observed. The KOS gradients contained nearly equal amounts of both B- and C-capsids, with only minor amounts of A-capsids. In contrast, the gradient for the v155i mutant contained less C-capsids and more A- and B-capsids, and the C-capsid band was barely detectable in the v155i gradient. The lysates of the UL25 mutants that did not replicate on Vero cells (vΔUL25, v143i, v212s, v560s, vΔ1-50, and KUL25NS) contained approximately equal numbers of A- and B-capsids but no DNA-containing C-capsids. The high proportion of A-capsids found along with the absence of C-capsids in all of these UL25 mutants is identical to what was previously described with the UL25-null mutant KUL25NS (121).

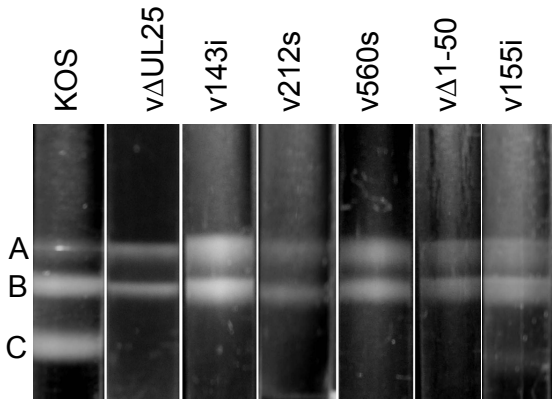

Figure 13. Capsid phenotypes of UL25 mutant viruses. Vero cells infected at a MOI of 5 with KOS or the indicated virus were harvested at 18 h post infection. Nuclear lysates were layered onto 20 to 50% sucrose gradients and centrifuged at 24,000rpm (SW41 rotor) for 1 h. The position of A-, B-, and C-capsid bands are indicated. This figure was amended with permission from reference (30).

To determine whether the UL25 protein was present in these capsids, the sucrose gradient fractions were analyzed by Western blot (Figure 14). The KOS gradient showed that pUL25 was found in the fractions that contained A-, B-, and C-capsids. The 155i mutant was found to associate with A- and B-capsids, but since there were so few C-capsids present on the gradient, there was little if any of this protein detected with these DNA-containing capsids. The UL25 linker insertion mutant 143i and the nonsense mutants 212s and 560s were found associated with A- and B-capsids isolated from cells infected with viruses expressing those proteins. The vΔ1-50 mutant expressed a truncated UL25 protein that was missing residues 1 to 50, and although this protein could be detected in the cell extract, it failed to bind either the A- or B-capsids. This result demonstrates the importance of the N-terminus of pUL25 for its capsid association. These data also demonstrate that similar to the result of the *in vitro* capsid-binding assay (Figure 11), the pUL25 capsid-binding domain resides within its first 50 amino acids. Furthermore, the studies with the UL25 mutant viruses demonstrate that the pUL25 capsid-binding domain is essential but not sufficient for production of infectious virus, as both virus progeny and C-capsids were significantly reduced in non-complementing cells infected with the 155i mutant (Table 6).

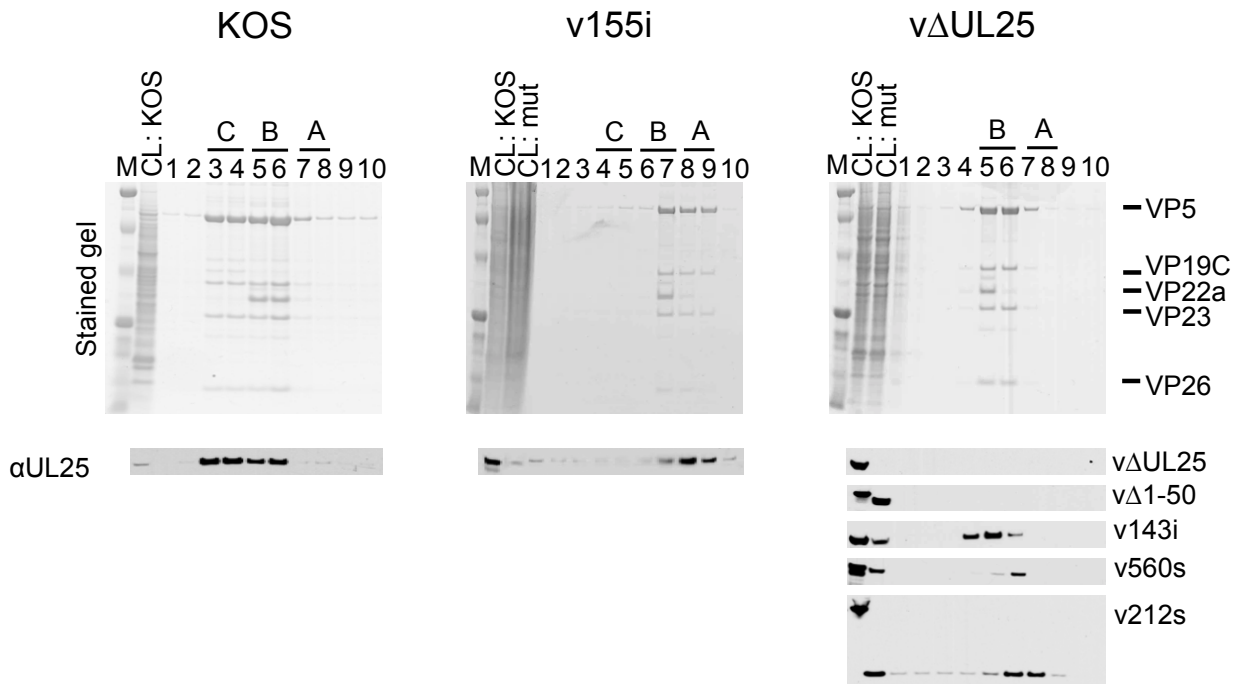

Figure 14. Analysis of capsid bound pUL25. (Top panels) The protein composition for each gradient fraction was determined by SDS-PAGE (stained gel). Lane 1 is the bottom and lane 10 is the top of the gradient. Gradient fractions that contained A-, B-, and C-capsids are indicated. The positions of the capsid proteins (major capsid protein, VP5; triplex proteins, VP19C and VP23; scaffold protein, VP22a; smallest capsid protein, VP26) are indicated at far right. The stained gel in the right panel contains capsids isolated from the UL25 null virus ΔUL25, which is representative of the mutants (vΔ1-50, v143i, v212s, v560s) that fail to replicate on Vero cells. (Bottom panels) Gradient fractions were analyzed by SDS-PAGE followed by immunoblotting for pUL25 using the 25E10 antibody. Lane CL: KOS, cell lysate from KOS-infected cells. Lane CL: mut, cell lysate from UL25 mutant-infected cells. Molecular mass standards are visible in lane M (from top, 194, 109, 59, 30, 22, 13, 6 kDa). This figure was amended with permission from reference (30).

2.4.5 Deletion of the pUL25 N-terminus does not inhibit pUL25 nuclear localization

The virus-expressed UL25 protein deleted of amino acids 1-50 is present in infected cell lysates but is not associated with capsids purified from infected cell nuclei (30). It is possible that this truncated protein is structurally unstable and consequently, sequestered in the cytoplasm. In this

case, the nuclear exclusion of Δ1-50 protein would prevent contact with intranuclear capsids and could have led us to erroneously conclude that the capsid-binding domain was located in amino acids 1-50.

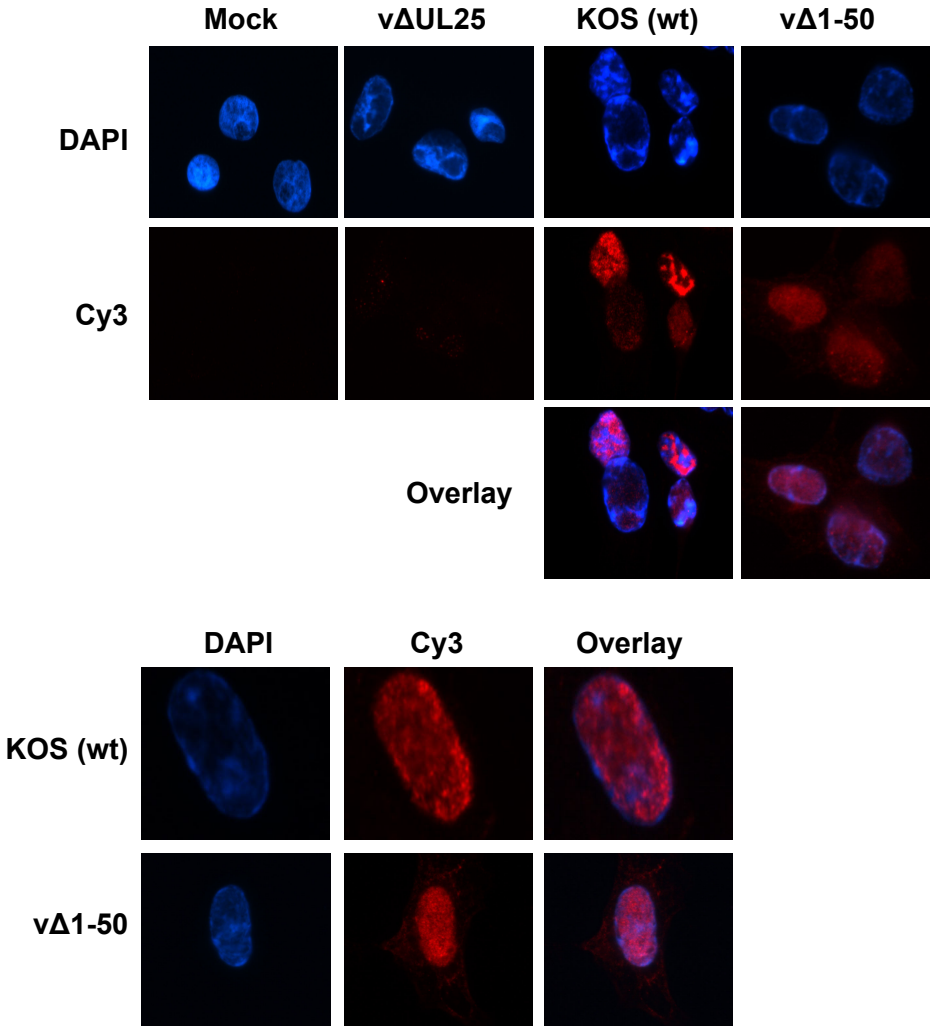

Figure 15. The truncated UL25 protein Δ1-50 localizes to infected cell nuclei. Vero cells were mock-infected or infected with ΔUL25, wt KOS, or vΔ1-50. Cells were fixed at 16 hpi and stained for pUL25 with the monoclonal antibody 25E10, the Cy3-congugated secondary antibody, and DAPI. The following parameters were used for image capture: exposure time 0.9-1.3 seconds, gain 1x, and gamma 1-1.4.

To rule out this possibility, indirect immunofluorescence was used to track pUL25 in infected cells. Vero cells were mock-infected or infected at a MOI of 5 with KOS, vΔUL25, or Δ1-50 viruses and fixed at 16 hours post-infection. Cells were stained with the pUL25 monoclonal antibody, 25E10, the Cy3-conjugated secondary antibody, and DAPI. In mock-infected cells, nuclei retained clearly defined nucleoli and roughly spherical symmetry, while infected cells had distorted nuclei with marginalized host DNA. The Δ1-50 UL25 protein was visible in infected cells, and it was predominantly located in cell nuclei (Figure 15). Like the wt protein, Δ1-50 protein was visible in compartments segregated from the host DNA. These compartments have been described as assemblons or replication compartments (234). We conclude that the Δ1-50 UL25 protein is stably expressed and trafficked to the nucleus, and the observed defects in virus replication and DNA packaging are specifically due to the inability of the truncated protein to attach to capsids.

2.4.6 Characterization of viruses expressing pUL25 with small deletions and point mutations in the highly conserved N-terminal region

Several residues within the putative capsid-binding domain are highly conserved throughout the alphaherpesviruses, particularly through amino acids 26-39 of HSV-1 (Fig 16A). We hypothesized that these highly conserved residues represented the essential amino acids required for pUL25 interaction with capsid proteins. In order to determine the effects of small deletions within the UL25 N-terminus on *in vivo* capsid attachment and virus replication, recombinant viruses were generated by manipulation of the HSV-1 KOS strain genome maintained in a bacterial artificial chromosome (BAC), as previously described (30, 71, 218). These deletions spanned the highly conserved region within amino acids 1-50 and removed amino acids 1-36,

27-37, 40-50, and 27-50 (Figure 16B). Point mutations of the most conserved residues—F26, I27, F35, and W36—were also made in pairs (F26 and I27, F35 and W36) or in quadruplet (F26, I27, F35, and W36). For each of the alanine substitution mutants, a restriction site was embedded into the primers used for BAC recombination (see Methods, Tables 10 and 11). These mutations inserted a unique restriction site while making only conservative changes to the codons surrounding the mutated residues.

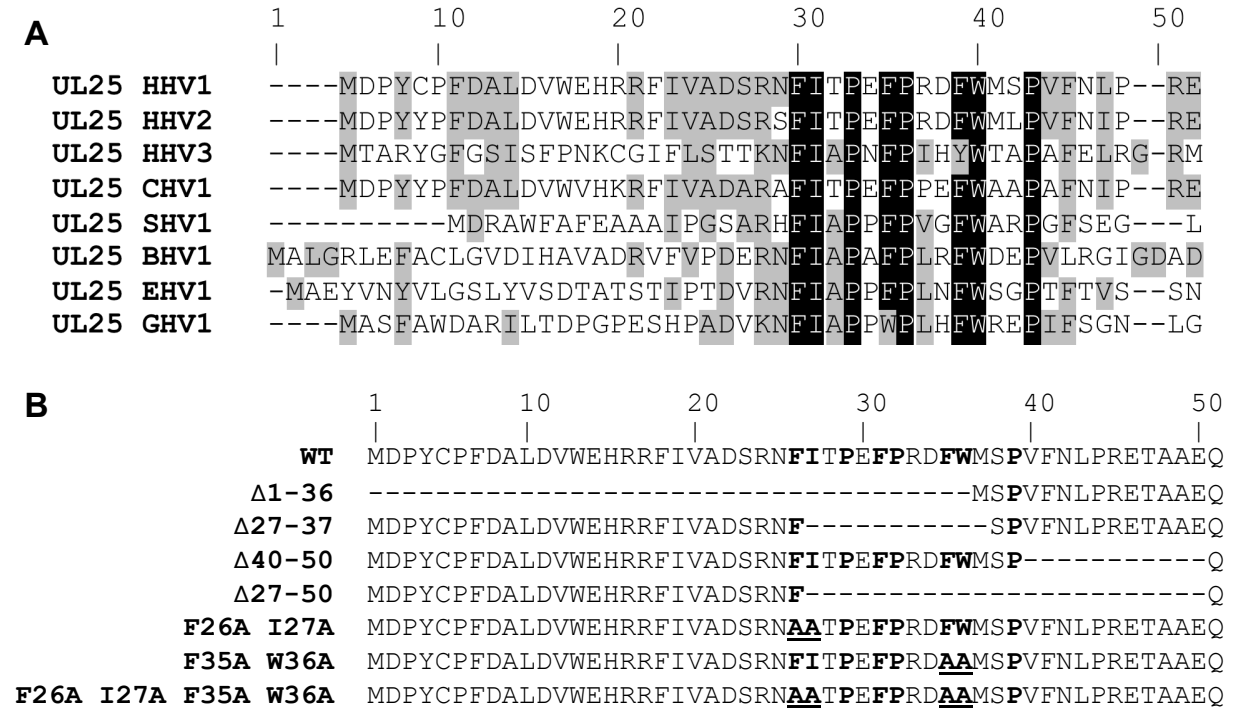

Figure 16. Generation of HSV-1 mutant viruses containing small deletions or point mutations in the highly conserved region of the pUL25 N-terminus. A. Alignment of pUL25 amino acids 1-50 from eight alphaherpesviruses including human herpesviruses 1, 2, and 3 (HHV1, 2, 3); chimpanzee herpesvirus 1 (CHV1), suid herpesvirus 1 (SHV1); bovine herpesvirus 1 (BHV1); equine herpesvirus 1 (EHV1); and gallid herpesvirus 1 (GHV1). Sequences were acquired from the NCBI website (GenBank). The alignment was generated with VectorNTI software. Similar or conservative residues are highlighted in gray; identical residues are highlighted in black. The highly conserved region comprises HSV-1 amino acids F26-P39. B. UL25 recombinant viruses. The highly conserved residues in the WT sequence are shown in bold. Deletions are shown as dashes (-), and alanine substitutions are underlined.

BACs were transfected onto Vero cells and the UL25 complementing cell line, 8-1, and the recovered viruses were plaque-purified on Vero or 8-1 cells. Viral DNA was prepared and used in PCR with primers flanking the UL25 locus (Figure 17A). In order to detect very small deletions in UL25, the PCR products were digested with *Sac*I, which cleaved within the wt UL25 gene near its 5' end. *Sac*I digestion of the wt PCR product liberated DNA fragments of 2.1 and 0.8 kb; the 0.8 kb fragment is shifted to a lower molecular weight by the small deletions in viruses vΔ1-36, vΔ27-37, vΔ40-50 and vΔ27-50 (Figure 17B). This method allowed observation of the small (≤ 100 bp) shifts in the UL25 gene, which would have been difficult to detect by Southern blot. PCR-amplified DNA from viruses vF26A I27A, vF35A W36A, and vF26A I27A F35A W36A was digested with the restriction enzymes *Xba*I, *Bcg*I, or *Bsm*I in order to detect the inclusion of these unique restriction sites in the recombinant viruses. For additional confirmation that the anticipated mutations were in place, the 2.9 kb PCR product from each virus was sequenced through the region of the mutations. Each mutant virus was titrated on Vero and 8-1 cells (Table 7).

TABLE 7. Virus stock titers: Small N-terminal deletion and point mutants

	PFU/ml in:	
Virus strain	Vero cells	8-1 cells
KOS (wild type)	2×10^8	2×10^8
vΔUL25	$<1 \times 10^2$	9×10^7
vΔ1-36	$< 10^3$	5.9×10^8
vΔ27-37	$< 10^3$	3.8×10^8
vΔ40-50	1.9×10^8	2.5×10^8
vΔ27-50	$< 10^3$	2.7×10^7
vF26A I27A	$< 10^3$	7.5×10^8
vF35A W36A	3×10^7	1.5×10^8
vF26A I27A F35A W36A	$< 10^3$	7.1×10^7

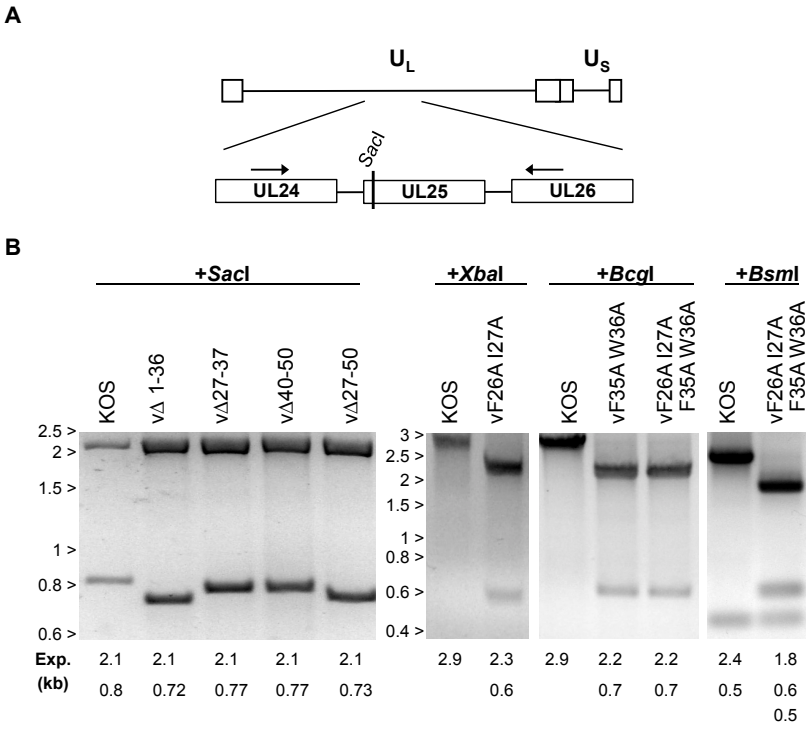

Figure 17. Confirmation of UL25 mutations in viral DNA. A. Diagram of the HSV-1 genome showing the 2.9 kbp region amplified from viral DNA by PCR. Forward and reverse primers are shown as black arrows. The *Sac*I restriction site is shown. B. PCR products were digested with the restriction enzymes *Sac*I, *Xba*I, *Bcg*I, or *Bsm*I. These unique restriction sites were embedded in the primers used for BAC recombination (Tables 10 and11). Digested PCR products were run on 2.2% agarose in TAE and stained with ethidium bromide. The expected restriction fragments are listed below the gel. Molecular weight markers are indicated in kbp.

Although the vF35A W36A virus produced plaques on Vero cells, the plaques were very small and difficult to quantify by plaque assay. Likewise, the titer of the vF26A I27A F35A W36A virus was difficult to quantify because infected cells tended to fuse into syncytia. To assay the changes in virus replication due to UL25 mutations, single-step growth curves were calculated for each UL25 mutant (Figure 18). Briefly, Vero and 8-1 cells were infected at a MOI of 3 with each virus. At 0, 6, and 24 hours post-infection (hpi) (deletion mutants) or 0, 6, 12, 22, and 30 hpi (point mutants), viral progeny in the cell lysates was harvested and quantified by titration on 8-1 cells. While the aa 40-50 deletion had no effect on virus growth, other small

deletions (Δ1-36, Δ27-37, Δ27-50) inhibited virus replication on Vero cells. All point mutants exhibited growth defects on Vero cells. Surprisingly, replication of the F35A W36A mutant on Vero cells was not comparable to wt virus at 24 hpi, which was unexpected given the virus stock formed plaques on Vero cells (Table 7). This result indicates that F35A W36A replication in its initial stages is slowed compared to wt but continues through several rounds of virus replication, unlike the UL25 deletion virus, which is unable to replicate on Vero cells.

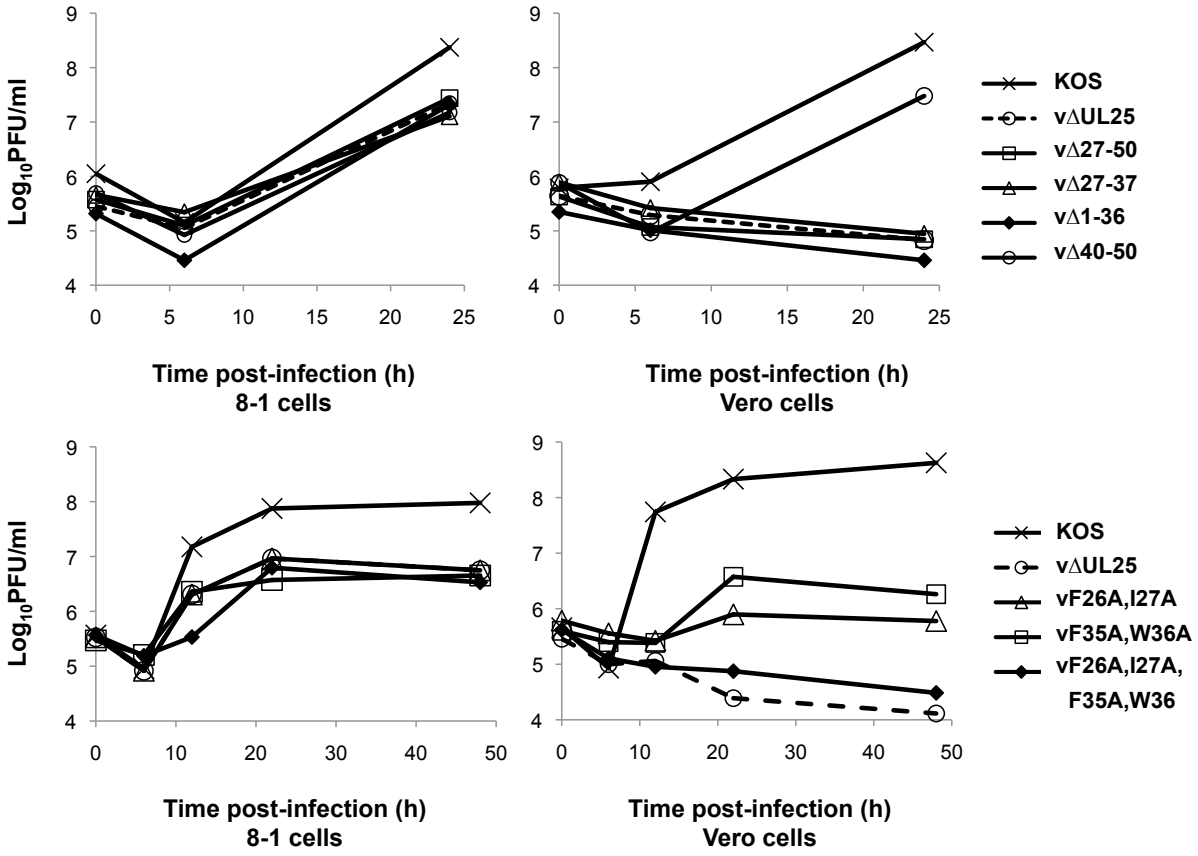

Figure 18. Analysis of viral replication. 1 x 10^6 Vero or 8-1 cells were infected with each virus at a MOI of 3 on ice for 1 h, rinsed twice with DMEM, and incubated in DMEM at 37°C to the indicated timepoints. Cells were lysed by freeze-fracture, and viral progeny in cell lysates was quantified by titration and plaque assay on 8-1 cells. The results shown are averages of duplicate experiments. (Top) Small deletion mutants. (Bottom) Point mutants.

2.4.7 The minimal capsid-binding domain is located within pUL25 amino acids 1-36

Purified capsids from Vero cells infected with each mutant were assayed for the presence of pUL25 by Western blot. Viruses that did not replicate on Vero cells were deficient in DNA packaging, as demonstrated by the absence of C-capsids (Figure 19, bottom panels). Of the deletions within aa 1-50, only the aa 40-50 deletion did not preclude formation of C-capsids. The UL25 mutant proteins Δ27-37 and Δ27-50 were found associated with capsids although these mutations to UL25 inhibited replication of the virus. Only the Δ1-36 mutant protein was undetectable on A- and B-capsids purified from cells infected with that mutant virus. This result was similar to that observed in the mutant virus vΔ1-50. These data indicate that within the putative capsid-binding domain of UL25, amino acids 1-36 were absolutely required for capsid attachment, while amino acids 27-50 were dispensable for capsid attachment but not for DNA packaging and viral replication.

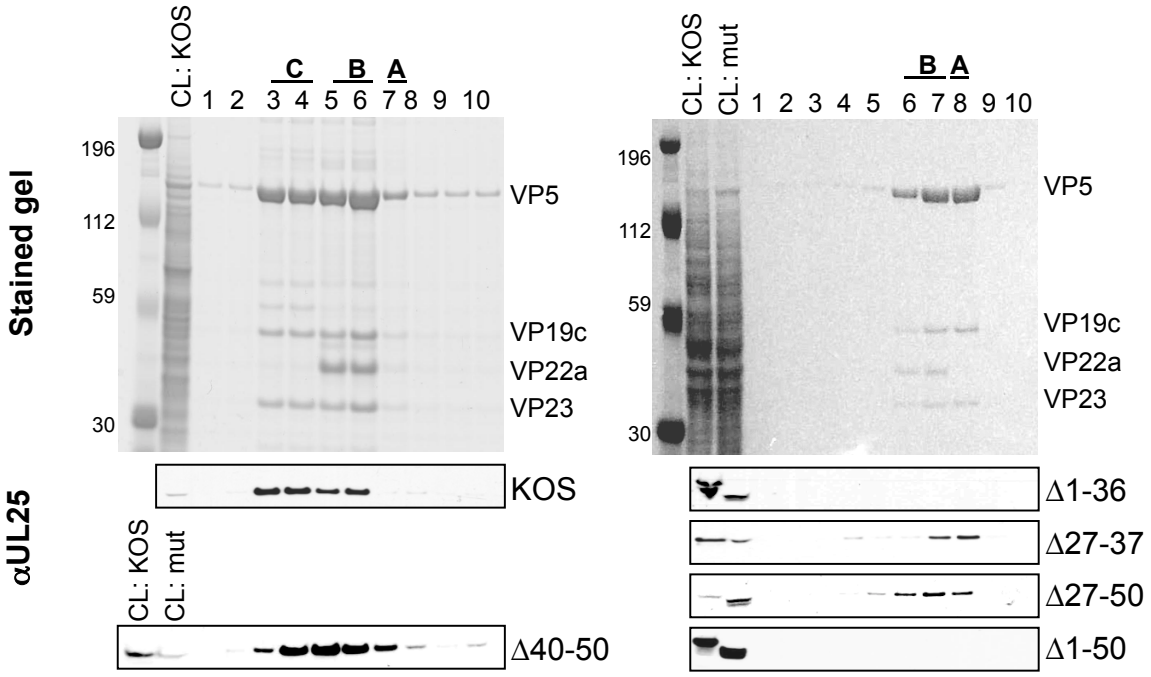

Figure 19. Deletion of amino acids 1-36 prevents pUL25 capsid attachment. Lane 1 is the bottom of the gradient, and lane 10 is the top. Gradient fractions that contained A-, B-, and C-capsids are indicated; the different capsid fractions can also be identified by the presence or absence of the scaffold protein, VP22a, since only B-capsids contain the scaffold protein. The positions of the capsid proteins (major capsid protein, VP5; triplex proteins, VP19C and VP23; scaffold protein, VP22a) are indicated. CL: cell lysate from KOS or UL25 mutant. The representative stained gels shown contain capsids isolated from KOS and the UL25-null virus vΔ27-50, respectively. Of the deletions within aa 1-50, only the aa 40-50 deletion did not preclude formation of C-capsids. (Bottom panels) Gradient fractions were analyzed by immunoblotting for UL25.

Gradients prepared with capsids from both the double point mutants vF26A I27A and vF35A W36A contained faint but visible bands of C-capsids, although the majority of capsids produced were the A- and B-types (data not shown). In each case, the gradient fractions containing C-capsids were positive for pUL25 by Western blot (Figure 20). The quadruple mutant vF26A I27A F35A W36A only produced A- and B-capsids. Immunoblots of the vF26A

I27A F35A W36A gradient fractions showed that these capsids contained very reduced amounts of pUL25 (Figure 20).

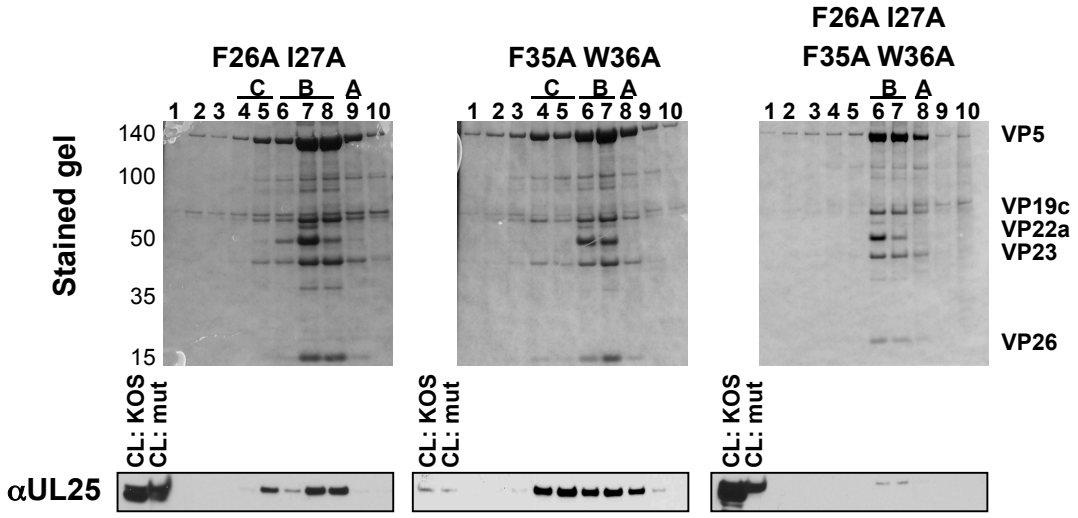

Figure 20. pUL25 point mutant capsid phenotypes. Capsids were prepared as previously described and observed as light-scattering bands on sucrose density gradients. Fractions from gradients were run on SDS-PAGE and tested for pUL25 by Western blot. Lane 1 is the bottom of the gradient, and lane 10 is the top. Gradient fractions that contained A-, B-, and C-capsids are indicated; the different capsid fractions can also be identified based on the presence or absence of the scaffold protein, VP22a, since only B capsids contain the scaffold protein. The positions of the capsid proteins (major capsid protein, VP5; triplex proteins, VP19C and VP23; scaffold protein, VP22a) are indicated. CL: cell lysate from KOS or UL25 mutant.

2.4.8 Point mutations of pUL25 aa26 and 27 or 35 and 36 block nuclear egress of capsids

The viruses vF26A I27A and vF35A W36A clearly exhibited defects in viral replication (Figure 18), but the production of C-capsids by these viruses was inconsistent with a null DNA packaging phenotype. Very small plaques were observed on Vero cells during titering of the vF35A W36A virus stock (data not shown), suggesting that the reduced viral replication may have been due to a defect in cell-to-cell spread. We postulated that the point mutations at amino

acids 26, 27, 35, and 36 interfered with capsid transport after packaging, causing an accumulation of C-capsids in infected nuclei or in other sub-cellular compartments.

To investigate the possibility that the point mutations F26A I27A and F35A W36A inhibited primary or secondary envelopment of capsids after DNA packaging, Vero cells were infected with either point mutant, fixed, and prepared for imaging by thin-section electron microscopy. The location of capsids in these infected cells was compared to those found in wt KOS-infected cells or cells infected with the viruses vΔUL25 and vF26A I27A F35A W36A, which are both deficient in DNA packaging. In wt-infected cells, scaffold-containing B-capsids and DNA- containing C-capsids were visible in the nuclei of infected cells (Figure 21, dashed and black arrows). Wt C-capsids were also observed as unenveloped particles in the cytoplasm, in enveloped inclusions in the cytoplasm, and in virions in the extracellular space. The UL25 deletion mutant produced A- and B-capsids—and an occasional C-capsid—that were all contained in the nucleus (Figure 21E). In the replication-defective but DNA packaging-competent point mutants vF26A I27A and vF35A W36A, A-, B-, and C-capsids were visible in the nucleus but not the cytoplasm (Figure 21A and B). During infection of Vero cells with the quadruple point mutant vF26A I27A F35A W36A, many of the cells fused to form syncytia that were visible under the light microscope. In thin-sections, multi-nucleated cells were observed in which up to five nuclei were adjacent to each other. We observed many C-capsids in the nuclei of cells infected with this virus (Figure 21C). This result was surprising because we could not purify C-capsids from Vero cells infected with vF26A I27A F35A W36A, and the A- and B-capsids that were present in the gradients contained very reduced amounts of pUL25 (Figure 20). These data suggest that point mutations within the highly conserved region of the pUL25 N-

terminus destabilize the pUL25 connection to the capsid, leading to detachment of the protein and destruction of C-capsids during purification.

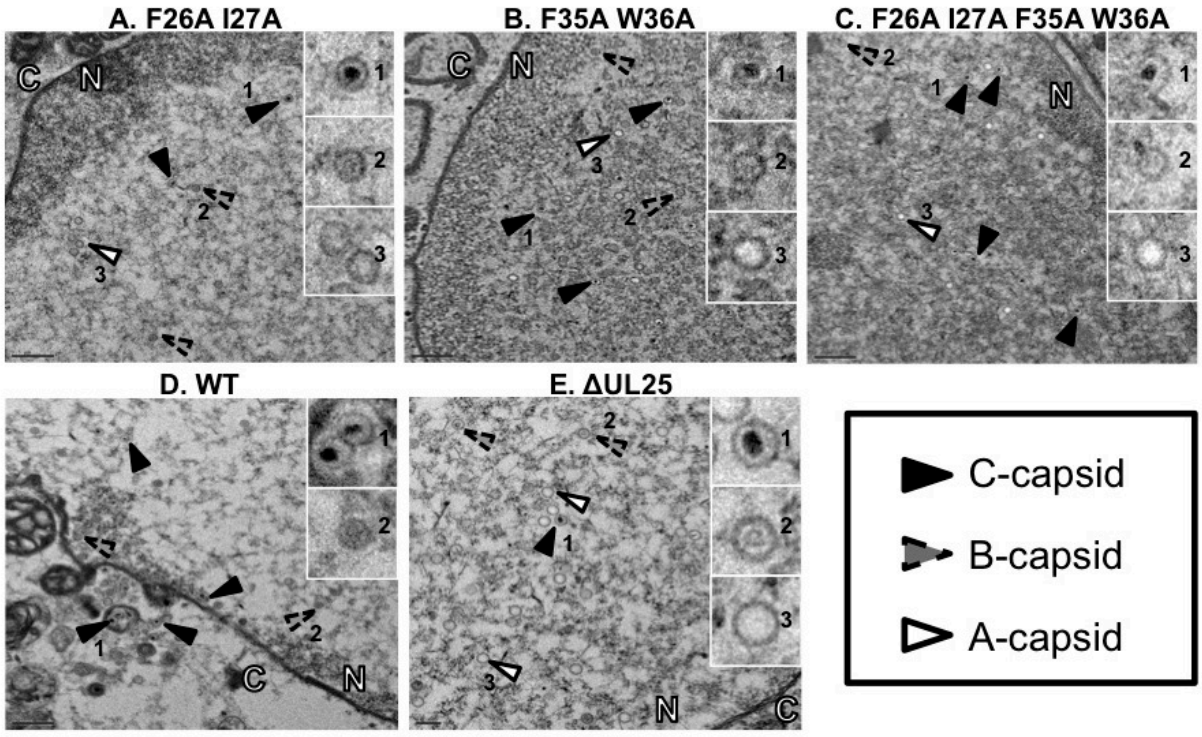

Figure 21. Thin-section electron microscopy. Vero cells were infected at a MOI of 5 and incubated to 18 hpi. Cells were fixed, sectioned, and embedded on carbon grids for imaging. White arrows, A-capsids. Dashed arrows, B-capsids. Black arrows, C-capsids. The nucleus and cytoplasm are marked with N and C, respectively. A-D. 4400x magnification, scale bar 0.5um. E. 6500X magnification, scale bar 0.2 um. Insets show C-capsids (1), B-capsids (2), and A-capsids (3).

2.5 DISCUSSION

The HSV-1 UL25 protein is one of seven viral proteins that are required for DNA cleavage and packaging. pUL25 is found near of the vertices of DNA-containing C-capsids. The capsid-bound

pUL25 appears to be a multifunctional protein required (i) to stabilize capsids after DNA is packaged; (ii) to trigger nuclear egress of the capsid once a stable DNA-containing capsid is formed; (iii) to anchor VP1/2, the major tegument protein to capsids; and (iv) to uncoat the incoming viral genome early during infection (32, 121, 137, 169, 205, 224). Random mutagenesis of the HSV-1 UL25 gene was used to identify regions of UL25 protein important for virus replication and for pUL25 capsid attachment. Although the five amino acid insertions disrupted core portions of the folded protein, most UL25 transposon mutants were able to complement the UL25 deletion virus. Four mutants (12s, 143i, 212s, 560s) were defective in the complementation assay. Insertion of stop codons after amino acids 212 and 560 resulted in the expression of nonfunctional truncated proteins that attached to capsids *in vitro* and when expressed from a recombinant virus. Similarly the 143i insertion mutant expressed a nonfunctional protein that failed to complement the UL25-null virus but retained the ability to bind capsids. The 12s mutant was predicted to encode a small UL25 peptide, but *in vitro* translation of the 12s plasmid produced a nearly wild-type-size protein that did not bind to capsids. Examination of the UL25 DNA sequence indicated that the resulting protein was probably the result of translation initiation at an internal start codon (M37) in the UL25 gene. This result was confirmed by constructing a UL25 mutant in which the codons for amino acids 1 to 37 were deleted and replaced with an ATG codon. *In vitro* translation of this construct produced a protein the same size as the 12s mutant that also failed to bind capsids. Deletion of the UL25 N-terminus to amino acid 50 eliminated *in vitro* capsid binding; conversely, the UL25-TAP fusion protein containing UL25 amino acids 1 to 50 was able to bind capsids *in vitro*. A recombinant virus expressing the UL25 51–580 protein was replication defective and produced capsids lacking the virus-expressed mutant protein, suggesting that the capsid binding domain

resides solely within amino acids 1 to 50. This conclusion was supported by the capsid-binding studies in which the UL25 1-50-TAP protein was shown to bind capsids (Figure 11C). Taken together, these data indicate that amino acids 1 to 50 are necessary and sufficient for pUL25 capsid binding and therefore comprise the pUL25 capsid-binding domain. In order to rule out the possibility that deletion of the N-terminus caused aberrant localization of pUL25, indirect immunofluorescence was used to track pUL25 in infected cells. Δ1-50 pUL25 was properly localized to the nucleus, indicating that while the deletion blocked attachment to capsids, it did not prevent the interactions required for transport of the protein to the nucleus. Furthermore, binding of pUL25 to the capsid through the N-terminal capsid-binding domain is not sufficient for virus production. The two truncation mutants v212s and v560s both express proteins that associate with capsids, but these mutants do not produce infectious virus, indicating that the final 19 amino acids of UL25 are also essential for function.

Within the putative capsid-binding domain, the most highly conserved residues lie between HSV-1 aa 26-39. Small deletions and point mutations were made through amino acids 1-50 in order to further define the capsid-binding domain and to determine the importance of the highly conserved residues for pUL25 function. While deletion of aa 1-36 prevented capsid attachment, deletion mutants missing aa 27-37 or 27-50 were capsid-associated. Point mutations of four of the highly conserved residues—aa 26, 27, 35, and 36—generated mixed phenotypes. These mutants did not replicate well on Vero cells, as determined by single-step growth curves. The double point mutants vF26A I27A and vF35A W36A produced C-capsids that were positive for pUL25, but the quadruple mutant vF26A I27A F35A W36A appeared to be a typical UL25 null virus, in that only A- and B-capsids could be purified from infected cells. On Western blots of these A- and B-capsids, only a very faint pUL25 immunoreactive band was observed.

Although we did not test each of the smaller deletion mutants in the indirect immunofluorescence assay, we expect that mutations within aa 1-50 that prevented capsid attachment—Δ1-36 and F26A I27A F35A W36A—represent disruptions of pUL25 interaction with the capsid but not its localization to the nucleus, since deletion of amino acids 1-50 did not mislocalize pUL25. Unexpectedly, we found that cells infected with vF26A I27A F35A W36A contained many intranuclear C-capsids. These data suggest that the F26A I27A F35A W36A mutation renders the pUL25 connection to the capsid—and hence, the packaging of viral DNA—very tenuous. Purification of vF26A I27A F35A W36A capsids caused detachment of pUL25 and conversion of unstably packaged C-capsids to A-capsids. Interestingly, thin-sections of cells infected with the deletion mutant vΔ27-37 contained only intranuclear A- and B-capsids (data not shown); pUL25 was detected on these purified capsids by Western blot. Therefore, it appears that deletion—but not substitution—of the hydrophobic residues between pUL25 aa 26-36 was tolerated with respect to pUL25 capsid attachment.

Atomic force microscopy has been used to measure the force required to puncture A-, B-, and C- capsids (183). A- and C-capsids exhibit almost the same resistance to disruption, but B-capsids are broken with much less force. These results suggest that although scaffold proteolysis and DNA packaging are thought to be concomitant, it is scaffold removal, and not DNA insertion, that catalyzes the structural transformation and stabilizes the capsid. Furthermore, removal of the penton vertices of all capsid types by treatment with guanidine hydrochloride equalized the force required to disrupt the capsid, suggesting that the distinguishing structural features of the angularized capsid are the vertices containing the pUL17/pUL25 heterodimer. It would be interesting to use this assay to test pUL25 null mutants that do not support DNA packaging but do remain able to bind capsids. It is possible that these mutations inhibit pUL25

ability to buttress the vertex by interrupting its attachment to pUL17 or other capsid proteins. Thus, we would expect that A-capsids of mutants vΔ27-37, vΔ27-50, vF26A I27A, vF35A W36A, and vF26A I27A F35A W36A would break with less force than the wild type A-capsid.

Analysis of the crystal structure of pUL25 (amino acids 134 to 580) showed that UL25 protein consists of numerous flexible loops extending from a rigid core composed of several tightly packed alpha helices (19). We expected that mutations disrupting any of the alpha helices located in the core would alter the overall structure of the protein and hence inhibit its function. However, most of the transposon mutants isolated in this study contained insertions in the pUL25 core that did not reduce function of the plasmid-expressed mutant protein. For example, the 354i and 538i mutations were both located in internal alpha helices, but neither of these mutations caused significant reduction in complementation of the UL25-null virus. The 143i, 151i, and 155i insertion mutations occur within a region where the predicted amino acid sequence is strongly conserved within homologues of the UL25 gene of other herpesviruses. In the folded protein, this region is part of a loop that bridges the unstructured N-terminus (residues 1 to 45) with the highly structured C-terminus (residues 133 to 580); there are two small antiparallel beta sheets located between amino acids 133 and 155 (19). The 143i insertion maps to the turn between the two beta sheets, and the 151i insertion occurs shortly after the end of the second beta sheet. The 155i insertion is located within the first alpha helix found in the core structure. Interestingly, the 143i and 155i insertions altered virus replication, but the 151i insertion did not. Our results suggest that this region does not contribute to capsid binding but is important for UL25 function, possibly as a bridge from the flexible capsid- binding region (residues 1 to 50) of UL25 to the more structured C-terminus. Other structural features of UL25 protein include electropositive and electronegative faces and clusters of conserved surface

residues (19). The 151i and 155i mutations are located in the electropositive face of UL25, while the other mutations occur along the periphery or in the interior of the folded protein. The 151i and 155i mutations also fall within one of the conserved surface clusters identified by Bowman *et al*. (19).

A recent report detailed the significance of the loop domains and conserved surface clusters of pUL25 for DNA packaging and capsid incorporation into virions (147). O'Hara *et al*. reported that point mutations between aa 396-402 or deletion of aa 417-425 of pUL25 allowed DNA packaging but inhibited nuclear egress of capsids; this defect was characterized by an accumulation of C-capsids in nuclei. We observed a similar phenotype in our point mutants vF26A I27A and vF35A W36A. C-capsids produced by vF26A I27A and vF35A W36A were stable and could be purified from cells. The double point mutations appeared to inhibit capsid egress from the nucleus without significantly reducing pUL25 capsid attachment or DNA packaging. Thus, the residues at pUL25 positions 26, 27, 35, and 36 also may be involved in egress of capsids from the nucleus. Another interesting mutant described by O'Hara *et al*. was deleted of aa 578-580 and released virions that were defective in propagating infection into the extracellular space (147). In contrast, our v560s mutant, deleted of aa 561-580, completely eliminated DNA packaging and accumulated A-capsids that were visualized in micrographs of infected cells (not shown). Taken together, these data indicate that both the N- and C-termini of pUL25 are important for capsid stability and transport.

3.0 STRUCTURAL ANALYSES OF CAPSIDS CONTAINING PUL25 FUSION PROTEINS DEMONSTRATE THAT THE PUL25 N-TERMINUS CONTACTS HEXONS AND TRIPLEXES ADJACENT TO THE PENTON

3.1 ABSTRACT

The HSV-1 virion is a large macromolecular complex that is engaged in a dynamic set of interactions. These interactions coordinate the attachment, removal, rearrangement, and deconstruction of virion components in a precise temporal manner in order to propagate the virus lytic cycle. Studies of virion composition and structure have elucidated many aspects of the viral replication process, including virus attachment and entry, capsid assembly, and tegumentation. The DNA packaging protein pUL25 is located on the exterior surface of HSV-1 capsids on their vertices. Previous reports have shown that pUL25 interacts with the capsid structural proteins pUL19 (VP5) and pUL38 (VP19c) and that it incorporates the packaging protein pUL17 into capsids. Because definition of pUL25 location on the capsid surface—and consequently, identification of the interactions required for that placement—are important for elucidating the mechanisms by which pUL25 supports DNA packaging, we have visualized the connections between the pUL25 capsid-binding domain and the capsid. Cryoelectron microscopy and 3D image reconstructions were performed with capsids containing pUL25 fused at or near its N-terminus to GFP or to a tandem affinity purification (TAP) tag. In the composite image of

NTAP-UL25 and GFP-UL25 capsids, the precise location of pUL25 was visualized. The pUL25 capsid-binding domain appears to make contact with the triplexes and hexons adjacent to the penton vertex.

3.2 INTRODUCTION

The HSV-1 virion consists of 44 different viral proteins and many host cell proteins, and it can be segregated into three major compartments: the host-derived lipid envelope, the tegument protein layer, and the nucleocapsid (112). The first structural analysis of HSV-1 was completed by negative staining and transmission electron microscopy of purified virions. From these micrographs, it was determined that the HSV-1 capsid is angular with icosahedral symmetry, and its 162 subunits, or capsomers, are composed of 5- and 6-membered rings (pentons and hexons) (238). The capsid structural proteins were identified by SDS-PAGE analysis of infected cells and purified virions. Following sequencing and annotation of the complete HSV-1 genome, the gene products that constituted these structural proteins were designated (70, 118, 198). The major constituent of capsids is pUL19 (VP5), which forms the hexameric and pentameric capsomers. The other predominant structural proteins are pUL18 (VP23) and pUL38 (VP19c)—which together form a heterotrimer termed the "triplex" that lodges between capsomers—and pUL35 (VP26), which decorates the outer surfaces of hexons. Other minor components of capsids—including the DNA packaging proteins pUL6, pUL25, and pUL17—were discovered by Western blot analysis of purified capsids (192, 216, 252).

Several strategies have been used to define the arrangement of the capsid proteins. In the initial attempts, capsids were reacted with antibodies raised against individual capsid proteins.

Electron microscopy and biochemical analyses of these antibody-coated capsids proved that the capsomers were made of the largest capsid protein, pUL19, and that pUL19 adopted distinct conformations in hexons and pentons (31, 223, 230). More recently, EM mapping studies with monoclonal antibodies have located the portal protein, pUL6, and the packaging proteins, pUL17 and pUL25, at capsid vertices (24, 137, 143, 148, 216). Other methods for resolving the organization of capsid proteins involved chemical extraction of parts of the capsid, with visualization and biochemical identification of the proteins that remained (17, 134, 135, 145). Extraction of capsid components was achieved by exposing B-capsids to an ionized argon beam, guanidine hydrochloride (GuHCl), or urea, and the composition of the depleted capsids was ascertained by SDS-PAGE. Treated capsids retained their overall structure so that changes in capsid morphology could be observed by electron microscopy. Plasma etching of capsids revealed that pUL18, pUL19, and pUL38 were the first proteins removed, suggesting that these components were readily accessible on the capsid surface; removal of the scaffold proteins pUL26 and pUL26.5 required longer exposure times and probably occurred after the capsid was stripped of the outer proteins (135). In contrast, B-capsids treated with guanidine hydrochloride or urea lost most of the pUL26 and pUL26.5 while pUL18, pUL19, and pUL38 remained mostly intact (134, 145). Subsequent cryo-electron microscopy and 3D reconstruction of these capsid structures showed that GuHCl or urea treatment removed the vertices, allowing pUL26 and pUL26.5 to escape. In sum, these studies defined the internal scaffold as consisting of pUL26 and pUL26.5, while pUL18, pUL19, and pUL38 formed the external capsid lattice. Furthermore, the stoichiometry of the capsomers was elucidated; changes in the mass and protein composition of treated capsids could only be accounted for if both the pentons and hexons were made of pUL19 and the triplexes were made, on average, of two copies of pUL18 and one copy

of pUL38. Using similar methods, the small capsid protein pUL35 was traced to the outer tips of hexons but not pentons (17). More recently, genetic deletion of capsid components has allowed assignment of structural features to the capsid proteins that form them without destruction of the native capsid (27, 184, 255). Difference imaging techniques have been used also to describe the contacts between the capsid and the tegument and the asymmetry of the tegument within the virion (27, 73, 253). Finally, *in vitro* assembly studies have been carried out with HSV-1 capsid proteins expressed from Baculovirus and purified from infected insect cells (138-141, 143, 144, 220) (see Section 1.5). *In vitro* studies of pUL6 showed that the capsid portal is a dodecamer ring of pUL6; formation of the portal precedes the accumulation of scaffold proteins into the procapsid. Additionally, these studies elucidated the transition between procapsid and mature capsid forms, including the rearrangements of pUL19 and the addition of the triplex proteins onto the procapsid floor.

The HSV-1 UL25 gene product is a 580 amino acid, 62 kDa protein that contains an unstructured N-terminal tail and core of packed alpha helices (19). UL25 protein (pUL25) attaches to the external vertices of HSV-1 capsids with a capsid-binding domain that is located within its first 50 amino acids (30, 137, 224) (see Chapter 2). Based on comparative structural and biochemical analyses of wt and UL25-null capsids, pUL25 is predicted to form a heterodimer with the packaging protein pUL17 (216, 224). The putative pUL25-pUL17 complex—called the C-capsid specific component (CCSC)—is present in up to five copies at each capsid vertex and contacts the two triplexes and the hexons adjacent to the penton. While formation of the pUL25-pUL17 complex is independent of interactions with other structural proteins (188), pUL25 has several other potential binding partners at the capsid vertex: the major capsid protein pUL19 in pentons and hexons, and the triplex proteins pUL18 and pUL38.

Immunoprecipitation and far-Western assays have shown that pUL25 interacts directly with pUL19 and pUL38, suggesting that the CCSC connection to pUL18 is mediated by UL17 (148, 188). Additionally, transiently expressed pUL25 immunoprecipitates pUL6, which forms a dodecameric ring that serves as the portal of entry for DNA into the procapsid (143, 156, 221). It has yet to be determined if and how pUL25 binds to the capsid-integrated portal, or what importance this potential interaction might have for DNA packaging.

In this study, recombinant viruses were generated that expressed UL25 protein fused to either green-fluorescent protein (GFP) or a tandem affinity purification (TAP) tag. Each of these fusions served a dual purpose. First, tagged pUL25 could potentially be isolated from other viral proteins in infected cells. While GFP-fused pUL25 could be tracked in cells by fluorescence microscopy, TAP-tagged pUL25 could be purified by affinity chromatography. Secondly, the tags added extra density to the pUL25 N-terminus in cryo-electron micrographs, facilitating pUL25 location in 3D reconstructions of capsids. Based on the crystal structure of truncated pUL25, pUL25 was predicted to occupy the penton-distal region of the CCSC (224). Using the GFP and TAP tags as markers of the pUL25 N-terminus in capsid reconstructions, the location and orientation of pUL25 on the capsid surface has been mapped. pUL25 is present in the penton-distal region of the CCSC, as previously suggested, and its N-terminal capsid-binding domain makes contact with hexons and triplexes adjacent to the penton vertex.

3.3 MATERIALS AND METHODS

3.3.1 Cells, viruses, and antibodies

African green monkey kidney cells (Vero; American Type Culture Collection, Rockville, MD) and UL25-transformed 8-1 cells (121) were propagated in 5% FBS/DMEM with penicillin (10U/ml) and streptomycin (10μg/ml) at 37°C and 5% CO_2. HSV-1 wild-type KOS virus has been previously described (121). Baculovirus-expressed UL25 protein (121) was purified and used to prepare a UL25 monoclonal antibody, 25E10, that was provided by W. Newcomb, University of Virginia (33).

3.3.2 Introduction of GFP and the TAP tag into the virus genome

To create specific UL25 mutations, the HSV-1 KOS BAC clone was transferred to GS1783 bacteria (gift from G. Smith), and mutagenesis was performed using the two-step bacteriophage Red-mediated homologous recombination system described by Tischer *et al*. (218). PCR with template plasmids p-EGFP-in or p-EP-TAP-in (gift from P. Kinchington) was used to produce a construct that contained the Kan^R gene (alphAI) flanked by UL25 homologous sequences and repeat sequences containing the desired insertion. Integration of this construct into the BAC was followed by a second recombination that removed alphaAI and left the seamless insertion within the UL25 gene. Resolution of the integrated PCR product resulted in insertion of the GFP gene between UL25 codons 50 and 51 and the TAP sequence before UL25 codon 1. The list of primers for production of PCR amplicons that were used for isolation of the UL25 insertion mutants can be found in Table 10 (Appendix A). To confirm mutations in UL25 mutant viruses,

viral DNA was amplified by PCR with the primers 5'-GCAGAAGGTCTCCGG TAATATCACC-3' and 5'-GGTGATCAGGTACAACAGGCGCTC-3'. The PCR product was extracted from agarose gels and used for restriction digest and for sequencing with primers 5'-GCGGCGGCCGCAAGACTCATTTGGATCCG-3' and 5'-TCTCCGCGACGGCCAGAC-3' (GeneWiz sequencing facility).

3.3.3 Virus generation and propagation

To recover mutant viruses, BAC DNA (5 μg) was transfected into 8-1 cells with Lipofectamine. Recombinant viruses were harvested from transfected cell lysates and were plaque purified three times on Vero cells. The third round plaque isolate was used to generate a mini-stock of virus in a T25 flask of Vero cells. Cell lysates were freeze-thawed, and virus mini-stock concentrations were determined by plaque assay on Vero cells. Briefly, serial dilutions of virus preparation were absorbed to cells for 1 h, then incubated on cells three days under methylcellulose. Plaques were counted after staining cells with crystal violet (0.1% in 50% ethanol). To prepare a large stock of virus, 1.5 x 10^8 Vero cells were infected at a multiplicity of infection (MOI) of 0.01. At 3 days post-infection, cell lysates were harvested by freeze-thaw. Clarified cell lysates were centrifuged at in a Sorvall SS34 rotor at 10000 RPM for 2 h to pellet virions from the media. The virion pellet was resuspended in 10% glycerol/DMEM overnight on ice. The resultant virus stock was titrated on Vero and 8-1 cells.

3.3.4 Preparation of viral DNA

Viral DNA was prepared essentially as described in (21), with the following modifications. A T-175 flask of Vero cells (3 x 10^7 cells) was infected with virus at a MOI of 1 PFU per cell. At 48 h post-infection, the medium was removed and the cells were washed in 1x PBS, scraped off the plate, and pelleted. The cells were resuspended in TE and lysed in Triton X-100 (1.5%) on ice for 15 minutes. Nuclei were pelleted by centrifugation at 2000rpm for 10 minutes and subsequently discarded. Virus was lysed by incubation at 50°C with SDS (0.5%) and Proteinase K (0.5μg/μl) for 1 h. DNA was extracted with phenol twice and chloroform once before being precipitated with 1/10 volume sodium acetate and 2 volumes ethanol. Pelleted DNA was dried and resuspended in TE or sterile ddH_2O with RNAse A.

3.3.5 Immunoblotting

Protein extracts were separated on a 5 to 12% SDS–polyacrylamide gel and transferred to nitrocellulose. The nitrocellulose was washed in Tris-buffered saline (TBS) and blocked overnight or 1 h at room temperature in T-TBS (20 mM Tris, 0.5 M NaCl [pH 7.5] plus 0.5% Tween 20) supplemented with 10% nonfat dry milk. The UL25 monoclonal antibody, 25E10 was diluted to 1:5000 in blocking buffer. The diluted antibody was reacted with the blocked nitrocellulose for 1 h at room temperature, washed 6 times in T-TBS, and reacted with horseradish peroxidase-conjugated anti-mouse immunoglobulin G (IgG) diluted at 1:5000 in blocking buffer. The bound Igs were revealed by enhanced chemiluminescence (Pierce ECL kit).

3.3.6 Capsid preparation

Vero cells (1.5 x 10^8) were infected overnight (18 h at 37°C) at a MOI of 5 PFU/cell. Infected cells were harvested, rinsed with PBS, and resuspended in 20 mM Tris (pH 7.5) plus protease inhibitors (Roche), adjusted to 1% Triton X-100, and incubated for 30 min on ice. The resulting nuclei were harvested by low-speed centrifugation, resuspended in 10 ml TNE (500 mM NaCl, 10 mM Tris, 1 mM EDTA [pH 7.5]), and then sonicated to lyse the nuclei. The nuclear lysate was adjusted to 20 mM $MgCl_2$ and incubated with DNase I (100 μg/ml) at room temperature for 30 min. The lysate was then cleared by low-speed centrifugation, and the resulting supernatant was layered on top of a 10-ml cushion of 35% sucrose (SW28 rotor; 23000 rpm for 1 h). The pellets were suspended in 3 ml TNE and adjusted to 1 mM dithiothreitol, and capsids were separated by centrifugation on 20 to 50% sucrose (in TNE) gradients (SW41 rotor at 24000 rpm for 1 h). The positions of A-, B-, or C-capsids were observed as light-scattering bands, with A-capsids being found highest (least dense) on the gradient and C-capsids found lowest (dense fractions) on the gradients. The fractions were collected using a Beckman fraction recovery system (Beckman catalog no. 34890). The apparatus has a mechanism to puncture the bottoms of the tubes, and fractions are collected from the bottom to top. Fractions (0.75 ml) were collected, and protein was precipitated by adding an equal volume of 16% trichloroacetic acid. Pellets were resuspended in 35 μl of 2x PAGE loading buffer (Invitrogen) supplemented with 0.4 M Tris-base. Gradient fractions were run on 5 to 12% SDS-PAGE, and the gels were either stained with Imperial blue (Pierce) to visualize capsid proteins or analyzed by immunoblotting with the UL25 (25E10) antibody. On the stained gel, the different capsid types were identified based on the presence or absence of the scaffold protein, VP22a, since only B-capsids contain the scaffold protein.

To isolate capsids for cryo-electron microscopy, capsid bands were collected from sucrose gradients, diluted 1:4 in TNE, and pelleted for 1hr (SW41 rotor, 24000 rpm). Capsid pellets were resuspended overnight in a low volume (50μl) of low salt TNE (150 mM NaCl). Samples were prepared for cryo-electron microscopy (cryo-EM) by James Conway and Katerina Toropova (University of Pittsburgh, Department of Structural Biology) as described (33). Cryo-EM and image analysis was performed by James Conway (UL25-GFP) and Katerina Toropova (NTAP-UL25 and composite images).

3.4 RESULTS

3.4.1 Generation of viruses expressing GFP-UL25 and NTAP-UL25 fusion proteins

In order to facilitate the location of pUL25 on the capsid surface, viruses were generated that expressed pUL25 fused to either GFP or a tandem affinity purification (TAP) tag. The 234bp TAP sequence encoded a calmodulin-binding peptide, linker, and streptavidin-binding peptide (Figure 22). Insertions to the UL25 ORF were recombined into a HSV-1 (KOS) genome maintained in a bacterial artificial chromosome (BAC). BAC recombination resulted in targeted insertion of the GFP gene in-frame between codons 50 and 51 of the UL25 gene (Figure 23A). The TAP tag was inserted into the UL25 ORF in-frame before UL25 codon 1. Thus, each insertion was adjacent to the putative capsid-binding domain of pUL25 (aa 1-50).

To confirm insertion of these sequences, BAC DNA was digested with *Bam*HI and analyzed by agarose gel electrophoresis. The UL25 ORF is contained within the 2.3 kbp *Bam*HI U fragment of HSV-1 DNA (118, 164), and in the restriction enzyme digestion of the KOS-BAC

preparation, a prominent 2.3 kbp fragment was observed (Figure 23B, black arrows). The UL25-GFP BAC contained an additional 726 bp in UL25, which was detected as an upward shift in the mobility of the *Bam*HI U fragment (Figure 23B). Likewise, the NTAP-UL25 BAC *Bam*HI U fragment was shifted to a molecular weight consisted with insertion of the 234 bp TAP sequence. These results demonstrated that that the UL25 mutant BACs had the desired insertions.

NTAP-UL25 1 **MKRRWKKNFIAVSAANRFKKISSSGAL***GSGSGT*MDEKTTGWRGGHVEGLA 50
51 GELEQLRARLEHHPQGQREPSGGCKLGMDPYCPFDALDVWEHRRFIVADS 100

Figure 22. Amino acid sequence of the N-terminus of NTAP-UL25 protein. The TAP tag (Stratagene) is inserted between pUL25 amino acids 1 and 2. Bold, calmodullin-binding peptide; italic, linker peptide, underline, streptavidin-binding peptide.

To recover viruses, BACs were transfected onto UL25-complementing 8-1 cells. Transfected cell lysates were freeze-thawed and re-plated on Vero cells. Single plaques were isolated during three subsequent rounds of virus purification on Vero cells. From these clonal plaques, virus stocks of vUL25-GFP and vNTAP-UL25 were prepared as described in Materials and Methods. To determine the concentration of virus particles in each stock, virus preparations were titrated on Vero and 8-1 cells. The virus stock concentrations, expressed as plaque-forming units (PFU) per ml, are listed in Table 8. The virus yield calculation was similar for both cell lines tested (Vero and 8-1) for both the vUL25-GFP and vNTAP-UL25 viruses.

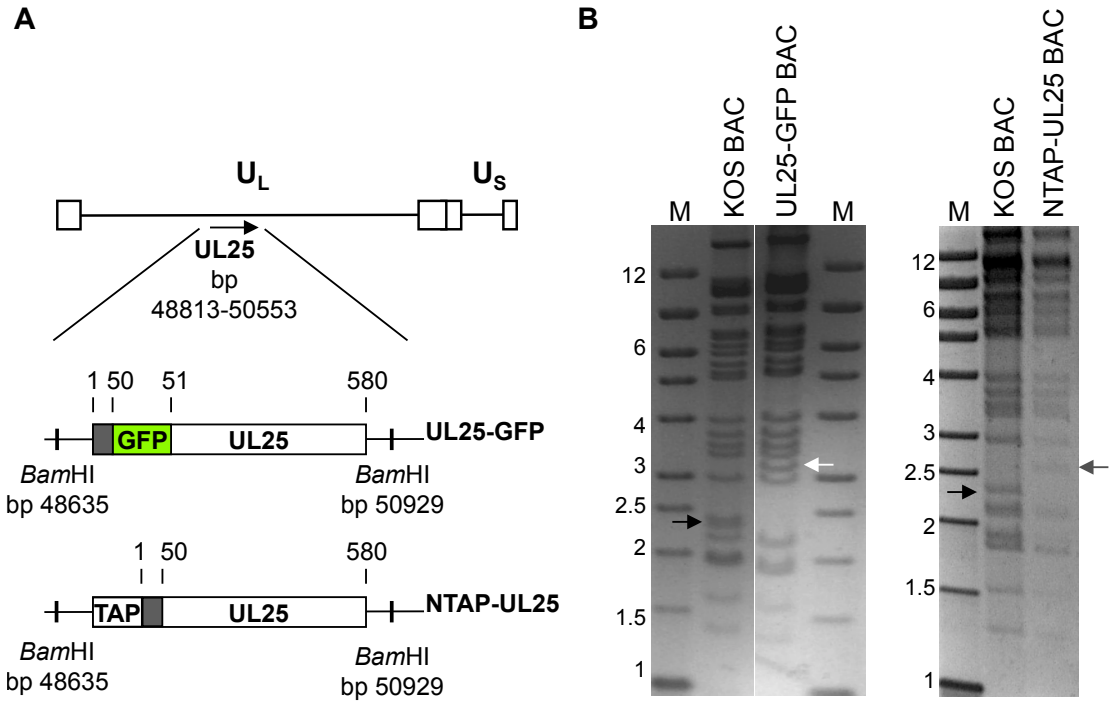

Figure 23. Insertion of GFP and TAP sequences to BAC DNA. A. (Top) Schematic representation of the HSV-1 genome and the UL25 locus at kbp 48813-50555. (Bottom) Diagram of the UL25 gene in UL25-GFP BAC and NTAP-UL25 BAC. Numbers above each box represent codon positions; numbers below the line are the nucleotide position within the viral genome. The UL25 gene is located within the *Bam*HI U fragment that contains nucleotides 48635-50929. The pUL25 capsid binding domain is encoded by codons 1-50 and is shown as a gray box. UL25-GFP BAC contained an in-frame insertion of the 726 bp GFP coding sequence after the codon for UL25 amino acid 50. NTAP-UL25 BAC had the 234 bp TAP sequence inserted in-frame before UL25 codon 1. B. BAC DNA was digested with *Bam*HI and run on a 1.2% agarose gel. The wild-type 2.3 kbp *Bam*HI fragment is present in the KOS BAC lanes (black arrows). The UL25 fragments of UL25-GFP BAC and NTAP-UL25 BAC are shifted to 3.2 kbp (white arrow) and 2.6 kbp (gray arrow), respectively. M, DNA markers in kbp.

TABLE 8. Virus stock titers: UL25-fusion mutants

Virus strain	UL25 protein expressed (amino acid positions)	PFU/ml in: Vero cells	8-1 cells
KOS	Wild type (1–580)	2×10^8	2×10^8
vUL25-GFP	UL25-GFP (1-50-GFP-51-580)	4×10^7	4×10^7
vNTAP-UL25	NTAP-UL25 (TAP-1-580)	3.4×10^7	3.2×10^7

The presence of the mutations in the progeny virus was verified by PCR and restriction digest. Viral DNA was prepared from infected cells and was amplified by PCR with primers that were external to UL25 (Figure 24A). Wt KOS, vUL25-GFP, and vNTAP-UL25 PCR products were then digested with the restriction enzymes *Not*I or *Sac*I, which cleaved within the wt UL25 gene near its 5' end. *Not*I digestion of the wt PCR product produced fragments of 0.9 and 1.9 kb (Figure 24B). Insertion of the GFP sequence in vUL25-GFP shifted the smaller fragment to 1.7 kb. Likewise, *Sac*I digestion of wt and vNTAP-UL25 PCR products showed that the smaller wt fragment (0.8 kb) is shifted to a higher molecular weight (1.1 kb) by the TAP sequence. Thus, both GFP and TAP sequences were present in the UL25 gene within the coding sequence for the N-terminus. These results were confirmed by sequencing of the PCR products through the 5' region of UL25.

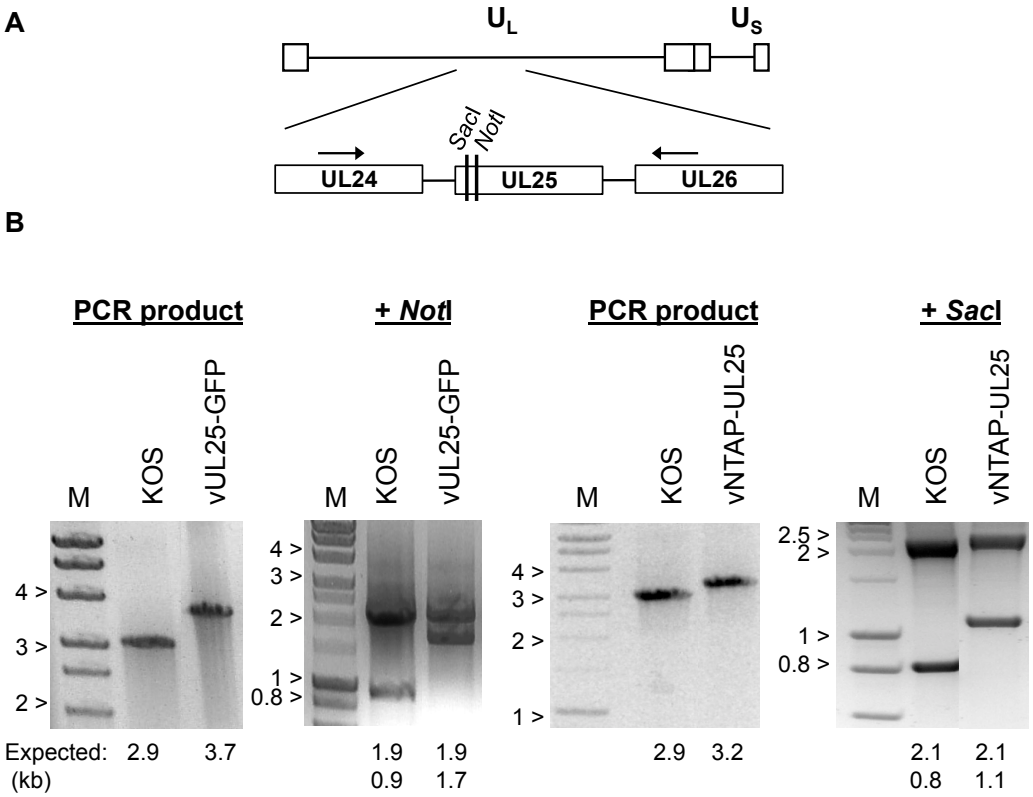

Figure 24. Confirmation of UL25 insertions in viral DNA. A. Diagram of the HSV-1 genome showing the 2.9 kb region amplified from viral DNA by PCR. Black arrows indicate the forward and reverse primers. The *Sac*I and *Not*I restriction sites are shown. B. PCR products were run on 1% agarose in TAE and stained with ethidium bromide. The GFP and TAP sequences added 0.8 kb and 0.3 kb to the PCR products of vUL25-GFP and vNTAP-UL25, respectively. PCR products were digested with the restriction enzymes *Sac*I or *Not*I, which cleaved near the coding sequence for the pUL25 N-terminus. The expected restriction fragments are listed below the gels. The shift in molecular weight of the 5' region of UL25 indicates that both insertions were at the N-terminus of the UL25 protein. Molecular weight markers are indicated in kbp.

Single-step growth curves were calculated for both viruses to determine if addition of GFP or TAP tags interfered with virus replication on Vero cells. Briefly, Vero cells were infected at a MOI of 3 with each virus. At 0, 2, 4, 8, 12, 24 and 30 hours post-infection, viral progeny in the cell lysates was harvested and quantified by plaque assay on Vero cells. Virus titers at times after the initial infection were then plotted to form a graphical representation of viral replication. Replication of vUL25-GFP was very similar to wt KOS (Figure 25). Additionally, vUL25-GFP plaques were observed to be fluorescent. These results indicated that the internal insertion of GFP to pUL25 aa 50-51 did not inhibit the expression or function of the protein.

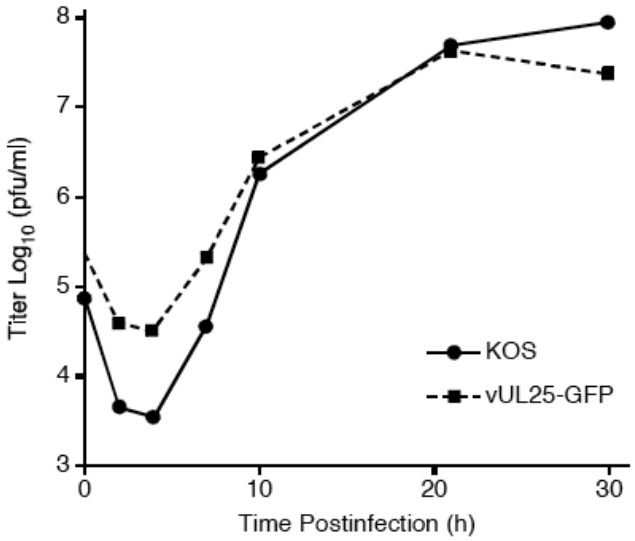

Figure 25. Analysis of vUL25-GFP viral replication. 1 x 10^6 Vero cells were infected with each virus at a MOI of 3 on ice for 1 h, rinsed twice with DMEM, and incubated in DMEM at 37° to the indicated timepoints. Cells were lysed by freeze-fracture, and viral progeny in cell lysates was quantified by titration and plaque assay on Vero cells. The results shown are averages of duplicate experiments. This figure was amended with permission from reference (33).

In contrast, replication of vNTAP-UL25 was diminished compared to wt beginning at 12 hours post infection, leading to a 100-fold reduction in viral progeny yields at 30 hours post infection (Figure 26A). The reduced growth of vNTAP-UL25 was also apparent in its plaque morphology. vNTAP-UL25 developed very small plaques on Vero cells that were difficult to ascertain by crystal violet staining (Figure 26B). The plaque size was on average 45% of wt, suggesting a deficiency in cell-to-cell spread.

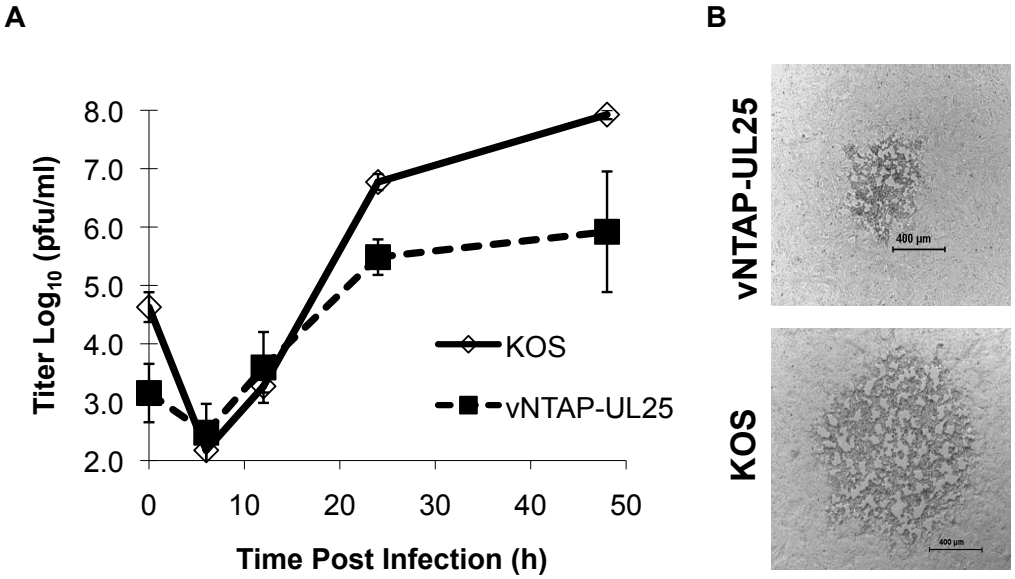

Figure 26. Analysis of vNTAP-UL25 viral replication. A. Single-step growth curve. 1 x 10^6 Vero cells were infected with each virus at a MOI of 3 on ice for 1 h, rinsed twice with DMEM, and incubated in DMEM at 37°C to the indicated timepoints. Cells were lysed by freeze-fracture, and viral progeny in cell lysates was quantified by titration and plaque assay on Vero cells. The results shown are averages of duplicate experiments. B. Comparison of vNTAP-UL25 and KOS plaque size at 3 days post-infection. Plaques were imaged at 50x magnification, and the diameter of each plaque was measured by Leica application software. The vNTAP-UL25 plaques were on average 45% of wt size (n=100). The scale bar is equal to 400 µm.

3.4.2 Association of tagged pUL25 with capsids.

The insertions were cloned into the UL25 ORF such that they flanked the pUL25 capsid-binding domain (aa 1-50; see Chapter 2). The TAP tag was at the amino-terminal end (aa 1) of the capsid-binding domain, and GFP was at the carboxy-terminal (aa 50). While the GFP insertion appeared to have no negative impact on pUL25 function, the diminished replication of vNTAP-UL25 could have been due to a disruption of the pUL25 capsid-binding domain. To ascertain if the capsid attachment of the UL25-GFP and NTAP-UL25 proteins were disrupted, intranuclear capsids were prepared from Vero cells infected with each mutant virus. Capsids were viewed as visible light-scattering bands on sucrose density gradients. The capsid preparations consisted mainly of C- and B-capsids, with a faint but observable A-capsid band. To determine whether the UL25 proteins were incorporated into these capsids, the sucrose gradient fractions were run on SDS-PAGE and analyzed by Western blot (Figure 27). Each of the tags was expected to shift the apparent molecular weight of pUL25. The GFP fusion protein contains an additional 239 aa, which corresponded to a 27 kDa molecular weight shift of pUL25 present in infected cell lysates (Figure 27). NTAP-UL25 protein ran with a smaller shift of 8.5 kDa (78 aa). Both GFP- and NTAP-UL25 proteins were observed on all capsid types, indicating that the capsid-binding domain of pUL25 was not obstructed by the GFP or TAP insertions (Figure 27, lower panels). Thus, while insertion of the TAP tag at the pUL25 N-terminus had negative effects on virus replication, it did not appear to alter the DNA packaging phenotype or the ability of the protein to attach to the capsid.

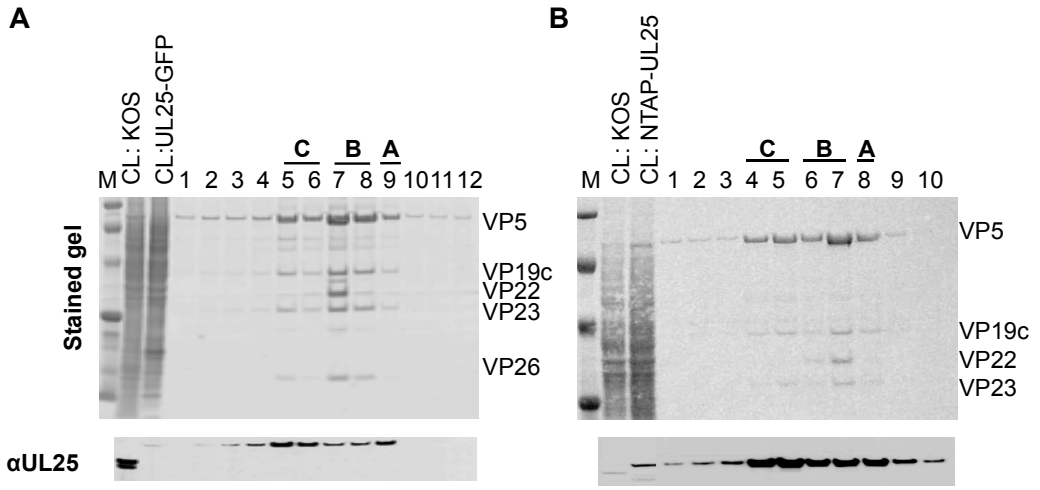

Figure 27. UL25-GFP and NTAP-UL25 proteins are capsid-associated. A. vUL25-GFP. B. v NTAP-UL25. Capsids purified from infected cells were separated on sucrose density gradients. (Top panels) Stained gels containing infected cell lysates and fractions from capsid gradients. Lane 1 is the bottom of the gradient, and lane 12 or 10 is the top. Gradient fractions that contained A-, B-, and C-capsids are indicated; the different capsid fractions can also be identified based on the presence or absence of the scaffold protein, VP22a, since only B-capsids contain the scaffold protein. The positions of the capsid proteins (major capsid protein, VP5; triplex proteins, VP19C and VP23; scaffold protein, VP22a) are indicated. CL: cell lysate from KOS, vUL25-GFP, or vNTAP-UL25. (Bottom) Gradient fractions were immunoblotted for pUL25. GFP adds 239 aa to pUL25, shifting the molecular weight by approximately 27 kDa. The TAP tag adds 78 aa (8.5 kDa) to pUL25.

3.4.3 Structural analysis of vGFP-UL25 capsids

To visualize the UL25-GFP protein on the capsid surface, purified B- and C-capsids of vGFP-UL25 were used for cryo-electron microscopy and 3D reconstruction. Cross-sections of C- and B-capsids produced by vUL25-GFP were then compared to the wt C-capsid (Figure 28, top panels). The C-capsid specific component (CCSC), which was previously identified on the wt C-capsid (224), is visible on the vUL25-GFP C-capsid as well; the vUL25-GFP B-capsid does not contain the CCSC. The vUL25-GFP C-capsid contains an extra density above the CCSC that was attributed to the GFP fusion in pUL25 (Figure 28A). In the surface views of these capsid

forms, the overall capsid morphology is similar, but there is no CCSC around the B-capsid penton (Figure 28, lower panels).

At the vGFP-UL25 C-capsid penton vertex, GFP is present as a globular domain that extends from the CCSC (Figure 29). The CCSC touches the proximal and distal triplexes and the hexon adjacent to the penton, and the GFP density contacts the underlying CCSC at its penton-distal region. Thus GFP localizes pUL25 within this region of the CCSC, confirming the placement by Trus *et al*. (224). GFP placement also allows prediction of the orientation of pUL25. Because the point of contact between pUL25 and GFP is at pUL25 amino acids 50-51, it appears that the pUL25 N-terminus makes contact with the capsid surface at the distal triplex, and another part of the CCSC touches the triplex proximal to penton. The exact orientation of pUL25 within the CCSC cannot yet be determined because the crystal structure of this portion of pUL25 is not available (19). In the model, GFP appears to occupy a larger volume of space than would be expected from its molecular weight. As shown in Figure 29D, GFP may adopt different positions as it pivots around its point of contact with pUL25. The larger-than-expected density in the reconstruction, therefore, is interpreted as being to the averaging of different positions of this flexible molecule.

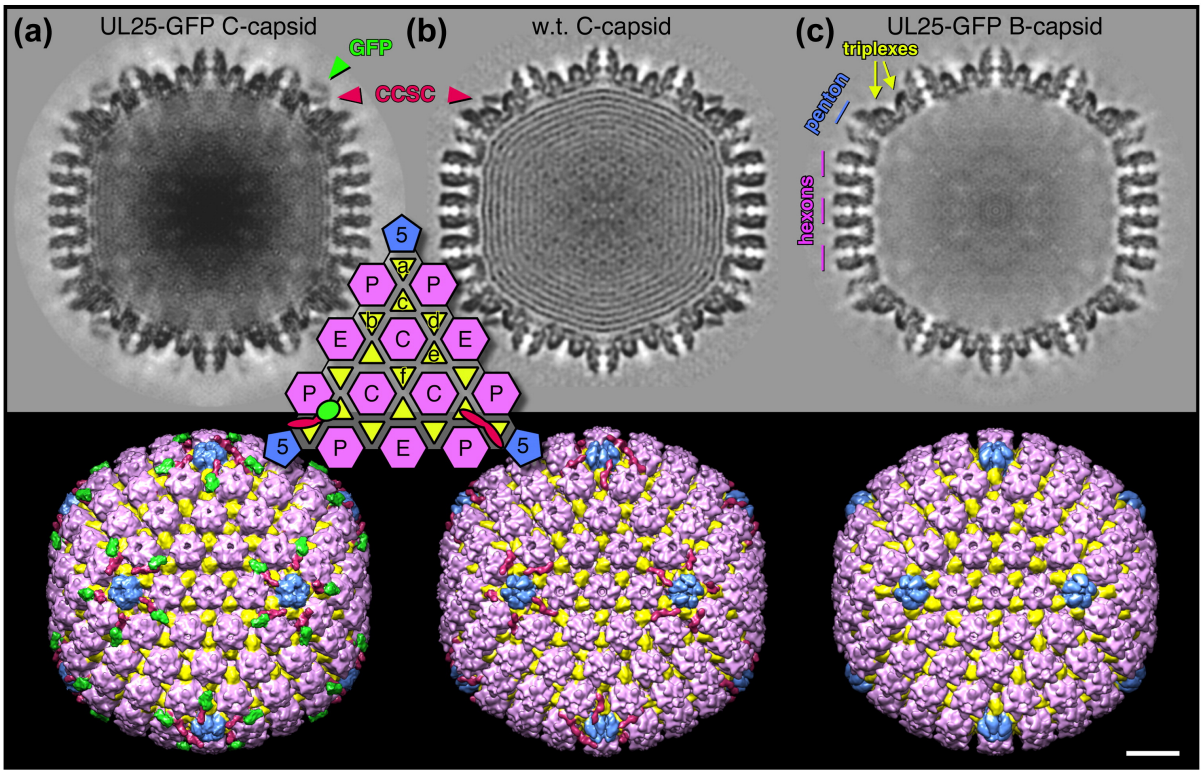

Figure 28. Density maps calculated from capsid micrographs. (a) C-capsids with UL25-GFP, (b) C-capsids with wt UL25 and (c) B-capsids that appear to lack the CCSC density as well as packaged DNA. Central sections are shown at top, and surface views along the 2-fold axis below. Capsomers, triplexes and the CCSC molecules are colored as indicated although the exact boundaries are not known in detail. The inset shows the positions of the four kinds of capsomers and six kinds of triplex on one triangular facet. The CCSC density common to both C-capsid samples (marked in red in a, b, and the inset) binds both the triplex (Ta) adjacent to the penton and the next closest (Tc) that are indicated in (c), as well as appearing to contact one of the two adjacent hexons. We attribute the additional density above the CCSC (green in a and the inset lower left) to the GFP protein inserted between residues 50 and 51 of UL25. Bar = 200Å. This figure was contributed by James Conway, Department of Structural Biology, University of Pittsburgh, and is published in reference (33).

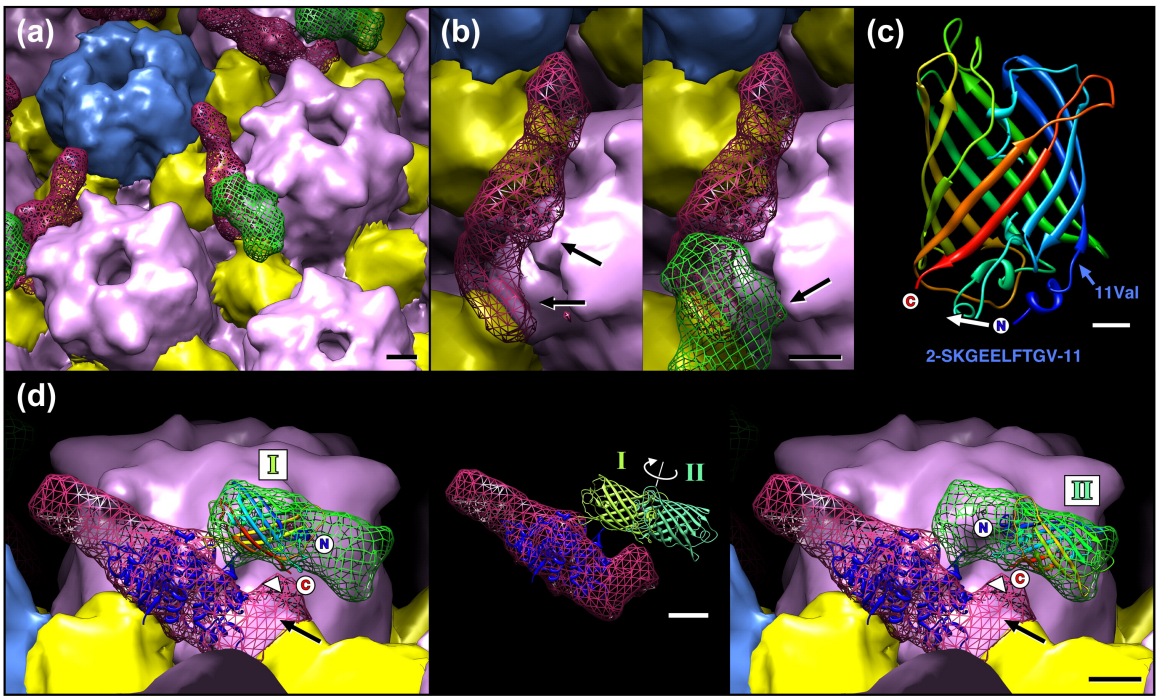

Figure 29. Close-up views of the UL25-GFP density. (a) The estimated boundaries for UL25 and GFP densities are shown as a purple and a green mesh, respectively. The scale bar represents 20 Å. (b) An alternative view revealing contacts (black arrows) between a hexon and the CCSC density (with GFP removed to aid visibility), at left, and between a hexon and the GFP density, at right. The scale bar represents 20 Å. (c) Ribbon representation of the GFP atomic model with termini and amino acid 11 (valine) marked, along with the sequence of GFP amino acids 2–11 (below). When inserted into UL25, the N- and C-termini of GFP may be closer together, possibly by refolding the 11 N-terminal amino acids moving the N-terminus as indicated (white arrow). The scale bar represents 5 Å. (d) Atomic models for UL25 (PDB ID: 2F5U, dark blue ribbons) and GFP (PDB ID: 1EMA, rainbow and green ribbons) positioned within the cryo-EM density. The UL25 atomic model (residues 134–580) is positioned so that the 133 missing N-terminal residues would occupy the distal region (black arrow) where contact with GFP appears most likely. The GFP model may be placed in two non-overlapping orientations to fill the green mesh, as indicated at left (position I) and at right (position II). These locations place the termini midway along the GFP density that closely approaches the CCSC density (arrowhead). The scale bar represents 20 Å. The inset shows the two GFP positions, represented by light and dark green models, superimposed on the CCSC density. The C-termini of the GFP are placed in the GFP density where it most closely approaches the UL25 density (arrowhead). This figure was contributed by James Conway, Department of Structural Biology, University of Pittsburgh, and is published in reference (33).

3.4.4 Reconstruction of capsids containing NTAP-UL25 protein

vNTAP-UL25 C-capsids were analyzed by cryo-EM, and surface maps for vNTAP-UL25 and wt C-capsids were calculated. Both vNTAP-UL25 and wt C-capsids contain the CCSC around the penton vertices (Figure 30). The NTAP-UL25 CCSC contains an additional small density

midway along the CCSC and adjacent to the hexon. This density is ascribed to the TAP tag. The region of the CCSC directly adjacent to the TAP tag (and more distal to the penton) makes contact with the hexon. The connection between the CCSC and the hexon is also observed on the wt capsid. Because the extreme N-terminus of pUL25 is fused to the C-terminus of the TAP tag, the region of the CCSC adjacent to the TAP tag must be occupied by the pUL25 N-terminus. Thus, we infer that the connection between the CCSC and the hexon is mediated by the extreme N-terminus of pUL25.

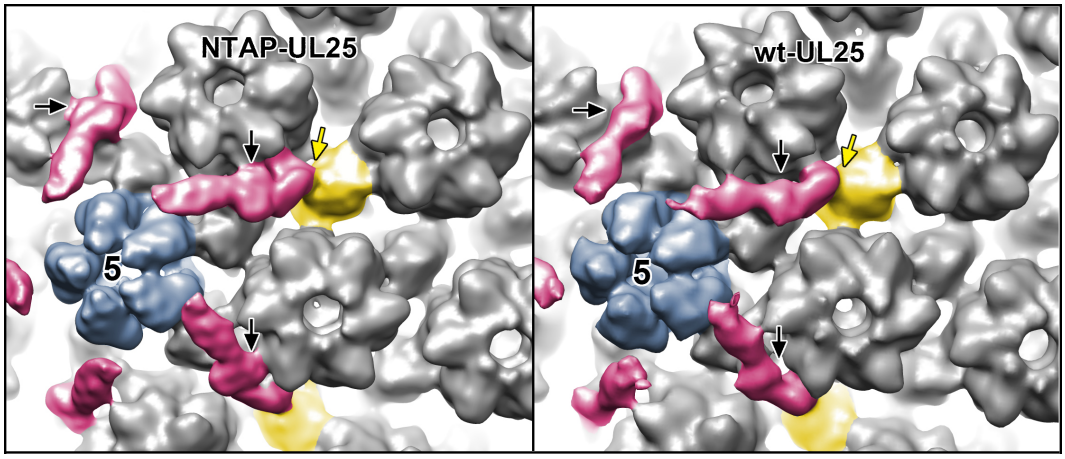

Figure 30. Comparison of the CCSC on vNTAP-UL25 and wt C-capsids. In this close-up view of the capsid vertices, the CCSC is colored dark pink. The blue penton is labeled 5, as it represents the five-fold axis of symmetry. Black arrows indicate the density attributed to the TAP tag, which is present in the vNTAP-UL25 CCSC but is missing from wt (right). A region of the CCSC to the right of the TAP tag makes contact with the hexon in both images. The penton-distal triplex is colored yellow. This figure was contributed by Katerina Toropova, Department of Structural Biology, University of Pittsburgh, and is unpublished material.

A composite view of the vUL25-GFP and vNTAP-UL25 CCSC molecules clarifies the boundaries of the pUL25 capsid-binding domain, located in aa 1-50 (Figure 31). In the composite CCSC, the TAP tag flanks pUL25 aa 1, and GFP connects to aa 50. The portion of

the CCSC between these two molecules touches both the hexon and the penton-distal triplex. These data suggest that the capsid-binding domain of pUL25 is able to bind both hexons and triplex proteins.

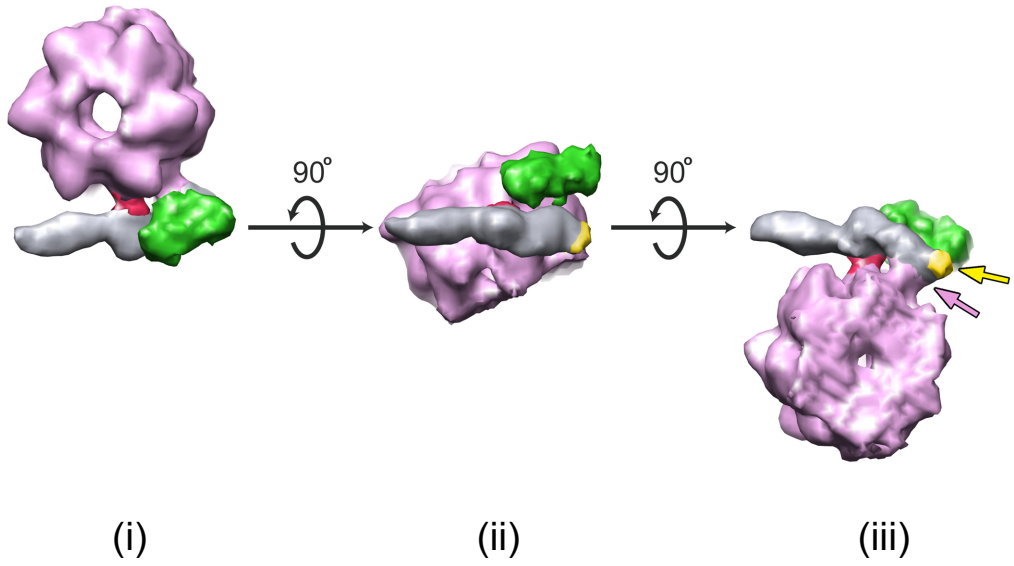

Figure 31. Composite image of the GFP and TAP labels. (i) Top view of the composite CCSC (gray), shown beside to the hexon (light pink) adjacent to the penton vertex. The GFP density is green, and the TAP tag is dark pink. The pUL25-hexon connection is obscured by GFP. (ii) Rotation of the image in (i) shows the side view from the surface of the capsid. The yellow region of the triplex makes contact with pUL25. (iii) View from underneath the hexon, looking out from the interior of the capsid. The region of pUL25 between the TAP and GFP densities makes contact with the hexon (pink arrow) and the triplex (yellow arrow). This figure was contributed by Katerina Toropova, Department of Structural Biology, University of Pittsburgh, and is unpublished material.

3.5 DISCUSSION

pUL25 is a minor component of HSV-1 capsids that is attached to their external surface. Based on immunogold labeling studies and difference imaging maps of wt and pUL25-deficient

capsids, pUL25 was predicted to bind the packaging protein, pUL17, to form a heterodimer that occupies 5 sites around each penton vertex. In order to verify this hypothesis and to discern the orientation of pUL25 in the pUL25-pUL17 complex, we generated viruses expressing pUL25 fused at its N-terminus to exogenous peptides—GFP or a tandem affinity purification (TAP) tag. While the TAP tag was inserted at the extreme N-terminus of pUL25 preceding aa 1, GFP was an internal fusion between aa 50 and 51. Hence, each tag was adjacent to the pUL25 capsid-binding domain in aa 1-50. Capsids containing the UL25-GFP and NTAP-UL25 fusion proteins were purified and analyzed by cryo-electron microscopy. Because GFP and the TAP tag add approximately 27 and 8.5 kDa of extra density to pUL25, respectively, the fusions were a convenient way to distinguish the location of pUL25 on the capsid surface. They also allowed visualization of a region of pUL25 that was not included in the crystal structure or the previous model of pUL25 in the CCSC. First, the reconstructions confirmed the predicted location of pUL25 in the CCSC. Furthermore, the tagged capsid reconstructions showed that the pUL25 N-terminus connects to the penton-distal triplex and the hexon adjacent to the penton. These data support the reports that pUL25 interacts with pUL19 (VP5) and pUL38 (VP19c), which are present in hexons and triplexes, respectively (148, 188). Finally, we postulate from the positions of the TAP and GFP molecules that the extreme N-terminus of pUL25 (aa 1) connects to the pUL19 in the hexon, while the region of the capsid-binding domain nearest to GFP (aa 50) binds to pUL38 in the triplex.

Preliminary quantitative analyses of pUL25 copy number on C-capsids indicates that pUL25 occupies more locations on the capsid than can be accounted for by its inclusion in the five CCSCs at each penton vertex (224). Recently, pUL25 was found to precipitate the portal protein pUL6 when the two were co-expressed in transfected cells (156). In structural studies,

pUL25 has not yet been observed around the portal. Interestingly, yeast-2-hybrid screens of UL25 homologues in KSHV and VZV predict that pUL25 also interacts with the putative terminase subunit, pUL15 (226). Because capsid-associated pUL25 prevents aberrant cleavage of viral genome termini (see Chapter 4), a potential role for pUL25 may be to stabilize terminase at its docking site on the portal while DNA is being actively packaged (237). A transient interaction between portal-associated pUL25 and pUL15 in the terminase complex could allow pUL25 to act as a tether that keeps terminase at the portal until the genome is completely packaged.

Its flexible nature and accessibility on the capsid surface has implicated pUL25 in interactions required for trafficking capsids through infected cells. Quantification of pUL25 copy numbers on intranuclear C-capsids and those in virions revealed that more pUL25 is present on capsids that leave the nucleus, suggesting that capsid-associated pUL25 is required for nuclear egress (98, 217, 224). UL25 involvement in nuclear egress has been confirmed in HSV-1 and pseudorabiesvirus (98, 102, 147, 169). pUL25 has been predicted to interact with pUL31, a viral protein involved in nuclear egress (124, 226). This interaction has not been tested in HSV-1, but if proven, could demonstrate the mechanism by which pUL25 capsid attachment promotes nuclear egress. Finally, pUL25 recruits the large tegument protein pUL36 to virus assembly compartments; in the virion, pUL36 likely connects to capsid pentons (27, 32, 156, 253). The studies presented here have confirmed that pUL25 is present on the capsid near the penton. Thus, indirectly, capsid-associated pUL25 drives maturation of the virion from the cell by the first addition of the inner tegument protein at the penton vertices. The pUL25/pUL36 complex may also contact microtubules and the nucleoporins; these interactions would transport capsids

from the cell periphery to the nucleus and dock them on the nuclear pore before the viral genome is released (93, 156, 169).

4.0 CAPSID-ASSOCIATED UL25 PROTEIN IS REQUIRED FOR SECONDARY CLEAVAGE OF THE VIRAL GENOME

4.1 ABSTRACT

The HSV-1 DNA packaging machinery cleaves unit-length genomes from a replicated DNA concatemer and packages them into preformed nucleocapsid precursors. Null mutations to the packaging gene UL25 promote the nuclear accumulation of two dead-end packaging products—empty A-capsids and unencapsidated, cleaved DNA—that are notable because they are not observed in other packaging mutants. In this study, pulsed field gel electrophoresis demonstrated that the UL25 deletion virus produced both genome-length DNA and a form that ran at a lower molecular weight. Southern blot analysis of viral DNA showed that in the absence of functional UL25, the U_S genome terminus was underrepresented with respect to the internal joint and U_L terminal fragments. In contrast to the discrete band observed in wt DNA, the UL25 mutant U_S terminus was detected as a smear of DNA that ran at lower molecular weight than wt, indicating that the U_S end of the genome was present but was shortened compared to the wt genome. These results suggest that in the UL25 mutants, aberrant cleavage takes place at the U_S end of the viral genome, producing truncated viral genomes that are not retained in capsids. Additionally, an *in vitro* binding assay tested the ability of soluble pUL25 prepared from infected cells to attach to DNA. pUL25 eluted from the DNA-cellulose resins at a low molarity of salt, suggesting that it

did not have a strong non-specific affinity for double-stranded or single-stranded DNA. Taken together, these data support a role for capsid-associated pUL25 in stabilizing the termination of cleavage and packaging without a direct interaction with viral DNA.

4.2 INTRODUCTION

In the HSV-1 virion, the linear, 152kbp, double-stranded DNA (dsDNA) genome is compressed into a nucleocapsid, where it is under immense pressure but not associated with any protein (16). The genome consists of two unique segments—U_L and U_S—that are flanked by the repeat sequences *a*, *b*, and *c*. The general arrangement of the genome is *a*-*b*-U_L-*b*'-*a*'-*c*'-US-*c*-*a*; each of the repeat sequences is inverted at the joint region between the unique segments. After the genome enters the nucleus of the newly infected cell, viral DNA is replicated into a concatemer of new genomes. Currently, there is a debate over the structure of the parent DNA and the mechanism of DNA replication. The concatemer may be generated by a rolling-circle mechanism, if the input DNA template is circular, or concatemerization may occur by recombination of linear DNA molecules, which is likely if the template itself is linear (87, 207, 239). Regardless of the mechanism of DNA replication, the concatemer is processed to single, unit-length genomes and packaged into precursor nucleocapsids by an ATP-driven terminase complex.

The cleavage and encapsidation of DNA requires specific packaging signals—pac1 and pac2—that are located in the *a* sequences present at the genome termini (128, 131, 206, 229). While pac2 is important for the initial cleavage that frees the U_L end of DNA, pac1 is required for the second cleavage, which frees the full-length genome from the concatemer and terminates

packaging (78). Within the pac1 and pac2 sites, GC or T-rich tracts are essential for DNA cleavage and packaging (219). In the overlapping *a* sequences of adjacent genomes in the concatemer, pac2 and pac1 are separated by a small (20 bp) direct repeat, DR1. Cleavage between genomes occurs within DR1 and leaves a single copy of the *a* sequence and a 3' overhang at the U_S terminus (128). In bacteriophage, the second cleavage of the concatemer can occur at a second packaging signal (phage λ) or after a headfull of DNA has been injected into the capsid (phages T4, P22, SPP1) (25). Although HSV-1 employs the pac1 site for secondary cleavage, there is evidence that there may also be a headfull component to HSV-1 DNA packaging. First, the packaging signals are in the multiple copies of the *a* sequence present at the joint region between the U_L and U_S segments, yet those pac sites are not cleaved in wild-type infection. Secondly, when the packaging signals were inserted into an amplicon of 4 kbp, tandem copies of the amplicon—measuring between 53 and 106 kbp—were stably packaged (78). These observations suggest that termination of packaging is coupled to a threshold amount of DNA inside the capsid, which is sensed by the terminase or some other component of the packaging machinery.

In the tightly coupled processes of DNA cleavage and packaging, some proteins must have direct contact with DNA, while others have indirect roles—or helper functions—in packaging. Several proteins that are assumed to contact DNA include the nuclease that cleaves near the packaging signals; architectural proteins that hold DNA in a particular conformation, much like the single-stranded DNA binding proteins of the DNA replication machinery; and proteins that hold DNA in place inside the capsid. Numerous examples of these DNA-binding mechanisms can be found in the DNA packaging machinery of the dsDNA bacteriophages [reviewed in (25)]. In λ phage, the terminase consists of two sub-units—gpNu1 and gpA—that

are the site-specific DNA binding component and endonuclease, respectively. Assembly of the terminase onto phage DNA concatemer requires the *E. coli* host cell proteins IHF and HU, which bind near the packaging signal and manipulate DNA into the conformation needed for gpNu1 binding (39, 115, 152, 209). In most phages, termination of packaging is followed by addition of head completion proteins, which seal the portal and form a connector that links the portal with the tail fiber. In the filled capsid of the bacteriophage SPP1, a short segment of packaged genome extrudes through the portal, probably making contact with the head completion proteins gp16 and gp15 (107, 151, 212). Some phages utilize decoration proteins that bind to the exterior of the partially packaged capsid to counteract the internal pressure of DNA; these include λ gpD and the Soc protein in phage T4 (86, 201, 249). Although these helper proteins do not contact DNA, they are required for the stable packaging of full-length genomes.

In HSV-1, some of the DNA packaging machinery with analogous functions to those in phage have been identified. UL6 forms the DNA entry portal at one vertex of the procapsid (143, 221). UL15, UL28, and UL33 presumably form the terminase complex (88, 246, 247). There is evidence that UL28 binds to HSV-1 packaging signals. Adelman *et al* used purified UL28 in electromobility shift assays with probes spanning the pac1 and pac2 sites (5). When the probes were tested as non-denatured dsDNA, no binding could be detected. However, pUL28 formed a nucleoprotein complex with both pac 1 and pac2 when they were used as boiled, ssDNA probes. It was also observed that pUL28 preferentially binds to the upper strand of the pac1 sequence and that GC-rich stretches are important for UL28 binding. These data confirmed a previous report (242) that like λ phage DNA, HSV-1 DNA needs to be in a specific architecture for cleavage. Thus, the HSV-1 packaging reaction may require DNA-bending proteins, but to date, none have been identified. Other HSV-1 proteins that have been

hypothesized to bind to the packaging signals include the viral nuclease UL12, the tegument protein UL36 (VP1/2), the disputed tegument US11 (ICP48), US12 (ICP47), and an unknown peptide of 140 kDa (28, 35). Of these, only UL12 has tangential relevance to packaging, as it is required to resolve branched intermediates in the DNA concatemer (116, 190).

The DNA packaging protein pUL25 plays an important role during the later stages of DNA packaging, prior to the release of capsids into the cytoplasm (205). Although pUL25 is primarily thought to reinforce the capsid (see Chapters 2 and 3), several features of pUL25 structure and function have encouraged the prediction that pUL25 associates with viral DNA during the packaging reaction: (i) the folded protein has a positively-charged face (19), (ii) purified pUL25 binds to immobilized HSV-1 DNA but not to Baculovirus DNA (148), (iii) pUL25 interacts with pUL6, the portal of viral DNA entry to the capsid (156), and (iv) capsid-associated pUL25 ensures retention of packaged DNA (30, 121). These observations have prompted suggestions that pUL25 seals the portal after the completion of packaging, much like the head completion proteins of bacteriophage [(151); reviewed in (25)]. Thus, UL25 could bind the viral genome (i) to remodel or maintain DNA in an appropriate structure that facilitates terminase cleavage or (ii) to anchor DNA within the portal for its retention within the capsid, but to date, neither of these functions has been experimentally determined. It is also possible that pUL25 could provide a platform for other proteins that interact directly with DNA. In the converse process of genome delivery to the nucleus of the newly infected cell, pUL25 is important for docking the capsid at the nuclear pore and for viral genome release (156, 169). If pUL25 is associated with viral DNA, it is possible that conformational changes in pUL25 during viral entry remove the constraint that pUL25 places on packaged DNA, allowing either pUL25 or other structural proteins to dissociate from the packaged genome. Furthermore, the UL25 null

mutant virus was shown to package shorter than unit-length genomes that were missing the U_S terminus (205); this observation conflicted with the initial characterization of the virus, when genomes of apparent full-length were detected (121). Since the U_L terminus is generated by the first concatemer cleavage (46), UL25 may have a role in the second site cleavage of DNA during packaging.

We have shown that the late defect in packaging in the UL25 null virus is due to the premature cleavage of the viral genome as it is being packaged, resulting in truncated genomes that failed to be retained in capsids. Thus, capsid-associated pUL25 stabilizes the secondary cleavage of DNA. Finally, in contrast to a previous report, we found that UL25 protein does not bind to DNA *in vitro*. These data suggest that pUL25 does not directly interact with DNA, but instead plays an accessory role in packaging.

4.3 MATERIALS AND METHODS

4.3.1 Cells, viruses, and antibodies

African green monkey kidney cells (Vero; American Type Culture Collection, Rockville, MD) and UL25-transformed 8-1 cells (121) were propagated in 5% FBS/DMEM with penicillin (10U/ml) and streptomycin (10μg/ml) at 37°C and 5% CO_2. HSV-1 wild-type KOS strain virus has been previously described (121). The UL25 mutant viruses vΔUL25, v143i, v212s, v560s, vΔ1-50, vΔ1-36, vΔ27-37, vΔ27-50, vΔ40-50, vF26A I27A, vF35A W36A, and vF26A I27A F35A W36A were described in Chapter 2. The UL28 null virus gCB is deleted of UL28 amino acids 78-706, and it serves as a negative control for DNA cleavage and packaging (214).

Baculovirus-expressed UL25 protein (121) was purified and used to prepare a UL25 monoclonal antibody, 25E10, that was provided by W. Newcomb, University of Virginia (33). Mouse monoclonal antibody 25E10 (αUL25) (33), rabbit polyclonal antibody NC1 (αUL19) (31), and mouse monoclonal antibody MAB8672 (αICP8; Millipore) were diluted to 1:5000, 1:10000, and 1:5000, respectively, in blocking buffer for immunoblotting. HRP-conjugated secondary antibodies goat anti-mouse or goat anti-rabbit (BioRad) were used at 1:5000 dilutions.

4.3.2 Preparation of total cell DNA

A T-175 flask of 8-1 or Vero cells was infected with virus at a MOI of 5 PFU per cell. At 18 h postinfection, the medium was removed and the cells were washed in 1x PBS, scraped off the plate, and pelleted. The cells were lysed in 20% SDS/Proteinase K at 37°C for 4 h. 5M NaCl (80 μl) was added, and the lysates were extracted 4 times with phenol, followed by 2 times with chloroform. Nucleic acids were precipitated with 1/10 volume 3M sodium acetate plus 2 volumes 100% ethanol. Pellets were rinsed in 70% ethanol, dried, and dissolved in 500 μl ddH_2O with 10μg/ml RNAse A. The concentration of DNA was determined by spectrophotometry.

4.3.3 Southern blots and hybridization analysis

To assess cleavage of viral DNA, total cell DNA (10μg) was digested with *Bam*HI or *Hind*III, separated by agarose gel electrophoreses, and transferred in alkaline buffer to a positively charged nylon membrane. Blots were rinsed in 2X SSC and stored at room temperature. The probes for hybridization analysis consisted of the HSV-1 genomic *Bam*HI J, K, Q fragments,

which were purified from the plasmid clones pFH218 (*Bam*HI K), pK1-2 (gift from Neal DeLuca; *Bam*HI Q), and pSG25 (gift from Sandra Weller; *Bam*HI J) by restriction digest and agarose gel electrophoresis. Double-stranded DNA probes were radiolabeled with ^{32}P-dCTP by nick translation reaction (GE Healthcare Nick Translation kit); unincorporated nucleotides were removed by gel filtration (Princeton Separations CentriSep column). Southern blots were pre-incubated with hybridization buffer (5X SSC, 5X Denhardt solution, 1% SDS, 100μg/ml denatured salmon sperm DNA) at 68°C for 3 h. Probes were boiled, quick-cooled on ice, added to hybridization buffer, and incubated with blots overnight at 68°C. Blots were washed 2 x 20 minutes with low stringency buffer (2X SSC/0.1% SDS) and 1 x 10 minutes with high stringency buffer (0.1X SSC/0.1% SDS) at 68°C. Blots were analyzed by autoradiography and phosphor screens, which were scanned with a Storm 840 Phosphor Imager. Specific bands were quantified with ImageQuant software.

4.3.4 Pulsed field gel electrophoresis

2 x 10^6 Vero cells were infected at a MOI of 2 and incubated to 24 hpi. Cells were rinsed in PBS, resuspended in 150 μl 2% low melt agarose (BioRad Clean Cut agarose), and molded into two wells. After hardening, the plugs were cut in half, rinsed in TE, and lysed overnight at 37°C in 20% Sarkosyl/0.5M EDTA. Plug slices were rinsed in EDTA treated with Proteinase K (0.5 mg/ml) overnight at 37°C. Plugs were rinsed in 1X TBE for 5 x 15 minutes before they were sealed into the wells of a 1% agarose/1X TBE gel (BioRad Pulse Field agarose). The gel was electrophoresed on BioRad CHEF-DRII module for 25 hrs with the following settings: 6V/cm; initial 50s; final 90s. The gel was stained with ethidium bromide to visualize DNA. To recover

viral DNA, agarose slices were extracted from the gel and incubated in TE at 50˚C overnight. Samples were extracted with phenol/chloroform. Nucleic acids in the aqueous phase were precipitated with ethanol and resuspended in ddH_2O. The recovered DNA was used in PCR with primers 5'-GCAGAAGGTCTCCGGTAATATCACC-3' and 5'-GGTGATCAGGTACAAC AGGCGCTC-3'. PCR products were run on 1% agarose in TAE and stained with ethidium bromide.

4.3.5 *In vitro* DNA binding assay

1.5 x 10^8 Vero cells were infected with wt HSV-1 (KOS strain) at a MOI of 5. At 24 hpi, cells were rinsed in PBS then incubated on ice in lysis buffer (50mM Tris pH 7.4, 1mM EDTA, 150mM NaCl, 1% NP-40, 0.25% sodium deoxycholate) plus 1X protease inhibitors (Roche) for 45 min. Nuclei were pelleted by low-speed centrifugation and then resuspended in a volume of low salt buffer (20mM Hepes pH 7.9, 1.5mM MgCl2, 20mM KCl, 0.2mM EDTA, 25% glycerol, 1X protease inhibitors) equal to half the nuclear pellet volume. High salt buffer (same as the previous buffer with KCl adjusted to 1.6M) was added dropwise to the suspension to 1/3 of the final volume. Extracts were gently rotated at 4°C for 30 minutes. Nuclei were pelleted in a microcentrifuge at max speed for 30 minutes. The supernatant was collected and dialyzed overnight into DNA-binding buffer (20mM Tris-HCl, pH 7.5; 50mM KCl; 1mM EDTA, pH 8; 2mM β-mercapto-ethanol, 10% glycerol) (165). Dialyzed protein was centrifuged for 30 minutes at maximum speed in a microcentrifuge to precipitate any remaining cellular debris or insoluble material. Resins containing double-stranded or single-stranded calf thymus DNA conjugated to cellulose (Sigma) were equilibrated to DNA-binding buffer overnight. After excess buffer was removed from the hydrated DNA-cellulose resins, an approximately equal volume of input

protein was added to the resin and incubated with agitation for 30 minutes at 4˚C. Flow-through was recovered by gentle centrifugation after the incubation of the input material and each successive wash. Proteins were precipitated from each sample with 16% TCA and resuspended in loading buffer (0.4M Tris-base, 2X NuPAGE loading buffer (Invitrogen)).

4.3.6 Immunoblotting

Protein extracts were separated on a 5 to 12% SDS–polyacrylamide gel and transferred to nitrocellulose. The nitrocellulose was washed in Tris-buffered saline (TBS) and blocked overnight or 1 h at room temperature in T-TBS (20 mM Tris, 0.5 M NaCl [pH 7.5] plus 0.5% Tween 20) supplemented with 10% nonfat dry milk. The UL25 monoclonal antibody 25E10 was diluted to 1:5000 in blocking buffer. The diluted antibody was reacted with the blocked nitrocellulose for 1 h at room temperature, washed 6 times in T-TBS, and reacted with horseradish peroxidase-conjugated anti-mouse immunoglobulin G (IgG) diluted at 1:5000 in blocking buffer. The bound Igs were revealed by enhanced chemiluminescence (Pierce ECL kit).

4.4 RESULTS

4.4.1 Isolation of whole viral genomes from infected cells

HSV-1 DNA replication generates concatemers that are subsequently cleaved into unit-length molecules and packaged into virions by the DNA packaging machinery. It was previously shown that the UL25-null virus KUL25NS cleaved replicated viral DNA into genomes that were

sensitive to DNAse (121). This result indicated that the virus processed viral DNA from the concatemer but failed to stably package the cleaved genomes. In a report that conflicted with the initial characterization of KUL25NS, unit-length and some smaller than unit-length DNA was stably packaged by KUL25NS, and the virus genomes appeared to be truncated from the U_S terminus (205). KUL25NS has a nonsense mutation at UL25 amino acid 104, and the virus has a growth defect resulting in a 10^3 PFU/ml reduction in plating efficiency on Vero cells compared to the UL25 complementing cell line 8-1 (121). However, the somewhat leaky null phenotype of KUL25NS on Vero cells—coupled with the possible rescue of the null gene by recombination with the complementing cell line—hindered efforts to evaluate the function of UL25 provided in *trans* (unpublished observation). To overcome this complication, the UL25 deletion virus, vΔUL25, was generated (see Chapter 2). In this virus, the entire UL25 ORF was replaced with the rpsL-neo antibiotic resistance cassette by BAC recombination. This virus expressed no UL25, and its reduction in replication on Vero cells was over 10^5 PFU/ml compared to the virus titer on 8-1 cells. In order to reconcile the reports of both complete and premature cleavage of UL25 null virus genomes, whole genomes produced by vΔUL25 were analyzed by pulsed field gel electrophoresis (PFGE). Vero or 8-1 cells were infected with wt KOS virus or vΔUL25. At 24 hours post-infection, the whole cell samples were embedded into agarose plugs, lysed, and run on PFGE (Figure 32). All the lanes retained DNA in the wells; this DNA consisted of highly branched concatemers that were not resolved by the gel (189, 190). Linear wt KOS DNA was present as a single band that migrated from the wells into the gel to a position consistent with the size of the HSV-1 genome (152 kbp) (Figure 32A). A similar band of DNA was observed in the vΔUL25 infection of 8-1 cells, which stably express UL25 and rescue the replication defect of the null virus. Vero cells infected with vΔUL25 contained only a faint band of the full-length

DNA, and there was also a faint and diffuse band of DNA that was several kbp smaller than wt. These bands were designated the "upper" and "lower" forms of vΔUL25 DNA. To further analyze each of the forms of vΔUL25 DNA, gel slices containing the bands were excised from the pulsed-field gel, and DNA was extracted from the gel. However, attempts to amplify the extracted DNA by PCR were unsuccessful (data not shown).

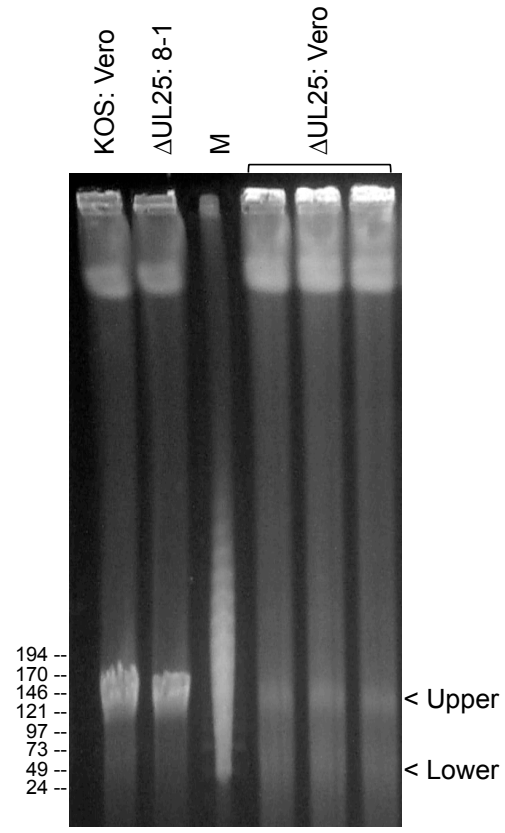

Figure 32. Pulsed Field Gel Electrophoresis. Vero or 8-1 cells were infected at a MOI of 2 and incubated to 24 hpi. Whole cells were embedded into low-melt agarose, lysed, and treated with Proteinase K. Agarose plugs were sealed into wells of a 1% agarose/1X TBE gel slab and run on a CHEF-DRII module for 25 h. The gel was stained with ethidium bromide to visualize DNA. A prominent band representing full-length genomes was observed in all samples (upper), and a minor band of smaller than unit-length DNA was observed in Vero cells infected with the UL25 deletion virus (lower).

4.4.2 Replication and cleavage of HSV-1 DNA by UL25 mutant viruses

Viral DNA cleaved from the concatemer contains free chromosomal termini, and the presence of chromosomal ends can be monitored by Southern blot analysis of total infected cell DNA. To better assess the genome processing of vΔUL25 and other UL25 mutant viruses (see Chapter 2), total DNA was prepared from Vero cells at 24 hpi and digested with *Bam*HI, which liberated both the internal and terminal repeat genome segments (Figure 33). The *Bam*HI K, S, and Q fragments contain the HSV-1 internal repeats (IR), long terminal repeat (TR_L), and short terminal repeat (TR_S), respectively. Only cleaved, genome-length viral DNA with free chromosomal ends will give rise to the terminal *Bam*HI Q and S fragments, while cleaved and concatemeric DNA contain the joint-spanning *Bam*HI K fragment.

Digested DNA was transferred to a nylon membrane and hybridized to a probe consisting of the *Bam*HI K fragment (Figure 33B(i)). The Q and S terminal fragments were detected in Vero cells infected with the wild type virus. The different sizes of the *Bam*HI S and K fragments are due to the presence of one to multiple copies of the *a* sequences, while the Q fragment contains only a single copy of the *a* sequence. An example of a mutant that fails to cleave replicated viral DNA is the null mutant GCB, which does not express the product of the HSV-1 UL28 gene (214). As shown in Figure 33B(i), the terminal Q and S fragments were absent from DNA isolated from Vero cells infected with GCB. All of the UL25 linker insertion mutants and vΔ1-50 replicated viral DNA when grown on Vero cells, as assessed by the presence of the joint K fragments. However, DNA isolated from Vero cells infected with the replication-defective UL25 mutants lacked the terminal Q fragments.

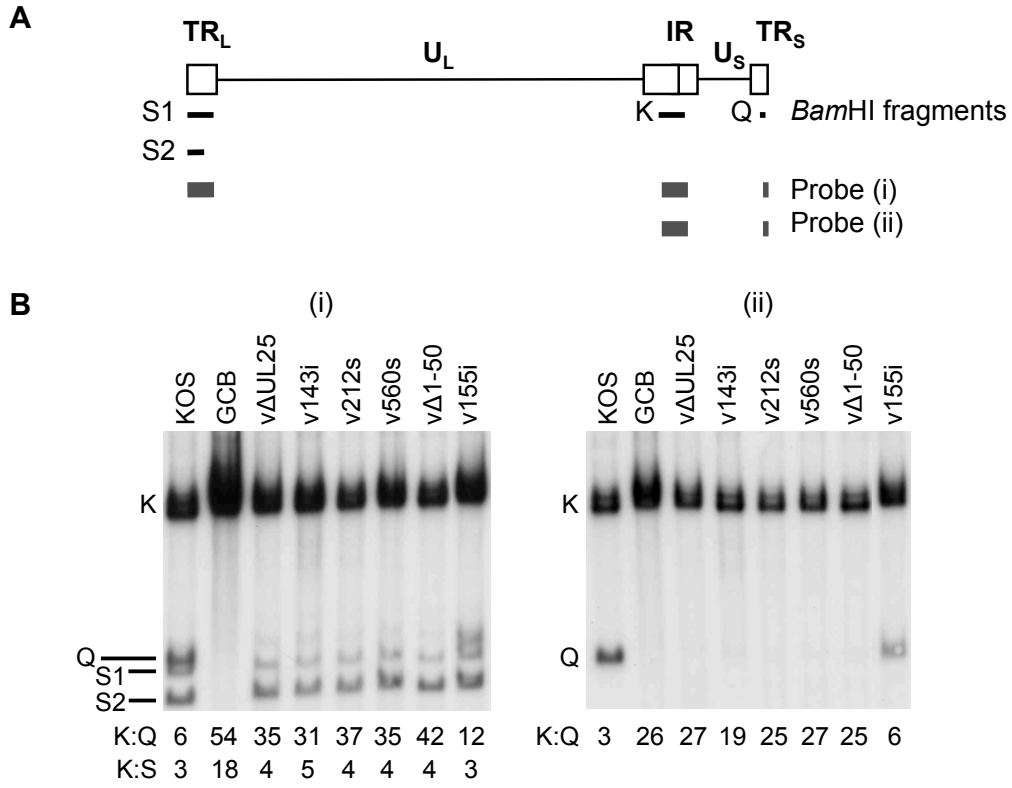

Figure 33. Processing of virus DNA. A. Schematic diagram of the HSV-1 genome showing the locations of the long and short terminal repeats (TR_L and TR_S), the joint or internal repeat (IR), and the *Bam*HI K, Q and S fragments. The different sizes of the *Bam*HI S fragment are due to the presence of one to multiple copies of the *a* sequence at the U_L terminus. B. Vero cells were infected with the indicated virus at a MOI of 5 PFU per cell. At 18 hours post-infection, total infected cell DNA was isolated, digested with *Bam*HI, and subjected to Southern blot analysis. The blots were probed with ^{32}P-labeled *Bam*HI K or *Bam*HI Q fragments of the HSV-1 genome, which hybridized to TR_L, IR, and TR_S (i) or IR and TR_S (ii), respectively. The ratio of the joint K fragment to U_S-end Q or U_L-end S fragments was determined by quantification of the hybridizing bands with a Phosphorimager and ImageQuant software. This figure was amended with permission from reference (30).

Since the Q and S fragments are similar in size, the blot was probed with a ^{32}P-labeled fragment that hybridizes specifically to the U_S terminus (Figure 33(ii)). The probe detected the Q fragment in the digests for the two viruses that replicated on Vero cells—wt KOS and the UL25 mutant v155i—but not in any of the viruses that did not; the junction fragment K was present in all samples. The amounts of radioactivity in the bands corresponding to the joint fragment, the

long terminus, and the short terminus (*Bam*HI fragments K, S, and Q, respectively) were measured, and the ratio of joint to each terminal fragment was calculated for each lane in Figure 33. In the case of the *Bam*HI S fragments from the U_L terminus, the measurement included both the S1 and S2 fragments. For wild-type HSV-1, the ratios of joint to end fragments were similar. For the UL25-null virus, vΔUL25, and the other UL25 mutants that do not replicate in Vero cells, the U_L terminus was present at levels similar to those in the wild-type virus, but the U_S terminus was absent or significantly underrepresented compared to the joint fragment (Figure 33 (i)). There was a twofold reduction in the U_S terminus for the 155i linker insertion mutant, v155i. This is consistent with the fact that replication of v155i is reduced (see Chapter 2, Table 6) and demonstrates a direct correlation of the defect with the cleavage of viral DNA, the production of stable C-capsids, and the production of infectious virus.

The absence of U_S terminal fragments from the UL25 mutants was surprising because previous studies from our laboratory demonstrated that genome-size (152 kbp) HSV-1 DNA is present in cells infected with the UL25-null virus, KUL25NS (121). To further examine the U_S terminus generated by the UL25 mutants, total infected cell DNA was digested with *Hind*III and subsequently analyzed by Southern blot analysis using the HSV-1 *Bam*HI J fragment as a probe (Figure 34). The probe spanned the *Hind*III restriction site that links the genome fragments containing the 13 kbp fragment from the U_S terminus (*Hind*III G fragment) and an internal 5 kbp fragment from the U_S region (*Hind*III N fragment). The two large hybridizing fragments that are present in all of the samples are viral DNA fragments that result from cleavage of the replicated DNA concatemers and consist of the joint-spanning fragments *Hind*III G plus *Hind*III B or, when the U_L region is inverted, *Hind*III G plus *Hind*III I. The *Hind*III G fragment was readily detected in DNA isolated from Vero cells infected with KOS and v155i, but this fragment was

absent from DNA isolated from Vero cells infected with the UL28 mutant, GCB (Figure 34). Although the *Hind*III G fragment was present in the blots of DNA isolated from the five UL25 mutants (vΔUL25, v143i, v212s, v560s, and vΔ1-50) that failed to grow on Vero cells, the hybridizing band was diffuse, suggesting that the probe detected multiple U_S terminal fragments. The presence of multiple U_S terminal fragments would indicate that either the cleavage reaction is taking place at several sites to generate *Hind*III G fragments of different sizes or that the full-length genomic DNA is not stable and is being degraded. The ratio of *Hind*III G fragment to the internal *Hind*III N fragment was calculated for each virus and showed that the cleavage at the U_S end is reduced approximately two-fold for the UL25 mutants.

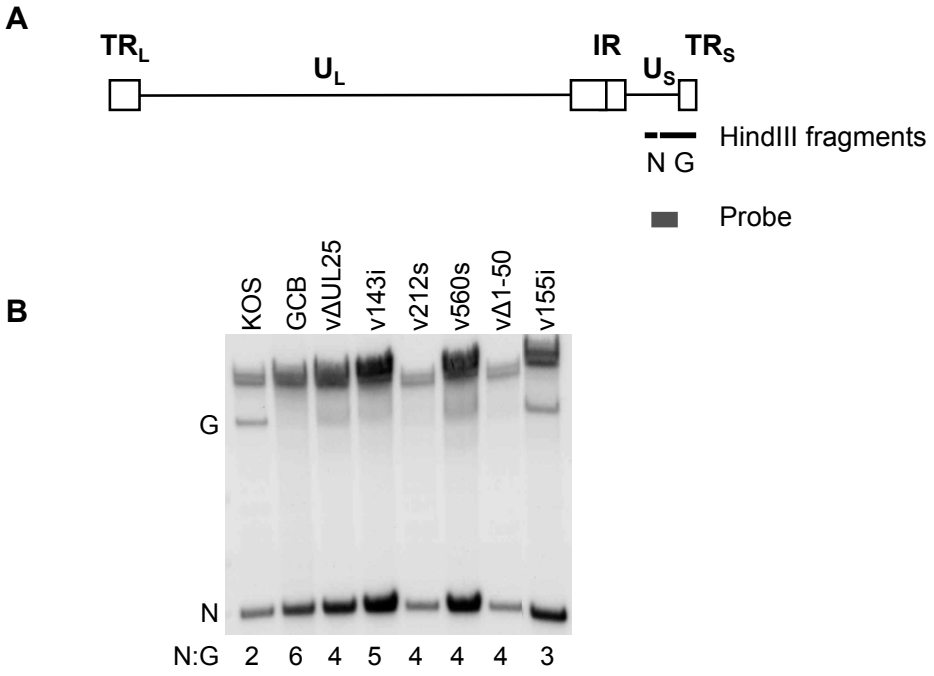

Figure 34. UL25 null viruses produce viral genomes with truncated U_S ends. A. Schematic diagram of the HSV-1 genome showing the locations of the *Hind*III G and N fragments. B. Total cell DNA from infected Vero cells digested with *Hind*III and subjected to Southern blot analysis. The blot was probed with the ^{32}P-labeled *Bam*HI J fragment of the HSV-1 genome. The ratio of the internal *Hind*III N fragment to the U_S end G fragment was determined by quantification of the hybridizing bands with a Phosphorimager and ImageQuant software. This figure was amended with permission from reference (30).

4.4.3 Characterization of viral genomes in UL25 small deletion and point mutation viruses

UL25 mutant viruses with small deletions within the putative capsid-binding domain (vΔ27-37, vΔ27-50) have similar phenotypes to the UL25 linker insertion mutants: they generate A- and B-capsids containing pUL25 (see Chapter 2). In contrast, viruses expressing pUL25 with point mutations at aa 26, 27, 35, and 36 have a different defect in virus replication. These viruses produce C-capsids that do not escape the nucleus. To characterize the viral genomes produced by these viruses upon infection, total DNA was isolated from Vero cells infected with wild-type and mutant viruses and subjected to Southern blot analysis as described in Section 4.4.2.

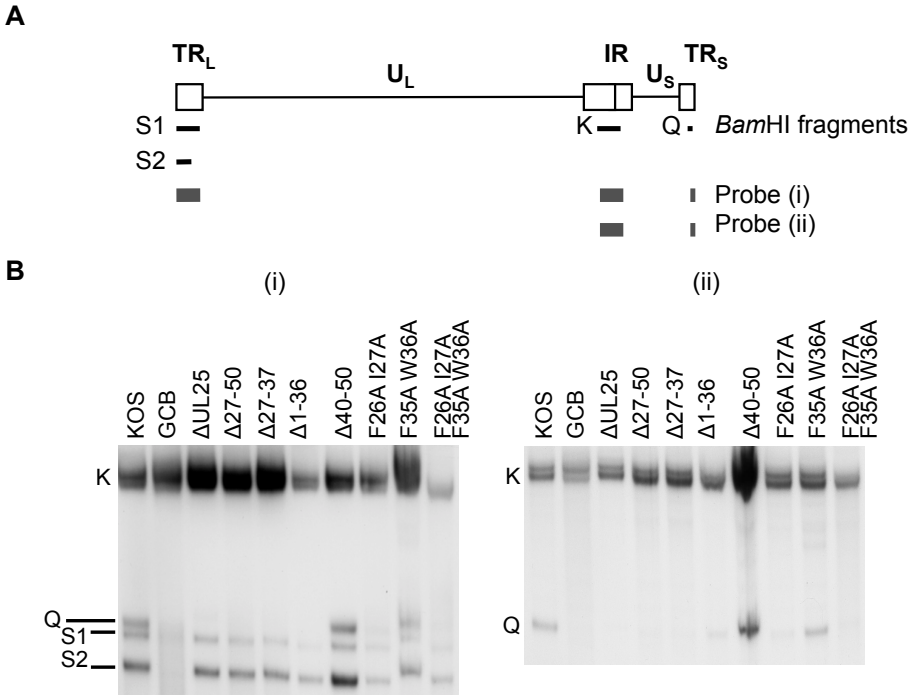

Figure 35. Processing of virus DNA. A. Schematic diagram of the HSV-1 genome showing the locations of the long and short terminal repeats (TR_L and TR_S), the joint or internal repeat (IR), and the *Bam*HI K, Q and S fragments. The different sizes of the *Bam*HI S fragment are due to variable copies of the *a* sequence at the U_L terminus. B. Total cell DNA was isolated from Vero cells, digested with *Bam*HI, and subjected to Southern blot analysis. The blots were hybridized to probes that detected TR_L, IR, and TR_S (i) or IR and TR_S (ii).

Wild-type KOS DNA contained all the expected fragments (Figure 35), indicating that cleavage of unit-length genomes from the replicated DNA concatemer produced both TR_L and TR_S genome ends. Like wt, the UL25 mutant vΔ40-50 DNA contained each of the genome fragments in approximately equimolar amounts. The UL28 null virus GCB was included as a negative control because it does not cleave DNA from the concatemer; in GCB DNA, the IR but neither TR_L nor TR_S were detected (Figure 35). As previously reported, the UL25 deletion mutant was negative for TR_S but not for TR_L. Most UL25 mutants exhibited a phenotype similar to vΔUL25, but point mutations that prevented replication on Vero cells—yet did not prevent packaging—appeared to carry out secondary cleavage of genomes at TRs, as demonstrated by the presence of the Q fragment in DNA from viruses vF26A I27A and vF35A W36A. To clarify this result, the identical Southern blot was probed with the *Bam*HI Q fragment, which selectively hybridized to the IR and TR_S but not TR_L. Prominent Q bands—representing TR_S—were observed in KOS, vΔ40-50, and vF35A W36A DNA, while fainter bands were present in vF26A I27A DNA. Thus, point mutations at aa 26, 27, and 35, 36 allowed completion of genome cleavage from the concatemer, but to a reduced extent compared to wt. This result was consistent with the observation of C-capsids in both gradients of purified intranuclear capsids and in the nuclei of infected cells.

4.4.4 pUL25 purified from wt-infected mammalian cells does not bind immobilized DNA *in vitro*

Ogasawara *et al*. showed that baculovirus-expressed pUL25 bound to HSV-1 genomic DNA when purified DNA and protein were mixed *in vitro* (148). We investigated the ability of UL25 protein present in infected mammalian cell nuclei to bind non-specifically to DNA immobilized

on a cellulose resin. Nuclear extracts were prepared by high salt extraction of cells infected with wt HSV-1 (KOS) (see Methods). The nuclear extract was dialyzed overnight into DNA binding buffer and was cleared of any remaining debris and aggregates. Double stranded (dsDNA) and single-stranded (ssDNA)-conjugated-cellulose resins were swelled overnight in DNA-binding buffer and gently pelleted. Clarified nuclear extracts were loaded onto the resins, and the flow-through supernatant was collected after a 30 minute incubation. Following an initial wash in DNA-binding buffer to remove any residual unattached protein, resins were washed for 30 minutes each with DNA binding buffers with stepwise increases in salt concentration, in a range from 0.1 to 2M KCl. The supernatant was separated from the resin after each wash by gentle centrifugation. After concentration of the protein in each wash by TCA precipitation, Western blot was used to detect the HSV-1 ssDNA binding protein ICP8, the major capsid protein pUL19 (VP5), and pUL25 in the DNA-cellulose eluates (Figure 36). The majority of ICP8 was eluted from the dsDNA and ssDNA at 0.5M KCl at 0.8M KCl, respectively, which is consistent with published values (68). In contrast, pUL25 eluted from the resin at very low concentrations of salt. This result was more similar to the pattern of salt elution for the major capsid protein pUL19. These data contradict previous assertions that pUL25 has the ability to bind to DNA (148). Instead, these results suggest that pUL25 is not a DNA-binding protein, as previously suggested, but more likely plays a structural role in DNA packaging.

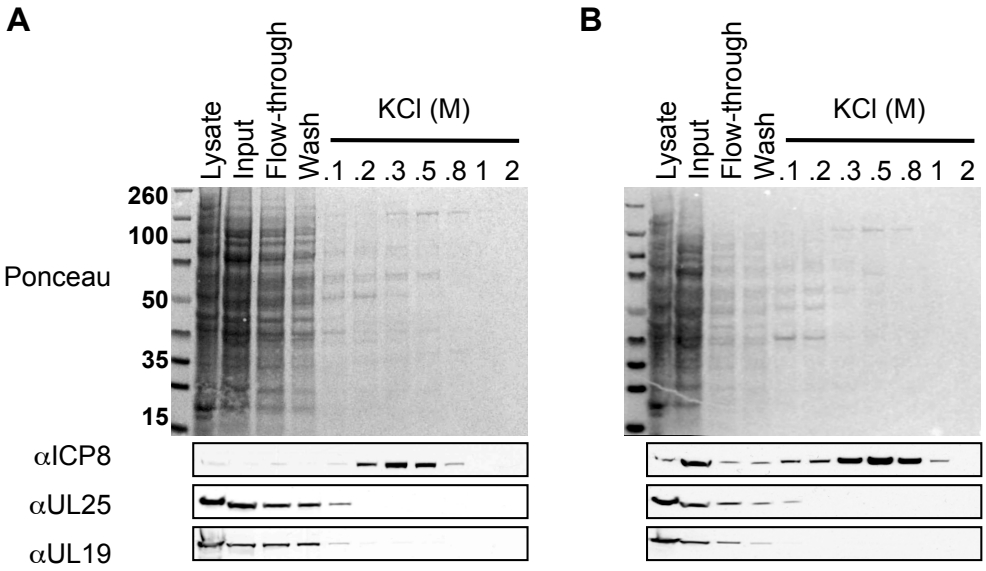

Figure 36. pUL25 purified from infected cell nuclei does not associate with dsDNA or ssDNA *in vitro*. A. Nuclear extracts from KOS-infected Vero cells were incubated with dsDNA-cellulose in a batch method in order to identify DNA-binding proteins. Increasing concentrations of salt (KCl) were used to elute proteins with higher DNA-binding affinity. (Top) Western blot with Ponceau stain shows the total protein loaded in each lane. Lysate, total infected cell lysate. Input, dialyzed nuclear extracts after centrifugation to remove precipitates. Flow-through, sample collected after initial incubation with resin. The molarity (M) of KCl of the washes is indicated above the lanes. Molecular weight markers are shown in kDa. (Bottom) The blot was probed for ICP8, the HSV-1 ssDNA binding protein (positive control (+)), pUL25, and pUL19, the major capsid protein. B. Nuclear extracts were tested for binding to ssDNA-cellulose. Labels are the same as above.

4.5 DISCUSSION

In the absence of the DNA packaging gene UL25, HSV-1 genomes are cleaved from the replicated DNA concatemer, but they are not retained in the capsid. In this study, the genomes produced by UL25 mutant viruses were examined by pulse field gel electrophoresis (PFGE) and by Southern blot. By PFGE of whole cells infected with the UL25 deletion virus, vΔUL25, two forms of vΔUL25 DNA were observed: an upper band corresponding to approximately genome-length (150kbp) DNA, and a lower band that migrated further into the gel. Both bands were extracted from the gel, but they were not successfully amplified with PCR and primers specific

to viral DNA. Southern blot and hybridization analysis of viral DNA was carried out to detect three DNA fragments released by *Bam*HI digest. The joint (*Bam*HI K fragment) is located between the U_L and U_S segments, and it is present in both concatemeric and cleaved DNA. The U_L and U_S genome termini correspond to the *Bam*HI S and Q fragments, respectively, and they are only present in linear DNA that has been cleaved from the concatemer. K and S fragments were observed for each UL25 mutant virus, but the Q fragment was present only in the UL25 mutants that replicated on Vero cells (Tables 6 and 7). Further analysis with a probe that hybridized to a region of DNA 5' to the Q fragment showed that the UL25 mutants produced a diffuse band of U_S terminal DNA that was reduced in intensity compared to wt. Thus, in UL25 null mutants, the U_S terminus was present but truncated. Because the diffuse band can be interpreted as a population of genome fragments that are many different sizes, it appears that in the absence of functional UL25, the second DNA cleavage event occurs randomly rather than at a distinct packaging sequence. Because the *Bam*HI Q fragment is absent from all of the UL25-defective mutants, the U_S terminus for these mutants appears to be located at least 3,000 bp 5' to the wild-type U_S terminus.

DNA translocation into the capsid is mediated by the terminase complex comprised of the HSV-1 proteins UL15, UL28, and UL33 (33, 88, 246, 247). The *cis*-acting HSV-1 packaging sequences, designated pac1 and pac2, are found near the genomic ends of viral DNA. At the U_L end of the genome, the pac2 site defines packaging directionality by mediating initiation, and pac1 serves to terminate packaging at the U_S end after a unit-length genome has entered the capsid (20). Terminase cleaves viral DNA at the pac2 site and then docks the free end of DNA at the capsid portal vertex. Packaging proceeds from the U_L end until a full-length genome has entered the capsid; DNA cleavage occurs at a pac1 site at the U_S end. The packaged genome is

then sealed within the capsid. Similar to the dsDNA bacteriophages, DNA cleavage is suppressed until a full genome (headfull mechanism) has entered the capsid because otherwise shorter packaged genomes would be formed from cleavage at the packaging sequences within the HSV-1 genome's internal repeat sequences. The addition of pUL25 to the capsid at or near the end of the packaging process suggests that it may function similarly to λ phage head completion proteins, gpD, or the Soc and Hoc proteins of phage T4; these proteins bind to the phage capsid surface after DNA has entered and are thought to reinforce the capsid structure (67, 84, 85, 249). Although most of our UL25 mutant proteins were able to attach to capsids, the failure of recombinant viruses to replicate on Vero cells was coincident with premature cleavage of the U_S end of the viral genome, as previously described for the UL25-null mutant KUL25NS (121, 168, 205). In CMV, the halogenated benzimidazoles BDCRB (2-bromo-5,6-dichloro-1-D-riborfuranosyl benzamidazole riboside) and TCRB (2,5,6-trichloro-1-D-riborfuranosyl benzimidazole riboside) induce premature cleavage events during DNA packaging such that the site of cleavage is located at a similar distance from the end of the genome as was observed with the UL25 mutants (146). These compounds are not active against HSV-1, but resistance mutations to BDCRB and TCRB map to the human CMV terminase genes UL89 and UL56, which are the homologues of HSV-1 UL15 and UL28, respectively (100, 228). While the drugs' mechanism of action is not known, they may relax the cleavage site sequence specificity of the terminase without relieving the headfull requirement. By extension, the absence of functional pUL25 on the capsid surface may relax the cleavage site specificity and allow aberrant cleavage by the terminase.

Based on the published observation that pUL25 binds HSV-1 DNA, we hypothesized that pUL25 could do so to remodel or maintain DNA in an appropriate structure that facilitates

terminase subunit assembly or DNA insertion into the capsid. To test pUL25 interaction with DNA, nuclear extracts were prepared from infected cells and incubated with double-stranded (ds) or single-stranded (ss) DNA-cellulose. pUL25 eluted from ss- and dsDNA-cellulose resins in the flow-through or the first wash of 0.1MKCl. In contrast, the known HSV-1 ssDNA binding protein ICP8 required up to 1M KCl to detach from the resins. These results suggest that pUL25 is unable to bind non-specifically to either ds- or ssDNA. This result conflicts with a previous report that pUL25 binds to immobilized DNA (148). We did not test pUL25 binding to HSV-1 DNA, so we cannot rule out the possibility that pUL25 does have affinity specifically for viral DNA. pUL25 could also require a specific DNA sequence or structure for its attachment to DNA; the putative terminase subunit UL28 interacted with packaging sequences only when DNA probes were denatured and reformed into single-strand or hairpin DNA (5). Our assay was limited in this aspect, as these variables were not tested. Future studies could address pUL25 attachment to the specific sequences by competition assay or electromobility shift assay with native and denatured probes, in the manner of (5, 28, 35), or chromatin immunoprecipitation could be used to isolate pUL25-DNA complexes from infected cells.

The UL25 mutants presented here fall into three groups: those that failed to cleave DNA at the proper packaging sequence (vΔUL25, v143i, v212s, v560s, vΔ1-50, vΔ1-36, vΔ27-50, vΔ27-37, vΔ1-50), those that cleaved and packaged DNA but did not support virion production (vF26A I27A, vF35A W36A), and those that behaved similar to the wt virus (v155i, vΔ40-50). In Chapter 2, the pUL25 capsid-binding domain was mapped to amino acids 1-36. The data presented here show that some pUL25 mutations outside of the putative capsid-binding domain promote the aberrant cleavage phenotype. Thus, it is possible that these mutations disrupt interactions between capsid-bound pUL25 and other proteins involved in DNA cleavage. It has

been hypothesized that undetected forms of the pUL17/pUL25 heterodimer (CCSC), or pUL25 in different protein complexes, may be present on the capsid at locations other than the pentons—specifically, at the vertex containing the portal complex (156, 224). Thus, while it is unlikely that pUL25 interacts directly with viral DNA as it is being packaged, if the CCSC or other form of pUL25 is near the portal, it could indirectly stabilize the DNA cleavage reaction by tethering the packaging machinery to the portal or by sealing off the portal after the second cleavage of DNA.

5.0 SUMMARY AND CONCLUSIONS

DNA packaging is a critical step in the lytic replicative cycle of herpes simplex virus type 1 (HSV-1). During the packaging reaction, replicated DNA is resolved from branched concatemers to single, unit-length genomes that are inserted into pre-assembled capsid precursors (46, 189). Seven HSV-1 genes have been identified that are required for DNA encapsidation (6, 103, 104, 121, 157, 186, 214). Null mutations of the UL6, UL15, UL17, UL28, UL32, and UL33 genes block cleavage of viral genomes from the replicated concatemer and promote the formation of B-capsids, which are dead-end products retaining the scaffold protein. In contrast, disruption of the UL25 gene results in the accumulation of both B-capsids and empty A-capsids in addition to unpackaged, genome-length DNA; packaging of shorter-than-wt genomes has also been reported (121, 205). Thus, it is inferred that UL25 is not required for the initial cleavage or insertion of DNA into the capsid but rather for termination of packaging and maintenance of the viral genome after the packaging event. UL25 protein (pUL25) attaches to the capsid exterior. Its occupancy coincides with capsid maturation, such that copy numbers of pUL25 increase from procapsids to B-, A-, C-capsids and virions (137, 192). Structural analysis of pUL25 indicates that it has multiple binding surfaces and flexible loop domains. These features may allow pUL25 to switch between conformational states in order to participate in dynamic interactions. On the capsid exterior, pUL25 has access to the viral proteins that promote capsid nuclear egress, tegumentation, and virion assembly. Taken together, the structure and location of pUL25 predict

that the capsid-associated protein interacts with multiple binding partners and has important roles in events downstream from initiation of the packaging reaction.

Due to similarities in null mutant phenotypes, UL25 has been likened to both the decoration proteins and head completion proteins of the double-stranded DNA bacteriophages. In the absence of the λ phage gpD decoration protein, capsids are unable to retain DNA, or shorter than unit-length genomes—missing the final 20% of sequence—are packaged (249). Furthermore, like pUL25, the gpD decoration protein is only added to the expanded capsid after the initiation of packaging. The T4 phage Soc decoration protein is dispensable for packaging, but it stabilizes the T4 capsid (86). The addition of pUL25 during DNA packaging likewise stabilizes the HSV-1 capsid (183). A major dissimilarity between pUL25 and these decoration proteins is the presence of decoration proteins at the capsid three-fold axes of symmetry. In HSV-1, the triplex proteins occupy these positions, and pUL25 is found around the five-fold axis of symmetry (33, 137, 145, 224). Bacteriophage head completion proteins seal off the portal after insertion of DNA (25). Like pUL25, the phage SPP1 head completion proteins gp15 and gp16 are required for retention of DNA inside the capsid, but not for DNA cleavage (151). These head completion proteins are arranged in rings on the exterior of the capsid portal (107). It has been suggested that pUL25 binds the HSV-1 portal protein pUL6 (156), but to date, there is no structural evidence for pUL25 at the portal. Therefore, in the distribution of protein on the capsid surface, pUL25 is not strictly analogous to either the decoration proteins or head completion proteins of the bacteriophage system.

Several functions of pUL25 have been mapped to regions of the protein. Figure 37 represents a summary of the current knowledge of pUL25 functional domains. pUL25 makes contact with the packaging protein pUL17—presumably in a heterodimer at the capsid vertices—

and this interaction is independent of the pUL25 N- and C-termini (137, 188, 216, 224). Two regions between amino acids 396 and 425 are important for egress of capsids from the nucleus after completion of packaging (147). The three C-terminal amino acids and one internal residue at position 233 are required for genome uncoating during viral entry to the cell (4, 147, 169). In this study, important functional regions were identified at the N-terminus, amino acid 143, and amino acids 560-580. While the N-terminus constitutes a capsid-binding domain, the latter two regions are important for the secondary cleavage of DNA and stable packaging of full-length DNA.

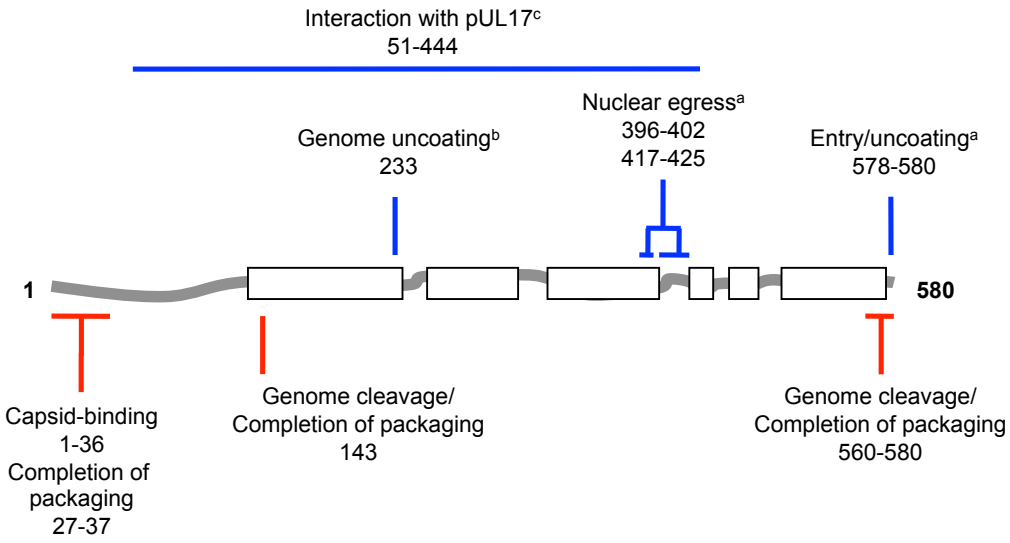

Figure 37. Summary of functional regions of pUL25. White bars represent the folded core of the protein, while gray lines are the flexible or unstructured N-terminus and internal loop domains. Conclusions drawn from this study are in red, while other published reports are in blue. [a]O'Hara, M. *et al.* 2010. *J Virol.* [b]Preston, V.G. *et al.* 2008. *J Virol.* [c]Scholtes L. and J.D. Baines. 2009. *J Virol.*

The pUL25 capsid-binding domain is located in its N-terminus. By mutational analysis of the UL25 gene coupled with *in vitro* and *in vivo* capsid-binding assays, a capsid-binding domain was identified within the first 50 amino acids of pUL25. Further investigation of

this region of pUL25 demonstrated that deletion of amino acids 1-36 was sufficient to eliminate capsid attachment, and point mutation of four residues highly conserved within the alphaherpesviruses—amino acids 26, 27, 35, 36—significantly reduced attachment. Structural analysis of capsids containing pUL25 fusion proteins showed that the pUL25 capsid-binding domain makes multiple contacts with the capsid surface. Its extreme N-terminus is close to the hexon adjacent to the penton vertex, and a portion of pUL25 close to amino acid 50 makes contact with the adjoining triplex. The mutant protein deleted of amino acids 1-50 was present in the nucleus in infected cells, indicating that deletion of the pUL25 N-terminus does not result in sequestering of the protein in the cytoplasm. It has been reported that nuclear localization of pUL25 is dependent on expression of the triplex protein, VP19c (148). While our data suggest that some residues between amino acids 1-50 contact VP19c, these contacts are not required for pUL25 localization to the nucleus. Together, these results could suggest that pUL25 has additional contacts with the capsid or another chaperone and that this connection directs pUL25 to the nucleus.

Capsid attachment is required but not sufficient for completion of packaging. Several UL25 mutants were generated that did not support viral replication. These mutations included a 5 amino acid insertion at position 143, C-terminal truncations to amino acids 212 or 560, and small deletions in the N-terminus between amino acids 27 and 50. These mutations did not disrupt the capsid-binding domain of pUL25, as demonstrated by the co-purification of the mutant proteins with A- and B-capsids produced by each recombinant virus. However, the mutations did preclude successful cleavage of the viral genome at the U_S terminus. Thus, pUL25 is recruited to the capsid surface via the N-terminal capsid-binding domain, but other functional regions are required to complete DNA packaging. In recent preliminary experiments, pUL25

copy number on PrV and HSV-1 capsids have been estimated to be greater than expected if pUL25 occupies 5 positions around each penton vertex (224). These data suggest that pUL25 is present at other locations on the capsid surface. Based on this suggestion and the data presented here, we propose that pUL25 potentially contacts other structural or packaging proteins with its amino acids 26-50, 143, and 560-580.

Thin-section electron microscopy was used to observe the morphology and location of capsids in cells infected with UL25 null mutant viruses. Unlike other UL25 null mutants that produced only A- and B-capsids, viruses with point mutations at amino acids 26, 27, 35, and 36 produced C-capsids that were trapped in the nucleus. This result was especially surprising for the virus vF26A I27A F35A W36A. This virus had very diminished replication on Vero cells, and only A- and B-capsids could be purified out of infected nuclei. The observation of intact C-capsids in cells infected with vF26A I27A F35A W36A suggests two conclusions: (i) the substitution of the four residues severely abrogates the pUL25 connection to the capsid, such that is easily disrupted upon capsid manipulation, and (ii) the four residues are important for nuclear egress or tegumentation of capsids.

It is has been established that UL25 is required for release of capsids from the nucleus (98, 102, 147) and that pUL25 interacts with the large tegument protein pUL36 (32, 156). At present, it is unclear if pUL36 is added to the capsid in the nucleus, and whether or not the pUL25-pUL36 interaction drives capsid nuclear egress. HSV-1 pUL36 has a functional nuclear localization signal in its N-terminus and can be detected in the nucleus, but UL36 is not required for egress of HSV-1 capsids (1, 22, 44). In PrV, truncated pUL36 is incorporated into nuclear capsid assembly compartments (32, 106), but full-length pUL36 is not detected on capsids until they exit the nucleus (64, 129). UL25 mutations that block virion assembly but not DNA

packaging could disrupt the pUL25-pUL36 interaction. pUL36 has two independent pUL25 binding domains at pUL36 aa 2037-2353 and 3105-3164 (32, 156). Because capsid trafficking defects can be isolated to different regions of pUL25—in this study, the N-terminus, and as previously reported (147), at aa 396-402 or aa 417-425—pUL25 potentially has multiple independent pUL36-binding domains. This hypothesis fits well with the suggestion that pUL25 forms distinct complexes with pUL36 that serve different roles at the vertex for assembly and egress and at the portal for genome uncoating (32, 156). On the other hand, the pUL25-pUL36 interaction may simply promote tegumentation of the capsid after it reaches the cytoplasm, in which case the nuclear egress defect observed in UL25 mutants must be attributed to disruption of UL25 interaction with proteins that promote primary envelopment of intranuclear capsids.

pUL25 stabilizes secondary cleavage of the viral genome, but does not appear to interact directly with DNA. The HSV-1 genome has two distinctive ends that are cleaved and packaged in a directional manner (46, 133). The U_L end is the first cleaved from the replicated concatemer, and the second cleavage frees the U_S end of DNA. To characterize changes in DNA cleavage due to UL25 mutations, viral DNA produced by UL25 mutants was extracted from infected cells for Southern blot and hybridization analysis. While the U_L end of the viral genome was present in viral DNA from all recombinant viruses, the U_S end was apparently missing from UL25 mutant viruses that failed to replicate on Vero cells. Further investigation showed that the U_S ends were present but truncated compared to the wt end fragment, suggesting that UL25 null mutations promote aberrant cleavage of the viral genome as it is being packaged. Virus-expressed pUL25 was purified and tested for non-specific binding to single-strand or double-strand DNA *in vitro*. In these assays, pUL25 demonstrated very low affinity for DNA, suggesting that pUL25 promotes completion of packaging without binding to the viral DNA.

Taken together, the data presented in these studies and elsewhere suggest that pUL25 has multiple sites of attachment on the capsid-surface and, potentially, distinct roles at these locations. At the five-fold axis of symmetry—the penton vertices—pUL25 forms a putative heterodimer with the DNA packaging protein pUL17, and inclusion of the heterodimer around the vertices stabilizes these vulnerable regions of the capsid. Because pUL25 has been shown to interact with the DNA packaging protein pUL6, pUL25 may also be present around the DNA portal, a twelve-mer ring of pUL6 that is present at a single capsid vertex. At this structurally distinct site, pUL25 may adopt a different conformation or engage in interactions with different viral proteins than at the vertex. These interactions could theoretically support completion of DNA packaging in two ways: (i) by stabilizing the terminase complex and the portal while DNA is being actively propelled through the portal or (ii) by sealing off the portal after the second DNA cleavage, much like a head completion protein function in the dsDNA bacteriophages.

In conclusion, we propose to integrate our current studies of UL25 into the HSV-1 DNA encapsidation model (Figure 38). DNA packaging is an energy-dependent process that requires conformational changes in the viral DNA (16, 36, 220). Presumably, ATP hydrolysis by the terminase-portal complex supplies the force required to compact DNA within the capsid. pUL25 association with the capsid may stabilize this transition. The pUL25 capsid-binding domain is responsible for the binding of pUL25 to the capsid surface, but other portions of the protein are essential for completion of DNA packaging. These essential functions could include a indirect role in the cleavage reaction via pUL25 interaction with the terminase and portal complexes. It is also possible that a threshold amount of capsid-associated pUL25 is required for the second cleavage event. Terminase sensing of the fully mature capsid, in combination with its recognition of the second packaging signal in the TR_S, precipitates cleavage of the U_S terminus.

In the absence of pUL25 capsid attachment or capsid-associated but non-functional pUL25, the capsid is unstable, and the equilibrium between the internal pressure of packaged DNA and the force exerted by the terminase is breached. The internal pressure may therefore inhibit DNA entry or cause DNA extrusion through the portal. When the terminase can no longer propel DNA into the nascent capsid, it stalls on the DNA and cleaves in a non-specific manner in order to abort packaging, thus forming the truncated genomes observed in replication-deficient UL25 mutants (30, 205). Ejection of the truncated genome leaves the empty A-capsid that is characteristic of UL25 null viruses.

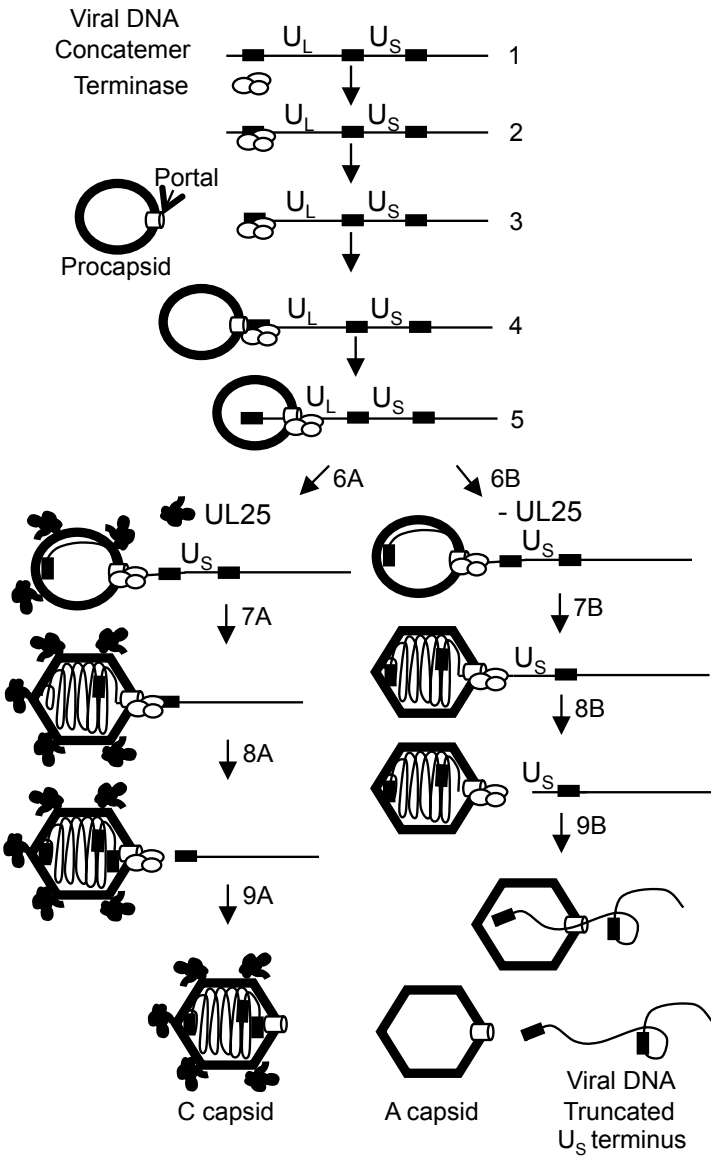

Figure 38. Model for the role of UL25 in DNA packaging. (1) DNA packaging initiates on concatemers when the terminase complex consisting of UL15, UL28, and UL33 binds (2) to packaging sequences and cleaves (3) the concatemer to generate a U_L end with the terminase still bound. The terminase/DNA complex then docks at the portal vertex on the procapsid (4) and the terminase initiates DNA packaging (5). As the procapsid is filled (6A) with DNA it angularizes and in the process, UL25 binding sites are exposed at the capsid vertexes. DNA cleavage is suppressed by a head-full mechanism (7A) until a full-length genome has entered. Cleavage occurs at a packaging site located at the U_S end of the genome (8A). More UL25 binds to the capsid, and the newly packaged genome is sealed within the C capsid (9A). In the absence of a functional UL25 protein the packaging reaction proceeds (6B) with the capsid filling and expanding until close to a genome-length has entered (7B). Without UL25 to stabilize the capsid against the pressure that the packaged genome generates, premature cleavage (8B) occurs just prior to the entry of the U_S end repeat resulting in genomes with truncated U_S termini. In the absence of UL25, the capsid is not stable and the DNA is released (9B) generating an empty A-capsid and a free viral genome that is truncated at the U_S end. This figure was amended with permission from reference (30).

APPENDIX A: PRIMERS USED FOR CLONING PLASMIDS AND BACS

TABLE 9. Primers used for plasmid cloning.

Plasmid clone	pUL25 amino acids coded	Sequence[A]
pFH274	37-580	5’ GGATCCATGTCGCCCGTCTTTAACC
		5’ GGATCCCTAAACCGCCGACAGGTAC
pFH284	51-580	5’ GAATTCGGATCCATGGACCCGTACTGCCCATT
		5’ GGATCCAACCGCCGACAGGTACTGTGGAATG
pFH368	1-50	5’ GGATCCGAATTCATGGACCCGTACTGCCCATT
		5’ GGATCCCTCCGCCGCCGTCTCCCG
pFH379	51-580	5’ GGATCCGAATTCATGCAGGTGGTCGTCCTACAGGCCCA
		5’ GGATCCAACCGCCGACAGGTACTGTGGAATG

[A]Uppercase letters represent the template sequence from HSV-1 UL25.

TABLE 10. Primers used for generation of recombinant HSV-1-BACs with UL25 insertions and point mutations.

BAC clone	UL25 mutation	RE	Sequence
bFH407	143i	*Pme*I	5'gccgtcgcggagatggaggtccagatcgtgcgcaac**tgtttaaac**a**gcaac**gacccgccg
			TAGGGATAACAGGGTAATCGATTT
		*Pme*I	5' ggaggttggtgtcgtatcgtagcggcgggtc**gttgctgtttaaac**agttgcgcacgat
			GCCAGTGTTACAACCAATTAACC
bFH416	212s	*Pme*I	5' actttcgggacggccggatgtccaagaccttcatgac**tgtttaaac**a**atgac**ggcgctggt
			TAGGGATAACAGGGTAATCGATTT
		*Pme*I	5' gccgcacgactgcagggacaggaccagcgcc**gtcattgtttaaac**agtcatgaaggtct
			GCCAGTGTTACAACCAATTAACC
bFH418	560s	*Pme*I	5' gctccaacaccaagcgtttctccgcgttcaacgttag**tgtttaaac**a**gttag**cagcgacta
			TAGGGATAACAGGGTAATCGATTT
		*Pme*I	5' gacataaaaagtacaacatgtcgtagtcgctg**ctaactgtttaaac**actaacgttgaacg
			GCCAGTGTTACAACCAATTAACC
bFH422	GFP insertion		5' gacttttggatgtcgcccgtctttaacctcccccgggagacggcggcggag
			ATGGTGAGCAAGGGCGAGGA
			5' ctccagggcagcggcagccgctgtgcgctgggcctgcaggacgaccacctg
			CTTGTACAGCTCGTCCATGCCG
bFH423	155i	*Pme*I	5' cgacccgccgctacgatacgacaccaacctccccg**tggtgtttaaac**a**cgt**ggatctgc
			TAGGGATAACAGGGTAATCGATTT
		*Pme*I	5' ccgcggcccgcgtacaccatatgtagcagatcc**acgtgtttaaac**a**cc**acggggaggttg
			GCCAGTGTTACAACCAATTAACC
bFH469	NTAP		5' cgaccgcagttctcgtgtgttattttcgctctccgcctctcgcag
			ATGAAGCGACGATGGAAAAAG
			5' gtgttcccagacgtccagagcgtcaaatgggcagtacgggtccat
			GCCCAGCTTGCAGCCGCCGGA
bFH480	F26A I27A	*Xba*I	5' aggcgcttcatagtcgccgatt<u>c*tag*a</u>aac**gc**c**gc**cacc
			TAGGGATAACAGGGTAATCGATTT
		*Xba*I	5' gtcccgggggaactcgggggtg**gc**g**gc**gttt<u>c*tag*a</u>atc
			GCCAGTGTTACAACCAATTAACC
bFH481	F35A W36A	*Bcg*I	5' gaaacttcatcacccccgagttcccccgggac**gcagc**gatgtcgccc
			TAGGGATAACAGGGTAATCGATTT
		*Bcg*I	5' aggttaaagacgggcgacatc**gctgc**gtcccgggggaactcgggggtg
			GCCAGTGTTACAACCAATTAACC
bFH482	F26A I27A F35A W36A	*Bsm*I	5' cttcatagtcgccgattcccg*gaat***gc**c**gc**caccccccgagttcccccggga
			TAGGGATAACAGGGTAATCGATTT
		*Bsm*I	5' tccaaaagtcccgggggaactcgggggtg**gc**g**gc***attc*cgggaatc
			GCCAGTGTTACAACCAATTAACC
		*Bcg*I	5' gaaacttcatcacccccgagttcccccgggac**gcagc**gatgtcgccc
			TAGGGATAACAGGGTAATCGATTT
		*Bcg*I	5' aggttaaagacgggcgacatc**gctgc**gtcccgggggaactcgggggtg
			GCCAGTGTTACAACCAATTAACC

RE, restriction enzyme. Underlined, restriction site. Italic, conservative substitution. Bold, mutation. Uppercase letters represent the template sequence (pEP-Kan-S; pEGFP-in; p-EP-TAP-in). Lowercase letters represent HSV-1 UL25 gene sequences.

TABLE 11. Primers used for generation of recombinant HSV-1-BACs with UL25 deletions.

BAC clone	UL25 deletion	RE	Sequence
bFH439	ORF replaced with rpsL-neo	*Bgl*II	5’ gacaacgaccgcagttctcgtgtgttattttcgctctccgcctctcgcagagatct GGCCTGGTGATGATGGCGGGATCG
		*Bgl*II	5’ ggctcttgttttttctccctaatgccccctcccccctcgcccaccacccaagatct TCAGAAGAACTCGTCAAGAAGGCG
bFH421	Δ1-50		5’ accgcagttctcgtgtgttattttcgctctccgcctctcgatgcaggtggtcgtcctgcag TAGGGATAACAGGGTAATCGATTT
			5’ cggcagccgctgtgcgctgggcctgcaggacgaccacctgcatcgagaggcggagagcga GCCAGTGTTACAACCAATTAACC
bFH472	Δ1-36		5’ tgtgttattttcgctctccgcctctcgcagacccccgagttcccccgg TAGGGATAACAGGGTAATCGATTT
			5’ atccaaaagtcccgggggaactcgggggtctgcgagaggcggagagc GCCAGTGTTACAACCAATTAACC
bFH471	Δ27-37		5’gaacacaggcgcttcatagtcgccgattcccgaaacttctcgcccgtctttaacctcccc TAGGGATAACAGGGTAATCGATTT
			5’cgccgccgtctcccgggggaggttaaagacgggcgagaagtttcgggaatcggc GCCAGTGTTACAACCAATTAACC
bFH473	Δ40-50		5’ gagttcccccgggacttttggatgtcgccccaggtggtcgtcctacag TAGGGATAACAGGGTAATCGATTT
			5’ tgtgcgctgggcctgtaggacgaccacctggggcgacatccaaaagtc GCCAGTGTTACAACCAATTAACC
bFH468	Δ27-50		5’gaacacaggcgcttcatagtcgccgattcccgaaacttccaggtggtcgtcctacaggcc TAGGGATAACAGGGTAATCGATTT
			5’ggcagccgctgtgcgctgggcctgtaggacgaccacctggaagtttcgggaatcggc GCCAGTGTTACAACCAATTAACC

RE, restriction enzyme. Underlined, restriction site. Italic, conservative substitution. Bold, mutation. Uppercase letters represent the template sequence (pEP-Kan-S). Lowercase letters represent HSV-1 sequences.

APPENDIX B: COPYRIGHTS AND PERMISSIONS

The text and figures included in chapters 2, 3, 4, and 5 and referencing viruses vΔUL25, v143i, v155i, v212s, v560s, vΔ1-50, and vGFP-UL25 are copyright © American Society for Microbiology, Journal of Virology, Volume 83, 2009, pages 47-57, DOI: 10.1128/JVI.01889-08 ("Role of the UL25 Protein in Herpes Simplex Virus DNA Encapsidation") and have been reproduced and amended with permission from the American Society for Microbiology (license number 2423801313520).

The text and figures included in chapter 4 referencing characterization and structural determination of the vGFP-UL25 virus are copyright © 2010 Elsevier Ltd, Journal of Molecular Biology, Volume 397, 2010, pages 575-586, DOI: 10.1016/J.JMB.2010.01.043 ("Labeling and Localization of the Herpes Simplex Virus Capsid Protein UL25 and Its Interaction with the Two Triplexes Closest to the Penton") and have been reproduced and amended with permission from Elsevier Ltd (license number 2433130182856).

BIBLIOGRAPHY

1. **Abaitua, F., and P. O'Hare.** 2008. Identification of a highly conserved, functional nuclear localization signal within the N-terminal region of herpes simplex virus type 1 VP1-2 tegument protein. J Virol **82:**5234-44.
2. **Abbotts, A. P., V. G. Preston, M. Hughes, A. H. Patel, and N. D. Stow.** 2000. Interaction of the herpes simplex virus type 1 packaging protein UL15 with full-length and deleted forms of the UL28 protein. J Gen Virol **81:**2999-3009.
3. **Adamson, W. E., D. McNab, V. G. Preston, and F. J. Rixon.** 2006. Mutational analysis of the herpes simplex virus triplex protein VP19C. J Virol **80:**1537-48.
4. **Addison, C., F. J. Rixon, J. W. Palfreyman, M. O'Hara, and V. G. Preston.** 1984. Characterisation of a herpes simplex virus type 1 mutant which has a temperature-sensitive defect in penetration of cells and assembly of capsids. Virology **138:**246-59.
5. **Adelman, K., B. Salmon, and J. D. Baines.** 2001. Herpes simplex virus DNA packaging sequences adopt novel structures that are specifically recognized by a component of the cleavage and packaging machinery. Proc Natl Acad Sci U S A **98:**3086-91.
6. **al-Kobaisi, M. F., F. J. Rixon, I. McDougall, and V. G. Preston.** 1991. The herpes simplex virus UL33 gene product is required for the assembly of full capsids. Virology **180:**380-8.
7. **Ali, M. A., B. Forghani, and E. M. Cantin.** 1996. Characterization of an essential HSV-1 protein encoded by the UL25 gene reported to be involved in virus penetration and capsid assembly. Virology **216:**278-83.
8. **Arduino, P. G., and S. R. Porter.** 2008. Herpes Simplex Virus Type 1 infection: overview on relevant clinico-pathological features. J Oral Pathol Med **37:**107-21.
9. **Atanasiu, D., J. C. Whitbeck, T. M. Cairns, B. Reilly, G. H. Cohen, and R. J. Eisenberg.** 2007. Bimolecular complementation reveals that glycoproteins gB and gH/gL of herpes simplex virus interact with each other during cell fusion. Proc Natl Acad Sci U S A **104:**18718-23.
10. **Baker, M. L., W. Jiang, F. J. Rixon, and W. Chiu.** 2005. Common ancestry of herpesviruses and tailed DNA bacteriophages. J Virol **79:**14967-70.
11. **Batterson, W., D. Furlong, and B. Roizman.** 1983. Molecular genetics of herpes simplex virus. VIII. further characterization of a temperature-sensitive mutant defective in release of viral DNA and in other stages of the viral reproductive cycle. J Virol **45:**397-407.
12. **Beilstein, F., M. R. Higgs, and N. D. Stow.** 2009. Mutational analysis of the herpes simplex virus type 1 DNA packaging protein UL33. J Virol **83:**8938-45.

13. **Billaud, G., D. Thouvenot, and F. Morfin.** 2009. Drug targets in herpes simplex and Epstein Barr Virus infections. Infect Disord Drug Targets **9:**117-25.
14. **Boehmer, P. E., and I. R. Lehman.** 1997. Herpes simplex virus DNA replication. Annu Rev Biochem **66:**347-84.
15. **Bogner, E., K. Radsak, and M. F. Stinski.** 1998. The gene product of human cytomegalovirus open reading frame UL56 binds the pac motif and has specific nuclease activity. J Virol **72:**2259-64.
16. **Booy, F. P., W. W. Newcomb, B. L. Trus, J. C. Brown, T. S. Baker, and A. C. Steven.** 1991. Liquid-crystalline, phage-like packing of encapsidated DNA in herpes simplex virus. Cell **64:**1007-15.
17. **Booy, F. P., B. L. Trus, W. W. Newcomb, J. C. Brown, J. F. Conway, and A. C. Steven.** 1994. Finding a needle in a haystack: detection of a small protein (the 12-kDa VP26) in a large complex (the 200-MDa capsid of herpes simplex virus). Proc Natl Acad Sci U S A **91:**5652-6.
18. **Bowman, B. R., M. L. Baker, F. J. Rixon, W. Chiu, and F. A. Quiocho.** 2003. Structure of the herpesvirus major capsid protein. EMBO J **22:**757-65.
19. **Bowman, B. R., R. L. Welschhans, H. Jayaram, N. D. Stow, V. G. Preston, and F. A. Quiocho.** 2006. Structural characterization of the UL25 DNA-packaging protein from herpes simplex virus type 1. J Virol **80:**2309-17.
20. **Brown, J. C., M. A. McVoy, and F. L. Homa.** 2002. Packaging DNA into Herpesvirus Capsids, p. 111-153. *In* H. a. Bogner (ed.), Structure-Function Relationships of Human Pathogenic Viruses. Kluwer Academic/Plenum Publishers, New York, NY.
21. **Brown, S. M., and A. R. MacLean.** 1998. Herpes Simplex Virus Protocols, Methods in Molecular Medicine 10. Humana Press Inc., Totowa, NJ.
22. **Bucks, M. A., K. J. O'Regan, M. A. Murphy, J. W. Wills, and R. J. Courtney.** 2007. Herpes simplex virus type 1 tegument proteins VP1/2 and UL37 are associated with intranuclear capsids. Virology **361:**316-24.
23. **Campadelli-Fiume, G., M. Amasio, E. Avitabile, A. Cerretani, C. Forghieri, T. Gianni, and L. Menotti.** 2007. The multipartite system that mediates entry of herpes simplex virus into the cell. Rev Med Virol **17:**313-26.
24. **Cardone, G., D. C. Winkler, B. L. Trus, N. Cheng, J. E. Heuser, W. W. Newcomb, J. C. Brown, and A. C. Steven.** 2007. Visualization of the herpes simplex virus portal in situ by cryo-electron tomography. Virology **361:**426-34.
25. **Catalano, C. E.** 2005. Viral genome packaging machines : genetics, structure, and mechanism. Kluwer Academic/Plenum Publishers, Georgetown, Tex. New York, N.Y.
26. **Chang, J. T., M. F. Schmid, F. J. Rixon, and W. Chiu.** 2007. Electron cryotomography reveals the portal in the herpesvirus capsid. J Virol **81:**2065-8.
27. **Chen, D. H., J. Jakana, D. McNab, J. Mitchell, Z. H. Zhou, M. Dougherty, W. Chiu, and F. J. Rixon.** 2001. The pattern of tegument-capsid interaction in the herpes simplex virus type 1 virion is not influenced by the small hexon-associated protein VP26. J Virol **75:**11863-7.
28. **Chou, J., and B. Roizman.** 1989. Characterization of DNA sequence-common and sequence-specific proteins binding to cis-acting sites for cleavage of the terminal a sequence of the herpes simplex virus 1 genome. J Virol **63:**1059-68.
29. **Church, G. A., and D. W. Wilson.** 1997. Study of herpes simplex virus maturation during a synchronous wave of assembly. J Virol **71:**3603-12.

30. **Cockrell, S. K., M. E. Sanchez, A. Erazo, and F. L. Homa.** 2009. Role of the UL25 protein in herpes simplex virus DNA encapsidation. J Virol **83:**47-57.
31. **Cohen, G. H., M. Ponce de Leon, H. Diggelmann, W. C. Lawrence, S. K. Vernon, and R. J. Eisenberg.** 1980. Structural analysis of the capsid polypeptides of herpes simplex virus types 1 and 2. J Virol **34:**521-31.
32. **Coller, K. E., J. I. Lee, A. Ueda, and G. A. Smith.** 2007. The capsid and tegument of the alphaherpesviruses are linked by an interaction between the UL25 and VP1/2 proteins. J Virol **81:**11790-7.
33. **Conway, J. F., S. K. Cockrell, A. M. Copeland, W. W. Newcomb, J. C. Brown, and F. L. Homa.** 2010. Labeling and localization of the herpes simplex virus capsid protein UL25 and its interaction with the two triplexes closest to the penton. J Mol Biol **397:**575-86.
34. **Copeland, A. M., W. W. Newcomb, and J. C. Brown.** 2009. Herpes simplex virus replication: roles of viral proteins and nucleoporins in capsid-nucleus attachment. J Virol **83:**1660-8.
35. **Dalziel, R. G., and H. S. Marsden.** 1984. Identification of two herpes simplex virus type 1-induced proteins (21K and 22K) which interact specifically with the a sequence of herpes simplex virus DNA. J Gen Virol **65 (Pt 9):**1467-75.
36. **Dasgupta, A., and D. W. Wilson.** 1999. ATP depletion blocks herpes simplex virus DNA packaging and capsid maturation. J Virol **73:**2006-15.
37. **Davison, A. J., and J. E. Scott.** 1986. The complete DNA sequence of varicella-zoster virus. J Gen Virol **67 (Pt 9):**1759-816.
38. **Davison, M. D., F. J. Rixon, and A. J. Davison.** 1992. Identification of genes encoding two capsid proteins (VP24 and VP26) of herpes simplex virus type 1. J Gen Virol **73 (Pt 10):**2709-13.
39. **de Beer, T., J. Fang, M. Ortega, Q. Yang, L. Maes, C. Duffy, N. Berton, J. Sippy, M. Overduin, M. Feiss, and C. E. Catalano.** 2002. Insights into specific DNA recognition during the assembly of a viral genome packaging machine. Mol Cell **9:**981-91.
40. **De Bolle, L., L. Naesens, and E. De Clercq.** 2005. Update on human herpesvirus 6 biology, clinical features, and therapy. Clin Microbiol Rev **18:**217-45.
41. **Decman, V., M. L. Freeman, P. R. Kinchington, and R. L. Hendricks.** 2005. Immune control of HSV-1 latency. Viral Immunol **18:**466-73.
42. **Deiss, L. P., J. Chou, and N. Frenkel.** 1986. Functional domains within the a sequence involved in the cleavage-packaging of herpes simplex virus DNA. J Virol **59:**605-18.
43. **Deiss, L. P., and N. Frenkel.** 1986. Herpes simplex virus amplicon: cleavage of concatemeric DNA is linked to packaging and involves amplification of the terminally reiterated a sequence. J Virol **57:**933-41.
44. **Desai, P. J.** 2000. A null mutation in the UL36 gene of herpes simplex virus type 1 results in accumulation of unenveloped DNA-filled capsids in the cytoplasm of infected cells. J Virol **74:**11608-18.
45. **Deshmane, S. L., and N. W. Fraser.** 1989. During latency, herpes simplex virus type 1 DNA is associated with nucleosomes in a chromatin structure. J Virol **63:**943-7.
46. **Deshmane, S. L., B. Raengsakulrach, J. F. Berson, and N. W. Fraser.** 1995. The replicating intermediates of herpes simplex virus type 1 DNA are relatively short. J Neurovirol **1:**165-76.

47. **Desloges, N., H. Boucher, and C. Simard.** 2001. Transcriptional and translational expression kinetics of the UL25 homologue of bovine herpesvirus 1.1. Arch Virol **146:**1693-704.
48. **Desloges, N., and C. Simard.** 2003. Implication of the product of the bovine herpesvirus type 1 UL25 gene in capsid assembly. J Gen Virol **84:**2485-90.
49. **Dezelee, S., F. Bras, P. Vende, B. Simonet, X. Nguyen, A. Flamand, and M. J. Masse.** 1996. The BamHI fragment 9 of pseudorabies virus contains genes homologous to the UL24, UL25, UL26, and UL 26.5 genes of herpes simplex virus type 1. Virus Res **42:**27-39.
50. **DiIanni, C. L., D. A. Drier, I. C. Deckman, P. J. McCann, 3rd, F. Liu, B. Roizman, R. J. Colonno, and M. G. Cordingley.** 1993. Identification of the herpes simplex virus-1 protease cleavage sites by direct sequence analysis of autoproteolytic cleavage products. J Biol Chem **268:**2048-51.
51. **Dohner, K., K. Radtke, S. Schmidt, and B. Sodeik.** 2006. Eclipse phase of herpes simplex virus type 1 infection: Efficient dynein-mediated capsid transport without the small capsid protein VP26. J Virol **80:**8211-24.
52. **Dohner, K., A. Wolfstein, U. Prank, C. Echeverri, D. Dujardin, R. Vallee, and B. Sodeik.** 2002. Function of dynein and dynactin in herpes simplex virus capsid transport. Mol Biol Cell **13:**2795-809.
53. **Dolan, A., C. Addison, D. Gatherer, A. J. Davison, and D. J. McGeoch.** 2006. The genome of Epstein-Barr virus type 2 strain AG876. Virology **350:**164-70.
54. **Dolan, A., C. Cunningham, R. D. Hector, A. F. Hassan-Walker, L. Lee, C. Addison, D. J. Dargan, D. J. McGeoch, D. Gatherer, V. C. Emery, P. D. Griffiths, C. Sinzger, B. P. McSharry, G. W. Wilkinson, and A. J. Davison.** 2004. Genetic content of wild-type human cytomegalovirus. J Gen Virol **85:**1301-12.
55. **Dolan, A., F. E. Jamieson, C. Cunningham, B. C. Barnett, and D. J. McGeoch.** 1998. The genome sequence of herpes simplex virus type 2. J Virol **72:**2010-21.
56. **Dominguez, G., T. R. Dambaugh, F. R. Stamey, S. Dewhurst, N. Inoue, and P. E. Pellett.** 1999. Human herpesvirus 6B genome sequence: coding content and comparison with human herpesvirus 6A. J Virol **73:**8040-52.
57. **Douglas, M. W., R. J. Diefenbach, F. L. Homa, M. Miranda-Saksena, F. J. Rixon, V. Vittone, K. Byth, and A. L. Cunningham.** 2004. Herpes simplex virus type 1 capsid protein VP26 interacts with dynein light chains RP3 and Tctex1 and plays a role in retrograde cellular transport. J Biol Chem **279:**28522-30.
58. **Fillet, A. M.** 2002. Prophylaxis of herpesvirus infections in immunocompetent and immunocompromised older patients. Drugs Aging **19:**343-54.
59. **Flint, S. J.** 2004. Principles of virology : molecular biology, pathogenesis, and control of animal viruses, 2nd ed. ASM Press, Washington, D.C.
60. **Forest, T., S. Barnard, and J. D. Baines.** 2005. Active intranuclear movement of herpesvirus capsids. Nat Cell Biol **7:**429-31.
61. **Fossum, E., C. C. Friedel, S. V. Rajagopala, B. Titz, A. Baiker, T. Schmidt, T. Kraus, T. Stellberger, C. Rutenberg, S. Suthram, S. Bandyopadhyay, D. Rose, A. von Brunn, M. Uhlmann, C. Zeretzke, Y. A. Dong, H. Boulet, M. Koegl, S. M. Bailer, U. Koszinowski, T. Ideker, P. Uetz, R. Zimmer, and J. Haas.** 2009. Evolutionarily conserved herpesviral protein interaction networks. PLoS Pathog **5:**e1000570.

62. **Frank, G. M., A. J. Lepisto, M. L. Freeman, B. S. Sheridan, T. L. Cherpes, and R. L. Hendricks.** 2010. Early CD4(+) T cell help prevents partial CD8(+) T cell exhaustion and promotes maintenance of Herpes Simplex Virus 1 latency. J Immunol **184:**277-86.
63. **Freeman, M. L., B. S. Sheridan, R. H. Bonneau, and R. L. Hendricks.** 2007. Psychological stress compromises CD8+ T cell control of latent herpes simplex virus type 1 infections. J Immunol **179:**322-8.
64. **Fuchs, W., B. G. Klupp, H. Granzow, and T. C. Mettenleiter.** 2004. Essential function of the pseudorabies virus UL36 gene product is independent of its interaction with the UL37 protein. J Virol **78:**11879-89.
65. **Fuchs, W., B. G. Klupp, H. Granzow, N. Osterrieder, and T. C. Mettenleiter.** 2002. The interacting UL31 and UL34 gene products of pseudorabies virus are involved in egress from the host-cell nucleus and represent components of primary enveloped but not mature virions. J Virol **76:**364-78.
66. **Fujisawa, H., and M. Morita.** 1997. Phage DNA packaging. Genes Cells **2:**537-45.
67. **Fuller, D. N., D. M. Raymer, J. P. Rickgauer, R. M. Robertson, C. E. Catalano, D. L. Anderson, S. Grimes, and D. E. Smith.** 2007. Measurements of single DNA molecule packaging dynamics in bacteriophage lambda reveal high forces, high motor processivity, and capsid transformations. J Mol Biol **373:**1113-22.
68. **Gao, M., and D. M. Knipe.** 1993. Intragenic complementation of herpes simplex virus ICP8 DNA-binding protein mutants. J Virol **67:**876-85.
69. **Gao, M., L. Matusick-Kumar, W. Hurlburt, S. F. DiTusa, W. W. Newcomb, J. C. Brown, P. J. McCann, 3rd, I. Deckman, and R. J. Colonno.** 1994. The protease of herpes simplex virus type 1 is essential for functional capsid formation and viral growth. J Virol **68:**3702-12.
70. **Gibson, W., and B. Roizman.** 1972. Proteins specified by herpes simplex virus. 8. Characterization and composition of multiple capsid forms of subtypes 1 and 2. J Virol **10:**1044-52.
71. **Gierasch, W. W., D. L. Zimmerman, S. L. Ward, T. K. Vanheyningen, J. D. Romine, and D. A. Leib.** 2006. Construction and characterization of bacterial artificial chromosomes containing HSV-1 strains 17 and KOS. J Virol Methods **135:**197-206.
72. **Granzow, H., B. G. Klupp, and T. C. Mettenleiter.** 2005. Entry of pseudorabies virus: an immunogold-labeling study. J Virol **79:**3200-5.
73. **Grunewald, K., P. Desai, D. C. Winkler, J. B. Heymann, D. M. Belnap, W. Baumeister, and A. C. Steven.** 2003. Three-dimensional structure of herpes simplex virus from cryo-electron tomography. Science **302:**1396-8.
74. **Haanes, E. J., C. C. Chen, and D. E. Lowery.** 1997. Nucleotide sequence and transcriptional analysis of a portion of the bovine herpesvirus genome encoding genes homologous to HSV-1, UL25, UL26 and UL26.5. Virus Res **48:**19-26.
75. **Hayward, G. S., R. J. Jacob, S. C. Wadsworth, and B. Roizman.** 1975. Anatomy of herpes simplex virus DNA: evidence for four populations of molecules that differ in the relative orientations of their long and short components. Proc Natl Acad Sci U S A **72:**4243-7.
76. **Heymann, J. B., N. Cheng, W. W. Newcomb, B. L. Trus, J. C. Brown, and A. C. Steven.** 2003. Dynamics of herpes simplex virus capsid maturation visualized by time-lapse cryo-electron microscopy. Nat Struct Biol **10:**334-41.

77. **Higgs, M. R., V. G. Preston, and N. D. Stow.** 2008. The UL15 protein of herpes simplex virus type 1 is necessary for the localization of the UL28 and UL33 proteins to viral DNA replication centres. J Gen Virol **89:**1709-15.
78. **Hodge, P. D., and N. D. Stow.** 2001. Effects of mutations within the herpes simplex virus type 1 DNA encapsidation signal on packaging efficiency. J Virol **75:**8977-86.
79. **Honess, R. W., and B. Roizman.** 1975. Regulation of herpesvirus macromolecular synthesis: sequential transition of polypeptide synthesis requires functional viral polypeptides. Proc Natl Acad Sci U S A **72:**1276-80.
80. **Honess, R. W., and B. Roizman.** 1974. Regulation of herpesvirus macromolecular synthesis. I. Cascade regulation of the synthesis of three groups of viral proteins. J Virol **14:**8-19.
81. **Hong, Z., M. Beaudet-Miller, J. Durkin, R. Zhang, and A. D. Kwong.** 1996. Identification of a minimal hydrophobic domain in the herpes simplex virus type 1 scaffolding protein which is required for interaction with the major capsid protein. J Virol **70:**533-40.
82. **Huang, E., E. M. Perkins, and P. Desai.** 2007. Structural features of the scaffold interaction domain at the N terminus of the major capsid protein (VP5) of herpes simplex virus type 1. J Virol **81:**9396-407.
83. **Huffman, J. B., W. W. Newcomb, J. C. Brown, and F. L. Homa.** 2008. Amino acids 143 to 150 of the herpes simplex virus type 1 scaffold protein are required for the formation of portal-containing capsids. J Virol **82:**6778-81.
84. **Imber, R., A. Tsugita, M. Wurtz, and T. Hohn.** 1980. Outer surface protein of bacteriophage lambda. J Mol Biol **139:**277-95.
85. **Ishii, T., Y. Yamaguchi, and M. Yanagida.** 1978. Binding of the structural protein soc to the head shell of bacteriophage T4. J Mol Biol **120:**533-44.
86. **Iwasaki, K., B. L. Trus, P. T. Wingfield, N. Cheng, G. Campusano, V. B. Rao, and A. C. Steven.** 2000. Molecular architecture of bacteriophage T4 capsid: vertex structure and bimodal binding of the stabilizing accessory protein, Soc. Virology **271:**321-33.
87. **Jackson, S. A., and N. A. DeLuca.** 2003. Relationship of herpes simplex virus genome configuration to productive and persistent infections. Proc Natl Acad Sci U S A **100:**7871-6.
88. **Jacobson, J. G., K. Yang, J. D. Baines, and F. L. Homa.** 2006. Linker insertion mutations in the herpes simplex virus type 1 UL28 gene: effects on UL28 interaction with UL15 and UL33 and identification of a second-site mutation in the UL15 gene that suppresses a lethal UL28 mutation. J Virol **80:**12312-23.
89. **Johnson, J. E., and W. Chiu.** 2007. DNA packaging and delivery machines in tailed bacteriophages. Curr Opin Struct Biol **17:**237-43.
90. **Johnson, J. E., and J. A. Speir.** 1997. Quasi-equivalent viruses: a paradigm for protein assemblies. J Mol Biol **269:**665-75.
91. **Jones, C.** 2003. Herpes simplex virus type 1 and bovine herpesvirus 1 latency. Clin Microbiol Rev **16:**79-95.
92. **Jovasevic, V., L. Liang, and B. Roizman.** 2008. Proteolytic cleavage of VP1-2 is required for release of herpes simplex virus 1 DNA into the nucleus. J Virol **82:**3311-9.
93. **Kaelin, K., S. Dezelee, M. J. Masse, F. Bras, and A. Flamand.** 2000. The UL25 protein of pseudorabies virus associates with capsids and localizes to the nucleus and to microtubules. J Virol **74:**474-82.

94. **Kelly, B. J., C. Fraefel, A. L. Cunningham, and R. J. Diefenbach.** 2009. Functional roles of the tegument proteins of herpes simplex virus type 1. Virus Res **145:**173-86.
95. **Khanna, K. M., R. H. Bonneau, P. R. Kinchington, and R. L. Hendricks.** 2003. Herpes simplex virus-specific memory CD8+ T cells are selectively activated and retained in latently infected sensory ganglia. Immunity **18:**593-603.
96. **Kleinschmidt-DeMasters, B. K., and D. H. Gilden.** 2001. The expanding spectrum of herpesvirus infections of the nervous system. Brain Pathol **11:**440-51.
97. **Klupp, B. G., H. Granzow, W. Fuchs, G. M. Keil, S. Finke, and T. C. Mettenleiter.** 2007. Vesicle formation from the nuclear membrane is induced by coexpression of two conserved herpesvirus proteins. Proc Natl Acad Sci U S A **104:**7241-6.
98. **Klupp, B. G., H. Granzow, G. M. Keil, and T. C. Mettenleiter.** 2006. The capsid-associated UL25 protein of the alphaherpesvirus pseudorabies virus is nonessential for cleavage and encapsidation of genomic DNA but is required for nuclear egress of capsids. J Virol **80:**6235-46.
99. **Koslowski, K. M., P. R. Shaver, J. T. Casey, 2nd, T. Wilson, G. Yamanaka, A. K. Sheaffer, D. J. Tenney, and N. E. Pederson.** 1999. Physical and functional interactions between the herpes simplex virus UL15 and UL28 DNA cleavage and packaging proteins. J Virol **73:**1704-7.
100. **Krosky, P. M., M. R. Underwood, S. R. Turk, K. W. Feng, R. K. Jain, R. G. Ptak, A. C. Westerman, K. K. Biron, L. B. Townsend, and J. C. Drach.** 1998. Resistance of human cytomegalovirus to benzimidazole ribonucleosides maps to two open reading frames: UL89 and UL56. J Virol **72:**4721-8.
101. **Krueger, G. R., B. Koch, N. Leyssens, Z. Berneman, J. Rojo, C. Horwitz, T. Sloots, M. Margalith, J. D. Conradie, S. Imai, I. Urasinski, M. de Bruyere, V. Ferrer Argote, and J. Krueger.** 1998. Comparison of seroprevalences of human herpesvirus-6 and -7 in healthy blood donors from nine countries. Vox Sang **75:**193-7.
102. **Kuhn, J., T. Leege, B. G. Klupp, H. Granzow, W. Fuchs, and T. C. Mettenleiter.** 2008. Partial functional complementation of a pseudorabies virus UL25 deletion mutant by herpes simplex virus type 1 pUL25 indicates overlapping functions of alphaherpesvirus pUL25 proteins. J Virol **82:**5725-34.
103. **Lamberti, C., and S. K. Weller.** 1998. The herpes simplex virus type 1 cleavage/packaging protein, UL32, is involved in efficient localization of capsids to replication compartments. J Virol **72:**2463-73.
104. **Lamberti, C., and S. K. Weller.** 1996. The herpes simplex virus type 1 UL6 protein is essential for cleavage and packaging but not for genomic inversion. Virology **226:**403-7.
105. **Lee, J. H., V. Vittone, E. Diefenbach, A. L. Cunningham, and R. J. Diefenbach.** 2008. Identification of structural protein-protein interactions of herpes simplex virus type 1. Virology **378:**347-54.
106. **Lee, J. I., G. W. Luxton, and G. A. Smith.** 2006. Identification of an essential domain in the herpesvirus VP1/2 tegument protein: the carboxy terminus directs incorporation into capsid assemblons. J Virol **80:**12086-94.
107. **Lhuillier, S., M. Gallopin, B. Gilquin, S. Brasiles, N. Lancelot, G. Letellier, M. Gilles, G. Dethan, E. V. Orlova, J. Couprie, P. Tavares, and S. Zinn-Justin.** 2009. Structure of bacteriophage SPP1 head-to-tail connection reveals mechanism for viral DNA gating. Proc Natl Acad Sci U S A **106:**8507-12.

108. **Liu, F., and B. Roizman.** 1993. Characterization of the protease and other products of amino-terminus-proximal cleavage of the herpes simplex virus 1 UL26 protein. J Virol **67:**1300-9.
109. **Liu, F., and B. Roizman.** 1992. Differentiation of multiple domains in the herpes simplex virus 1 protease encoded by the UL26 gene. Proc Natl Acad Sci U S A **89:**2076-80.
110. **Liu, F. Y., and B. Roizman.** 1991. The herpes simplex virus 1 gene encoding a protease also contains within its coding domain the gene encoding the more abundant substrate. J Virol **65:**5149-56.
111. **Liu, F. Y., and B. Roizman.** 1991. The promoter, transcriptional unit, and coding sequence of herpes simplex virus 1 family 35 proteins are contained within and in frame with the UL26 open reading frame. J Virol **65:**206-12.
112. **Loret, S., G. Guay, and R. Lippe.** 2008. Comprehensive characterization of extracellular herpes simplex virus type 1 virions. J Virol **82:**8605-18.
113. **Luxton, G. W., S. Haverlock, K. E. Coller, S. E. Antinone, A. Pincetic, and G. A. Smith.** 2005. Targeting of herpesvirus capsid transport in axons is coupled to association with specific sets of tegument proteins. Proc Natl Acad Sci U S A **102:**5832-7.
114. **Mabit, H., M. Y. Nakano, U. Prank, B. Saam, K. Dohner, B. Sodeik, and U. F. Greber.** 2002. Intact microtubules support adenovirus and herpes simplex virus infections. J Virol **76:**9962-71.
115. **Maluf, N. K., H. Gaussier, E. Bogner, M. Feiss, and C. E. Catalano.** 2006. Assembly of bacteriophage lambda terminase into a viral DNA maturation and packaging machine. Biochemistry **45:**15259-68.
116. **Martinez, R., R. T. Sarisky, P. C. Weber, and S. K. Weller.** 1996. Herpes simplex virus type 1 alkaline nuclease is required for efficient processing of viral DNA replication intermediates. J Virol **70:**2075-85.
117. **Matusick-Kumar, L., W. Hurlburt, S. P. Weinheimer, W. W. Newcomb, J. C. Brown, and M. Gao.** 1994. Phenotype of the herpes simplex virus type 1 protease substrate ICP35 mutant virus. J Virol **68:**5384-94.
118. **McGeoch, D. J., M. A. Dalrymple, A. J. Davison, A. Dolan, M. C. Frame, D. McNab, L. J. Perry, J. E. Scott, and P. Taylor.** 1988. The complete DNA sequence of the long unique region in the genome of herpes simplex virus type 1. J Gen Virol **69 (Pt 7):**1531-74.
119. **McGeoch, D. J., and D. Gatherer.** 2005. Integrating reptilian herpesviruses into the family herpesviridae. J Virol **79:**725-31.
120. **McGeoch, D. J., F. J. Rixon, and A. J. Davison.** 2006. Topics in herpesvirus genomics and evolution. Virus Res **117:**90-104.
121. **McNab, A. R., P. Desai, S. Person, L. L. Roof, D. R. Thomsen, W. W. Newcomb, J. C. Brown, and F. L. Homa.** 1998. The product of the herpes simplex virus type 1 UL25 gene is required for encapsidation but not for cleavage of replicated viral DNA. J Virol **72:**1060-70.
122. **Meckes, D. G., Jr., and J. W. Wills.** 2008. Structural rearrangement within an enveloped virus upon binding to the host cell. J Virol **82:**10429-35.
123. **Megaw, A. G., D. Rapaport, B. Avidor, N. Frenkel, and A. J. Davison.** 1998. The DNA sequence of the RK strain of human herpesvirus 7. Virology **244:**119-32.

124. **Mettenleiter, T. C.** 2004. Budding events in herpesvirus morphogenesis. Virus Res **106:**167-80.
125. **Mettenleiter, T. C., B. G. Klupp, and H. Granzow.** 2006. Herpesvirus assembly: a tale of two membranes. Curr Opin Microbiol **9:**423-9.
126. **Mettenleiter, T. C., B. G. Klupp, and H. Granzow.** 2009. Herpesvirus assembly: an update. Virus Res **143:**222-34.
127. **Mitchell, M. S., S. Matsuzaki, S. Imai, and V. B. Rao.** 2002. Sequence analysis of bacteriophage T4 DNA packaging/terminase genes 16 and 17 reveals a common ATPase center in the large subunit of viral terminases. Nucleic Acids Res **30:**4009-21.
128. **Mocarski, E. S., and B. Roizman.** 1982. Structure and role of the herpes simplex virus DNA termini in inversion, circularization and generation of virion DNA. Cell **31:**89-97.
129. **Mohl, B. S., S. Bottcher, H. Granzow, J. Kuhn, B. G. Klupp, and T. C. Mettenleiter.** 2009. Intracellular localization of the pseudorabies virus large tegument protein pUL36. J Virol **83:**9641-51.
130. **Naldinho-Souto, R., H. Browne, and T. Minson.** 2006. Herpes simplex virus tegument protein VP16 is a component of primary enveloped virions. J Virol **80:**2582-4.
131. **Nasseri, M., and E. Mocarski.** 1988. The cleavage recognition signal is contained within sequences surrounding an a-a junction in herpes simplex virus DNA. Virology **167:**25-30.
132. **Nellissery, J. K., R. Szczepaniak, C. Lamberti, and S. K. Weller.** 2007. A putative leucine zipper within the herpes simplex virus type 1 UL6 protein is required for portal ring formation. J Virol **81:**8868-77.
133. **Newcomb, W. W., F. P. Booy, and J. C. Brown.** 2007. Uncoating the herpes simplex virus genome. J Mol Biol **370:**633-42.
134. **Newcomb, W. W., and J. C. Brown.** 1991. Structure of the herpes simplex virus capsid: effects of extraction with guanidine hydrochloride and partial reconstitution of extracted capsids. J Virol **65:**613-20.
135. **Newcomb, W. W., and J. C. Brown.** 1989. Use of Ar+ plasma etching to localize structural proteins in the capsid of herpes simplex virus type 1. J Virol **63:**4697-702.
136. **Newcomb, W. W., S. K. Cockrell, F. L. Homa, and J. C. Brown.** 2009. Polarized DNA ejection from the herpesvirus capsid. J Mol Biol **392:**885-94.
137. **Newcomb, W. W., F. L. Homa, and J. C. Brown.** 2006. Herpes simplex virus capsid structure: DNA packaging protein UL25 is located on the external surface of the capsid near the vertices. J Virol **80:**6286-94.
138. **Newcomb, W. W., F. L. Homa, and J. C. Brown.** 2005. Involvement of the portal at an early step in herpes simplex virus capsid assembly. J Virol **79:**10540-6.
139. **Newcomb, W. W., F. L. Homa, D. R. Thomsen, F. P. Booy, B. L. Trus, A. C. Steven, J. V. Spencer, and J. C. Brown.** 1996. Assembly of the herpes simplex virus capsid: characterization of intermediates observed during cell-free capsid formation. J Mol Biol **263:**432-46.
140. **Newcomb, W. W., F. L. Homa, D. R. Thomsen, and J. C. Brown.** 2001. In vitro assembly of the herpes simplex virus procapsid: formation of small procapsids at reduced scaffolding protein concentration. J Struct Biol **133:**23-31.
141. **Newcomb, W. W., F. L. Homa, D. R. Thomsen, B. L. Trus, N. Cheng, A. Steven, F. Booy, and J. C. Brown.** 1999. Assembly of the herpes simplex virus procapsid from

purified components and identification of small complexes containing the major capsid and scaffolding proteins. J Virol **73:**4239-50.

142. **Newcomb, W. W., F. L. Homa, D. R. Thomsen, Z. Ye, and J. C. Brown.** 1994. Cell-free assembly of the herpes simplex virus capsid. J Virol **68:**6059-63.
143. **Newcomb, W. W., R. M. Juhas, D. R. Thomsen, F. L. Homa, A. D. Burch, S. K. Weller, and J. C. Brown.** 2001. The UL6 gene product forms the portal for entry of DNA into the herpes simplex virus capsid. J Virol **75:**10923-32.
144. **Newcomb, W. W., D. R. Thomsen, F. L. Homa, and J. C. Brown.** 2003. Assembly of the herpes simplex virus capsid: identification of soluble scaffold-portal complexes and their role in formation of portal-containing capsids. J Virol **77:**9862-71.
145. **Newcomb, W. W., B. L. Trus, F. P. Booy, A. C. Steven, J. S. Wall, and J. C. Brown.** 1993. Structure of the herpes simplex virus capsid. Molecular composition of the pentons and the triplexes. J Mol Biol **232:**499-511.
146. **Nixon, D. E., and M. A. McVoy.** 2004. Dramatic effects of 2-bromo-5,6-dichloro-1-beta-D-ribofuranosyl benzimidazole riboside on the genome structure, packaging, and egress of guinea pig cytomegalovirus. J Virol **78:**1623-35.
147. **O'Hara, M., F. J. Rixon, N. D. Stow, J. Murray, M. Murphy, and V. G. Preston.** 2010. Mutational analysis of the herpes simplex virus type 1 UL25 DNA packaging protein reveals regions that are important after the viral DNA has been packaged. J Virol **84:**4252-63.
148. **Ogasawara, M., T. Suzutani, I. Yoshida, and M. Azuma.** 2001. Role of the UL25 gene product in packaging DNA into the herpes simplex virus capsid: location of UL25 product in the capsid and demonstration that it binds DNA. J Virol **75:**1427-36.
149. **Ojala, P. M., B. Sodeik, M. W. Ebersold, U. Kutay, and A. Helenius.** 2000. Herpes simplex virus type 1 entry into host cells: reconstitution of capsid binding and uncoating at the nuclear pore complex in vitro. Mol Cell Biol **20:**4922-31.
150. **Okoye, M. E., G. L. Sexton, E. Huang, J. M. McCaffery, and P. Desai.** 2006. Functional analysis of the triplex proteins (VP19C and VP23) of herpes simplex virus type 1. J Virol **80:**929-40.
151. **Orlova, E. V., B. Gowen, A. Droge, A. Stiege, F. Weise, R. Lurz, M. van Heel, and P. Tavares.** 2003. Structure of a viral DNA gatekeeper at 10 A resolution by cryo-electron microscopy. EMBO J **22:**1255-62.
152. **Ortega, M. E., and C. E. Catalano.** 2006. Bacteriophage lambda gpNu1 and Escherichia coli IHF proteins cooperatively bind and bend viral DNA: implications for the assembly of a genome-packaging motor. Biochemistry **45:**5180-9.
153. **Padgett, D. A., J. F. Sheridan, J. Dorne, G. G. Berntson, J. Candelora, and R. Glaser.** 1998. Social stress and the reactivation of latent herpes simplex virus type 1. Proc Natl Acad Sci U S A **95:**7231-5.
154. **Padula, M. E., M. L. Sydnor, and D. W. Wilson.** 2009. Isolation and preliminary characterization of herpes simplex virus 1 primary enveloped virions from the perinuclear space. J Virol **83:**4757-65.
155. **Park, R., and J. D. Baines.** 2006. Herpes simplex virus type 1 infection induces activation and recruitment of protein kinase C to the nuclear membrane and increased phosphorylation of lamin B. J Virol **80:**494-504.

156. **Pasdeloup, D., D. Blondel, A. L. Isidro, and F. J. Rixon.** 2009. Herpesvirus capsid association with the nuclear pore complex and viral DNA release involve the nucleoporin CAN/Nup214 and the capsid protein pUL25. J Virol **83:**6610-23.
157. **Patel, A. H., F. J. Rixon, C. Cunningham, and A. J. Davison.** 1996. Isolation and characterization of herpes simplex virus type 1 mutants defective in the UL6 gene. Virology **217:**111-23.
158. **Peake, M. L., P. Nystrom, and L. I. Pizer.** 1982. Herpesvirus glycoprotein synthesis and insertion into plasma membranes. J Virol **42:**678-90.
159. **Perelygina, L., L. Zhu, H. Zurkuhlen, R. Mills, M. Borodovsky, and J. K. Hilliard.** 2003. Complete sequence and comparative analysis of the genome of herpes B virus (Cercopithecine herpesvirus 1) from a rhesus monkey. J Virol **77:**6167-77.
160. **Person, S., S. Laquerre, P. Desai, and J. Hempel.** 1993. Herpes simplex virus type 1 capsid protein, VP21, originates within the UL26 open reading frame. J Gen Virol **74 (Pt 10):**2269-73.
161. **Perucchetti, R., W. Parris, A. Becker, and M. Gold.** 1988. Late stages in bacteriophage lambda head morphogenesis: in vitro studies on the action of the bacteriophage lambda D-gene and W-gene products. Virology **165:**103-14.
162. **Poon, A. P., and B. Roizman.** 1993. Characterization of a temperature-sensitive mutant of the UL15 open reading frame of herpes simplex virus 1. J Virol **67:**4497-503.
163. **Porter, I. M., and N. D. Stow.** 2004. Replication, recombination and packaging of amplicon DNA in cells infected with the herpes simplex virus type 1 alkaline nuclease null mutant ambUL12. J Gen Virol **85:**3501-10.
164. **Post, L. E., A. J. Conley, E. S. Mocarski, and B. Roizman.** 1980. Cloning of reiterated and nonreiterated herpes simplex virus 1 sequences as BamHI fragments. Proc Natl Acad Sci U S A **77:**4201-5.
165. **Powell, K. L., and D. J. Purifoy.** 1976. DNA-binding proteins of cells infected by herpes simplex virus type 1 and type 2. Intervirology **7:**225-39.
166. **Preston, V. G., J. A. Coates, and F. J. Rixon.** 1983. Identification and characterization of a herpes simplex virus gene product required for encapsidation of virus DNA. J Virol **45:**1056-64.
167. **Preston, V. G., and I. M. McDougall.** 2002. Regions of the herpes simplex virus scaffolding protein that are important for intermolecular self-interaction. J Virol **76:**673-87.
168. **Preston, V. G., J. Murray, C. M. Preston, I. M. McDougall, and N. D. Stow.** 2008. The UL25 gene product of herpes simplex virus type 1 is involved in uncoating of the viral genome. J Virol **82:**6654-66.
169. **Preston, V. G., J. Murray, C. M. Preston, I. M. McDougall, and N. D. Stow.** 2008. The UL25 Gene Product of Herpes Simplex Virus type 1 is Involved in Uncoating of the Viral Genome. J Virol.
170. **Preston, V. G., F. J. Rixon, I. M. McDougall, M. McGregor, and M. F. al Kobaisi.** 1992. Processing of the herpes simplex virus assembly protein ICP35 near its carboxy terminal end requires the product of the whole of the UL26 reading frame. Virology **186:**87-98.
171. **Przech, A. J., D. Yu, and S. K. Weller.** 2003. Point mutations in exon I of the herpes simplex virus putative terminase subunit, UL15, indicate that the most conserved residues are essential for cleavage and packaging. J Virol **77:**9613-21.

172. **Qu, L., F. Jenkins, and D. J. Triulzi.** 2010. Human herpesvirus 8 genomes and seroprevalence in United States blood donors. Transfusion.
173. **Rajcani, J., V. Andrea, and R. Ingeborg.** 2004. Peculiarities of herpes simplex virus (HSV) transcription: an overview. Virus Genes **28:**293-310.
174. **Remillard-Labrosse, G., G. Guay, and R. Lippe.** 2006. Reconstitution of herpes simplex virus type 1 nuclear capsid egress in vitro. J Virol **80:**9741-53.
175. **Reynolds, A. E., Y. Fan, and J. D. Baines.** 2000. Characterization of the U(L)33 gene product of herpes simplex virus 1. Virology **266:**310-8.
176. **Reynolds, A. E., L. Liang, and J. D. Baines.** 2004. Conformational changes in the nuclear lamina induced by herpes simplex virus type 1 require genes U(L)31 and U(L)34. J Virol **78:**5564-75.
177. **Rezaee, S. A., C. Cunningham, A. J. Davison, and D. J. Blackbourn.** 2006. Kaposi's sarcoma-associated herpesvirus immune modulation: an overview. J Gen Virol **87:**1781-804.
178. **Rigaut, G., A. Shevchenko, B. Rutz, M. Wilm, M. Mann, and B. Seraphin.** 1999. A generic protein purification method for protein complex characterization and proteome exploration. Nat Biotechnol **17:**1030-2.
179. **Rixon, F. J., C. Addison, A. McGregor, S. J. Macnab, P. Nicholson, V. G. Preston, and J. D. Tatman.** 1996. Multiple interactions control the intracellular localization of the herpes simplex virus type 1 capsid proteins. J Gen Virol **77 (Pt 9):**2251-60.
180. **Roberts, A. P., F. Abaitua, P. O'Hare, D. McNab, F. J. Rixon, and D. Pasdeloup.** 2009. Differing roles of inner tegument proteins pUL36 and pUL37 during entry of herpes simplex virus type 1. J Virol **83:**105-16.
181. **Roizman, B., and J. Baines.** 1991. The diversity and unity of Herpesviridae. Comp Immunol Microbiol Infect Dis **14:**63-79.
182. **Roizman, B., R. J. Whitley, and C. Lopez.** 1993. The Human herpesviruses. Raven Press, New York.
183. **Roos, W. H., K. Radtke, E. Kniesmeijer, H. Geertsema, B. Sodeik, and G. J. Wuite.** 2009. Scaffold expulsion and genome packaging trigger stabilization of herpes simplex virus capsids. Proc Natl Acad Sci U S A **106:**9673-8.
184. **Saad, A., Z. H. Zhou, J. Jakana, W. Chiu, and F. J. Rixon.** 1999. Roles of triplex and scaffolding proteins in herpes simplex virus type 1 capsid formation suggested by structures of recombinant particles. J Virol **73:**6821-30.
185. **Sainz, B., J. M. Loutsch, M. E. Marquart, and J. M. Hill.** 2001. Stress-associated immunomodulation and herpes simplex virus infections. Med Hypotheses **56:**348-56.
186. **Salmon, B., C. Cunningham, A. J. Davison, W. J. Harris, and J. D. Baines.** 1998. The herpes simplex virus type 1 U(L)17 gene encodes virion tegument proteins that are required for cleavage and packaging of viral DNA. J Virol **72:**3779-88.
187. **Salmon, B., D. Nalwanga, Y. Fan, and J. D. Baines.** 1999. Proteolytic cleavage of the amino terminus of the U(L)15 gene product of herpes simplex virus type 1 is coupled with maturation of viral DNA into unit-length genomes. J Virol **73:**8338-48.
188. **Scholtes, L., and J. D. Baines.** 2009. Effects of major capsid proteins, capsid assembly, and DNA cleavage/packaging on the pUL17/pUL25 complex of herpes simplex virus 1. J Virol **83:**12725-37.

189. **Severini, A., A. R. Morgan, D. R. Tovell, and D. L. Tyrrell.** 1994. Study of the structure of replicative intermediates of HSV-1 DNA by pulsed-field gel electrophoresis. Virology **200:**428-35.
190. **Severini, A., D. G. Scraba, and D. L. Tyrrell.** 1996. Branched structures in the intracellular DNA of herpes simplex virus type 1. J Virol **70:**3169-75.
191. **Shanda, S. K., and D. W. Wilson.** 2008. UL36p is required for efficient transport of membrane-associated herpes simplex virus type 1 along microtubules. J Virol **82:**7388-94.
192. **Sheaffer, A. K., W. W. Newcomb, M. Gao, D. Yu, S. K. Weller, J. C. Brown, and D. J. Tenney.** 2001. Herpes simplex virus DNA cleavage and packaging proteins associate with the procapsid prior to its maturation. J Virol **75:**687-98.
193. **Simpson-Holley, M., R. C. Colgrove, G. Nalepa, J. W. Harper, and D. M. Knipe.** 2005. Identification and functional evaluation of cellular and viral factors involved in the alteration of nuclear architecture during herpes simplex virus 1 infection. J Virol **79:**12840-51.
194. **Singer, G. P., W. W. Newcomb, D. R. Thomsen, F. L. Homa, and J. C. Brown.** 2005. Identification of a region in the herpes simplex virus scaffolding protein required for interaction with the portal. J Virol **79:**132-9.
195. **Skaliter, R., and I. R. Lehman.** 1994. Rolling circle DNA replication in vitro by a complex of herpes simplex virus type 1-encoded enzymes. Proc Natl Acad Sci U S A **91:**10665-9.
196. **Sodeik, B., M. W. Ebersold, and A. Helenius.** 1997. Microtubule-mediated transport of incoming herpes simplex virus 1 capsids to the nucleus. J Cell Biol **136:**1007-21.
197. **Spear, P. G.** 2004. Herpes simplex virus: receptors and ligands for cell entry. Cell Microbiol **6:**401-10.
198. **Spear, P. G., and B. Roizman.** 1972. Proteins specified by herpes simplex virus. V. Purification and structural proteins of the herpesvirion. J Virol **9:**143-59.
199. **Spencer, J. V., W. W. Newcomb, D. R. Thomsen, F. L. Homa, and J. C. Brown.** 1998. Assembly of the herpes simplex virus capsid: preformed triplexes bind to the nascent capsid. J Virol **72:**3944-51.
200. **Staras, S. A., S. C. Dollard, K. W. Radford, W. D. Flanders, R. F. Pass, and M. J. Cannon.** 2006. Seroprevalence of cytomegalovirus infection in the United States, 1988-1994. Clin Infect Dis **43:**1143-51.
201. **Steven, A. C., H. L. Greenstone, F. P. Booy, L. W. Black, and P. D. Ross.** 1992. Conformational changes of a viral capsid protein. Thermodynamic rationale for proteolytic regulation of bacteriophage T4 capsid expansion, co-operativity, and super-stabilization by soc binding. J Mol Biol **228:**870-84.
202. **Steven, A. C., C. R. Roberts, J. Hay, M. E. Bisher, T. Pun, and B. L. Trus.** 1986. Hexavalent capsomers of herpes simplex virus type 2: symmetry, shape, dimensions, and oligomeric status. J Virol **57:**578-84.
203. **Stevens, J. G., E. K. Wagner, G. B. Devi-Rao, M. L. Cook, and L. T. Feldman.** 1987. RNA complementary to a herpesvirus alpha gene mRNA is prominent in latently infected neurons. Science **235:**1056-9.
204. **Stow, N. D.** 1982. Localization of an origin of DNA replication within the TRS/IRS repeated region of the herpes simplex virus type 1 genome. EMBO J **1:**863-7.

205. **Stow, N. D.** 2001. Packaging of genomic and amplicon DNA by the herpes simplex virus type 1 UL25-null mutant KUL25NS. J Virol **75:**10755-65.
206. **Stow, N. D., E. C. McMonagle, and A. J. Davison.** 1983. Fragments from both termini of the herpes simplex virus type 1 genome contain signals required for the encapsidation of viral DNA. Nucleic Acids Res **11:**8205-20.
207. **Strang, B. L., and N. D. Stow.** 2005. Circularization of the herpes simplex virus type 1 genome upon lytic infection. J Virol **79:**12487-94.
208. **Strauss, H., and J. King.** 1984. Steps in the stabilization of newly packaged DNA during phage P22 morphogenesis. J Mol Biol **172:**523-43.
209. **Swinger, K. K., and P. A. Rice.** 2004. IHF and HU: flexible architects of bent DNA. Curr Opin Struct Biol **14:**28-35.
210. **Tan, H. H., and C. L. Goh.** 2006. Viral infections affecting the skin in organ transplant recipients: epidemiology and current management strategies. Am J Clin Dermatol **7:**13-29.
211. **Taus, N. S., B. Salmon, and J. D. Baines.** 1998. The herpes simplex virus 1 UL 17 gene is required for localization of capsids and major and minor capsid proteins to intranuclear sites where viral DNA is cleaved and packaged. Virology **252:**115-25.
212. **Tavares, P., R. Lurz, A. Stiege, B. Ruckert, and T. A. Trautner.** 1996. Sequential headful packaging and fate of the cleaved DNA ends in bacteriophage SPP1. J Mol Biol **264:**954-67.
213. **Telford, E. A., M. S. Watson, K. McBride, and A. J. Davison.** 1992. The DNA sequence of equine herpesvirus-1. Virology **189:**304-16.
214. **Tengelsen, L. A., N. E. Pederson, P. R. Shaver, M. W. Wathen, and F. L. Homa.** 1993. Herpes simplex virus type 1 DNA cleavage and encapsidation require the product of the UL28 gene: isolation and characterization of two UL28 deletion mutants. J Virol **67:**3470-80.
215. **Thomsen, D. R., L. L. Roof, and F. L. Homa.** 1994. Assembly of herpes simplex virus (HSV) intermediate capsids in insect cells infected with recombinant baculoviruses expressing HSV capsid proteins. J Virol **68:**2442-57.
216. **Thurlow, J. K., M. Murphy, N. D. Stow, and V. G. Preston.** 2006. Herpes simplex virus type 1 DNA-packaging protein UL17 is required for efficient binding of UL25 to capsids. J Virol **80:**2118-26.
217. **Thurlow, J. K., F. J. Rixon, M. Murphy, P. Targett-Adams, M. Hughes, and V. G. Preston.** 2005. The herpes simplex virus type 1 DNA packaging protein UL17 is a virion protein that is present in both the capsid and the tegument compartments. J Virol **79:**150-8.
218. **Tischer, B. K., J. von Einem, B. Kaufer, and N. Osterrieder.** 2006. Two-step red-mediated recombination for versatile high-efficiency markerless DNA manipulation in Escherichia coli. Biotechniques **40:**191-7.
219. **Tong, L., and N. D. Stow.** 2010. Analysis of herpes simplex virus type 1 DNA packaging signal mutations in the context of the viral genome. J Virol **84:**321-9.
220. **Trus, B. L., F. P. Booy, W. W. Newcomb, J. C. Brown, F. L. Homa, D. R. Thomsen, and A. C. Steven.** 1996. The herpes simplex virus procapsid: structure, conformational changes upon maturation, and roles of the triplex proteins VP19c and VP23 in assembly. J Mol Biol **263:**447-62.

221. **Trus, B. L., N. Cheng, W. W. Newcomb, F. L. Homa, J. C. Brown, and A. C. Steven.** 2004. Structure and polymorphism of the UL6 portal protein of herpes simplex virus type 1. J Virol **78:**12668-71.
222. **Trus, B. L., F. L. Homa, F. P. Booy, W. W. Newcomb, D. R. Thomsen, N. Cheng, J. C. Brown, and A. C. Steven.** 1995. Herpes simplex virus capsids assembled in insect cells infected with recombinant baculoviruses: structural authenticity and localization of VP26. J Virol **69:**7362-6.
223. **Trus, B. L., W. W. Newcomb, F. P. Booy, J. C. Brown, and A. C. Steven.** 1992. Distinct monoclonal antibodies separately label the hexons or the pentons of herpes simplex virus capsid. Proc Natl Acad Sci U S A **89:**11508-12.
224. **Trus, B. L., W. W. Newcomb, N. Cheng, G. Cardone, L. Marekov, F. L. Homa, J. C. Brown, and A. C. Steven.** 2007. Allosteric signaling and a nuclear exit strategy: binding of UL25/UL17 heterodimers to DNA-Filled HSV-1 capsids. Mol Cell **26:**479-89.
225. **Turcotte, S., J. Letellier, and R. Lippe.** 2005. Herpes simplex virus type 1 capsids transit by the trans-Golgi network, where viral glycoproteins accumulate independently of capsid egress. J Virol **79:**8847-60.
226. **Uetz, P., Y. A. Dong, C. Zeretzke, C. Atzler, A. Baiker, B. Berger, S. V. Rajagopala, M. Roupelieva, D. Rose, E. Fossum, and J. Haas.** 2006. Herpesviral protein networks and their interaction with the human proteome. Science **311:**239-42.
227. **Umene, K., S. Oohashi, M. Yoshida, and Y. Fukumaki.** 2008. Diversity of the a sequence of herpes simplex virus type 1 developed during evolution. J Gen Virol **89:**841-52.
228. **Underwood, M. R., R. J. Harvey, S. C. Stanat, M. L. Hemphill, T. Miller, J. C. Drach, L. B. Townsend, and K. K. Biron.** 1998. Inhibition of human cytomegalovirus DNA maturation by a benzimidazole ribonucleoside is mediated through the UL89 gene product. J Virol **72:**717-25.
229. **Varmuza, S. L., and J. R. Smiley.** 1985. Signals for site-specific cleavage of HSV DNA: maturation involves two separate cleavage events at sites distal to the recognition sequences. Cell **41:**793-802.
230. **Vernon, S. K., M. Ponce de Leon, G. H. Cohen, R. J. Eisenberg, and B. A. Rubin.** 1981. Morphological components of herpesvirus. III. Localization of herpes simplex virus type 1 nucleocapsid polypeptides by immune electron microscopy. J Gen Virol **54:**39-46.
231. **Wadsworth, S., R. J. Jacob, and B. Roizman.** 1975. Anatomy of herpes simplex virus DNA. II. Size, composition, and arrangement of inverted terminal repetitions. J Virol **15:**1487-97.
232. **Wagner, M. J., and W. C. Summers.** 1978. Structure of the joint region and the termini of the DNA of herpes simplex virus type 1. J Virol **27:**374-87.
233. **Walters, J. N., G. L. Sexton, J. M. McCaffery, and P. Desai.** 2003. Mutation of single hydrophobic residue I27, L35, F39, L58, L65, L67, or L71 in the N terminus of VP5 abolishes interaction with the scaffold protein and prevents closure of herpes simplex virus type 1 capsid shells. J Virol **77:**4043-59.
234. **Ward, P. L., W. O. Ogle, and B. Roizman.** 1996. Assemblons: nuclear structures defined by aggregation of immature capsids and some tegument proteins of herpes simplex virus 1. J Virol **70:**4623-31.

235. **Weinheimer, S. P., P. J. McCann, 3rd, D. R. O'Boyle, 2nd, J. T. Stevens, B. A. Boyd, D. A. Drier, G. A. Yamanaka, C. L. DiIanni, I. C. Deckman, and M. G. Cordingley.** 1993. Autoproteolysis of herpes simplex virus type 1 protease releases an active catalytic domain found in intermediate capsid particles. J Virol **67:**5813-22.
236. **Weller, S. K., A. Spadaro, J. E. Schaffer, A. W. Murray, A. M. Maxam, and P. A. Schaffer.** 1985. Cloning, sequencing, and functional analysis of oriL, a herpes simplex virus type 1 origin of DNA synthesis. Mol Cell Biol **5:**930-42.
237. **White, C. A., N. D. Stow, A. H. Patel, M. Hughes, and V. G. Preston.** 2003. Herpes simplex virus type 1 portal protein UL6 interacts with the putative terminase subunits UL15 and UL28. J Virol **77:**6351-8.
238. **Wildy, P., W. C. Russell, and R. W. Horne.** 1960. The morphology of herpes virus. Virology **12:**204-22.
239. **Wilkinson, D. E., and S. K. Weller.** 2003. The role of DNA recombination in herpes simplex virus DNA replication. IUBMB Life **55:**451-8.
240. **Wills, E., L. Scholtes, and J. D. Baines.** 2006. Herpes simplex virus 1 DNA packaging proteins encoded by UL6, UL15, UL17, UL28, and UL33 are located on the external surface of the viral capsid. J Virol **80:**10894-9.
241. **Wingfield, P. T., S. J. Stahl, D. R. Thomsen, F. L. Homa, F. P. Booy, B. L. Trus, and A. C. Steven.** 1997. Hexon-only binding of VP26 reflects differences between the hexon and penton conformations of VP5, the major capsid protein of herpes simplex virus. J Virol **71:**8955-61.
242. **Wohlrab, F., S. Chatterjee, and R. D. Wells.** 1991. The herpes simplex virus 1 segment inversion site is specifically cleaved by a virus-induced nuclear endonuclease. Proc Natl Acad Sci U S A **88:**6432-6.
243. **Xu, F., M. R. Sternberg, B. J. Kottiri, G. M. McQuillan, F. K. Lee, A. J. Nahmias, S. M. Berman, and L. E. Markowitz.** 2006. Trends in herpes simplex virus type 1 and type 2 seroprevalence in the United States. JAMA **296:**964-73.
244. **Yamagishi, H., and M. Okamoto.** 1978. Visualization of the intracellular development of bacteriophage lambda, with special reference to DNA packaging. Proc Natl Acad Sci U S A **75:**3206-10.
245. **Yang, K., and J. D. Baines.** 2008. Domain within herpes simplex virus 1 scaffold proteins required for interaction with portal protein in infected cells and incorporation of the portal vertex into capsids. J Virol **82:**5021-30.
246. **Yang, K., and J. D. Baines.** 2006. The putative terminase subunit of herpes simplex virus 1 encoded by UL28 is necessary and sufficient to mediate interaction between pUL15 and pUL33. J Virol **80:**5733-9.
247. **Yang, K., F. Homa, and J. D. Baines.** 2007. Putative terminase subunits of herpes simplex virus 1 form a complex in the cytoplasm and interact with portal protein in the nucleus. J Virol **81:**6419-33.
248. **Yang, K., A. P. Poon, B. Roizman, and J. D. Baines.** 2008. Temperature-sensitive mutations in the putative herpes simplex virus type 1 terminase subunits pUL15 and pUL33 preclude viral DNA cleavage/packaging and interaction with pUL28 at the nonpermissive temperature. J Virol **82:**487-94.
249. **Yang, Q., N. K. Maluf, and C. E. Catalano.** 2008. Packaging of a unit-length viral genome: the role of nucleotides and the gpD decoration protein in stable nucleocapsid assembly in bacteriophage lambda. J Mol Biol **383:**1037-48.

250. **Yu, D., A. K. Sheaffer, D. J. Tenney, and S. K. Weller.** 1997. Characterization of ICP6::lacZ insertion mutants of the UL15 gene of herpes simplex virus type 1 reveals the translation of two proteins. J Virol **71:**2656-65.
251. **Yu, D., and S. K. Weller.** 1998. Genetic analysis of the UL 15 gene locus for the putative terminase of herpes simplex virus type 1. Virology **243:**32-44.
252. **Yu, D., and S. K. Weller.** 1998. Herpes simplex virus type 1 cleavage and packaging proteins UL15 and UL28 are associated with B but not C capsids during packaging. J Virol **72:**7428-39.
253. **Zhou, Z. H., D. H. Chen, J. Jakana, F. J. Rixon, and W. Chiu.** 1999. Visualization of tegument-capsid interactions and DNA in intact herpes simplex virus type 1 virions. J Virol **73:**3210-8.
254. **Zhou, Z. H., M. Dougherty, J. Jakana, J. He, F. J. Rixon, and W. Chiu.** 2000. Seeing the herpesvirus capsid at 8.5 A. Science **288:**877-80.
255. **Zhou, Z. H., J. He, J. Jakana, J. D. Tatman, F. J. Rixon, and W. Chiu.** 1995. Assembly of VP26 in herpes simplex virus-1 inferred from structures of wild-type and recombinant capsids. Nat Struct Biol **2:**1026-30.
256. **Zhou, Z. H., S. J. Macnab, J. Jakana, L. R. Scott, W. Chiu, and F. J. Rixon.** 1998. Identification of the sites of interaction between the scaffold and outer shell in herpes simplex virus-1 capsids by difference electron imaging. Proc Natl Acad Sci U S A **95:**2778-83.